Raquel Alexandra Ribeiro dos Santos

Mestre em Biotecnologia

Developing non-chromatographic strategies for biopharmaceuticals purification

Dissertação para obtenção do Grau de Doutor em
Biociências Moleculares

Orientadora:	Doutora Ana Luísa Moreira de Carvalho, Investigadora Auxiliar UCIBIO, Faculdade de Ciências e Tecnologia da Universidade Nova de Lisboa
Co-Orientadora:	Prof. Doutora Ana Cecília Afonso Roque, Professora Associada com Agregação, Faculdade de Ciências e Tecnologia da Universidade Nova de Lisboa

Júri:

Presidente:	Prof. Doutora Maria João Lobo de Reis Madeira Romão
Arguentes:	Prof. Doutor José António Mestre Prates
	Prof. Doutora Maria Raquel Murias dos Santos Aires Barros
Vogais:	Prof. Doutora Maria João Lobo de Reis Madeira Romão
	Prof. Doutor Victor Manuel Diogo de Oliveira Alves
	Doutora Ana Luísa Moreira de Carvalho

FACULDADE DE CIÊNCIAS E TECNOLOGIA
UNIVERSIDADE NOVA DE LISBOA

Fevereiro 2020

Developing non-chromatographic strategies for biopharmaceuticals purification

Dedicated to my family

Dedicado à minha família

Acknowledgments

Even though an academic thesis is by definition an individual project, this work would not be possible without the collaboration, understanding and help from the people I encountered over the last years.

For the last four years, I had the pleasure to work under the supervision of both Professor Ana Cecília Roque and Doctor Ana Luisa Carvalho. To them I would like to express my profound thank you for letting me take this challenging project. Many times the road was not as straight as one might wanted to, but they were always there to help me go forward, and for that, I am truly grateful.

Working in two very distinct groups, the biomolecular engineering and the macromolecular crystallography laboratories, enabled me to learn, experience and explore new scientific mindsets, paramount to develop a sense of critical analyses. For that, for making me feel welcome and for the good environment, I have to thank all the group members from both groups without any exception.

From the macromolecular crystallography laboratory, I would like to address a special acknowledgment to Professor Maria João Romão for welcoming me to her laboratory. To Cecília Bonifácio and Márcia Correia for helping me plan and perform all experiments in the crystallization robot. To Francisco Leisico, for the help around the lab and scientific discussions throughout the whole project.

From the biomolecular engineering laboratory, I would like to once again acknowledge Professor Ana Cecília Roque for welcoming me in her group. To Doctor Ana Sofia Pina, a very (big) thank you for all the scientific discussions, inputs, out of the box thinking and for always pushing further when I most needed during the course of this work. To Sara Carvalho, thank you for all the scientific input and help that many times I much needed, our discussions really made me grown as a scientific individual. To (future to be Doctor) Manuel Matos, many thanks for the time spent discussing each other's works, many times coming up with a solution, many times finding other way to make it work. To Iana Lychko, thank you for the experimental help during your short first stay at the laboratory. I also have to acknowledge the PureCatSelf sub-group, I really enjoyed working with you all, it was a true pleasure to discuss scientific experimental work and to work with you truly as a group.

But many times the work went beyond the walls of these two laboratories, and during the four years of this project I have the pleasure to have the help of many people beyond the walls of the two labs. To Professor João Gonçalves and his group from the Faculty of Pharmacy (Universidade de Lisboa, Portugal) thank you for all biological material and further analyses. To Doctor Maria

Leonor and to Professor Carlos Salgueiro, thank you for letting me use as many times as I needed your autoclave system. To Paula Chicau, I would like to thank for letting me use the zetasizer equipment and ultrasonic baths from ITQB-NOVA, and always helping me when I needed. To Mrs. Palminha a great thank you always making our material so clean and tidy. And because many times we had to care about administrative bureaucracies, I have to thank the help of Mrs. Maria José Carapinha and Mrs. Inês Santos.

To the Molecular Biosciences PhD program class of 2015, I do not have the words to express all the gratitude I have for all the support during the last for years. For sure we are the greatest class, and for sure we will be the greatest of the Doctors.

To the Novartis Pharma Lab at iBET, thank for the support and kind words during the year I dedicated to writing this thesis. You all known it was not always easy, but I can assure that all of you made it much easier.

With the absolute certainty that I did not mention everyone that helped during the four years. I would like to express my utmost apologies but be certain that your influence much helped me during my patch and your influence will continue to help me move on.

At last, I would like to acknowledge Fundação para a Ciência e Tecnologia (FCT-MCTES) - Portugal for the award of research fellowship PD/BD/105753/2014 in the scope of the PhD program Molecular Biosciences PD/00133/2012. This work was support by UCIBIO, funded by FCT/MEC (UID/Multi/04378/2013) and ERDF under the PT2020 Partnership Agreement (POCI-01-0145-FEDER-007728). European Community's Seventh Framework Programme H2020 under iNEXT (grant agreement N°283570) funded this research through the HTX lab.

The following personal acknowledgements will be addressed in Portuguese.

Mãe e mano, obrigada por tudo. Só vocês sabem o que eu vos fiz passar durante estes 4 anos. E estes não foram 4 anos fáceis, a cada passo fomos postos à prova, mas conseguimos superar tudo. Do fundo do coração não sei como alguma vez vos vou conseguir agradecer.

Pai, onde quer que estejas sei que estás orgulhoso.

À minha família um muito obrigado.

Abstract

The biopharmaceutical market shows a high annual growth, and the major contributors for this success are antibody molecules. The purification of high added value biological molecules is an important step in the manufacturing process of any biopharmaceutical, being currently focused on packed-bed chromatography, which does not cope with the high titers and working volumes obtained upstream. A new trend in downstream processing explores Anything But Chromatography (ABC) methodologies, including precipitation and crystallization techniques, as well as magnetic fishing.

This work aims at developing a new ABC method - magnetic precipitation - which combines crystallization and affinity magnetic separation in a single step providing simultaneous protein purification and concentration.

Firstly, the potential of small synthetic affinity ligands for protein capture was shown with the development of an affinity chromatographic adsorbent for human serum albumin capture. Secondly, the potential of affinity magnetic fishing in protein capture from complex mixtures was shown with affinity-functionalized magnetic particles targeting hen egg white lysozyme and antibodies from complex media, such as human serum plasma. As a first step to further investigate the potential of combining affinity magnetic particles in other ABC processes, we studied the influence of these particles in protein crystal growth as nucleation agents. As a proof-of-concept, functionalized and non-functionalized magnetic particles were used as additives in protein crystallization. A rational design for magnetic particles functionalization was achieved, having magnetic particles functionalized with affinity-triggering molecules for the crystallization of the target proteins - hen egg white lysozyme, bovine trypsin and green fluorescent protein from *Aequorea victoria*. The presence of functionalized magnetic particles did not hamper crystal growth nor the resolution of the diffracting crystal. The new magnetic crystallization method can overcome some protein crystallization difficulties, but also has the potential to be integrated in protein purification methods involving crystallization/precipitation steps. Finally, crystallization and magnetic fishing methods were used in synergy for antibody purification. A screening of precipitation conditions in the presence of magnetic particles functionalized with an affinity ligand for antibodies were tested against human plasma and mammalian cells supernatant. Affinity driven magnetic precipitation enabled crude extract fractionation and antibody recovery in the elution fraction with high purity and recovery yield, up to 99% and 97%, respectively.

This work shows the development of a new method using crystallization and magnetic particles - magnetic precipitation, with the potential implications to be implemented and integrated as a platform to improve protein crystal for X-ray diffraction or as a step in a protein's purification pipeline.

Resumo

O mercado biofarmacêutico apresenta um dos maiores crescimentos anuais, e os principais contribuintes para esse sucesso são as moléculas de anticorpos. A purificação de moléculas biológicas de alto valor de mercado é uma etapa importante no processo de produção de qualquer biofarmacêutico, sendo a sua purificação atualmente focada na cromatografia em coluna, que não consegue trabalhar com as elevadas concentrações e volumes obtidos a montante no processo de produção de biofármacos. Uma nova tendência no processo de purificação de biofármacos explora as metodologias Tudo Exceto Cromatografia (TEC), incluindo técnicas de precipitação e cristalização, bem como a captura magnética.

Este trabalho tem como objetivo desenvolver um novo método TEC combinando cristalização/precipitação e captura magnética por afinidade - precipitação magnética - proporcionando simultaneamente purificação e concentração de proteínas.

Em primeiro lugar, foi demonstrado o potencial da utilização de ligandos de afinidade sintéticos com o desenvolvimento de um adsorvente cromatográfico de afinidade para captura de albumina soro humano. Em segundo lugar, foi demonstrado o potencial de partículas magnéticas funcionalizados com um ligando de afinidade para capturar lisozima de clara de ovo e anticorpos de uma mistura proteica complexa, como plasma de soro humano. Como primeiro passo para investigar o potencial de combinar partículas magnéticas de afinidade em outros processos TEC, estudamos a influência destas partículas no crescimento de cristais de proteínas, como agentes de nucleação. Como prova de conceito, partículas magnéticas funcionalizadas e não funcionalizadas foram utilizadas como aditivos na cristalização proteínas. O design racional da funcionalização das partículas magnéticas foi conseguido, tendo as partículas funcionalizadas moléculas com afinidade para as proteínas alvo – lisozima de clara do ovo de galinha, tripsina bovina e proteína fluorescente verde de *Aequorea victoria*. A presença de partículas magnéticas funcionalizadas não afetou a cristalização das proteínas nem a prejudicou a resolução de difração do cristal. O novo método de cristalização magnética pode permitir a possibilidade de superar algumas dificuldades de cristalização de proteínas, mas também tem o potencial de ser integrado em métodos de purificação de proteínas que envolvam etapas de cristalização / precipitação.

Finalmente, a cristalização e separação magnética foram dois métodos explorados em sinergia para purificação de anticorpos. Uma triagem das condições de precipitação na presença de partículas magnéticas funcionalizados com um ligante de afinidade para anticorpos foi testada contra o plasma humano e o sobrenadante de células de mamífero. A precipitação magnética acionada por afinidade permitiu o fracionamento do extrato bruto e a recuperação de anticorpos na fração de eluição com alto grau de pureza e rendimento, até 99% e 97%, respetivamente.

Neste trabalho, o desenvolvimento de um novo método - precipitação magnética tem potenciais implicações não apenas como um processo de purificação integrado, mas também como uma ferramenta para determinação da estrutura tridimensional de proteínas por cristalografia de raios-X.

Table of Contents

Figure index

Table index

Abbreviations

Å	Ångstrom
Ab	Antibody
ABC	Anything But Chromatography
APTES	(3-aminopropyl)triethoxysilane
BCA	Bicinchoninic acid
BSA	Bovine serum albumin
CHO	Chinese ovary cell line
Da	Dalton
DF	Diafiltration
DLS	Dynamic light scattering
DSP	Downstream processing
DTT	Dithiothreitol
EDTA	Ethylenediaminetetraacetic acid
EPO	Erythropoietin
FcRn	Neonatal Fc receptor
FT-IR	Fourier Transform Infrared
GFP	Green fluorescent protein
HER2	Human epidermal growth factor receptor 2
HEWL	Hen egg white lysozyme
hIgG	Human Immunoglobulin G
HSA	Human serum albumin
HTP	High-throughput
Ka	Affinity constant
LB medium	Luria Broth medium
mAbs	Monoclonal antibodies
MP(s)	Magnetic particle(s)
nH	Hill factor
OD_{600nm}	Optical density at 600 nm
PAB	*peptostreptococcal* albumin-binding
pAbs	Polyclonal antibodies
PBS	Phosphate saline buffer
PBST	Phosphate saline buffer with Tween20
PDB	Protein data bank
PEG	Polyethylene glycol
Qmáx	Maximum binding capacity

RMSD	Root mean square deviation
RPM	Rotations per minute
SDS-PAGE	Sodium dodecyl sulfate–polyacrylamide gel electrophoresis
sulfo-SMCC	Sulfosuccinimidyl-4-(*N*-maleimidomethyl)cyclohexane-1-carboxylate
TEM	Transmission electron microscopy
TEOS	Tetraethyl orthosilicate
TNF	Tumor necrosis factor
UF	Ultrafiltration
v/v	Volume/volume
w/v	Weight/volume
λex	Fluorescence excitation wavelength
λem	Fluorescence emission wavelength

Background and objectives

The biopharmaceutical market is the sector of the pharmaceutical industry with the higher growth for the past years and it is forecasted to continue its growth for the next five years. In 2018 the pharmaceutical market represented $865 billion, of those $219 billion corresponded to the biopharmaceutical market [1]. By 2017 more than 50% of the top 10 blockbuster pharmaceuticals (more than $1 billion of revenue) corresponded to biopharmaceuticals comprising monoclonal antibodies, vaccines and insulin [2]. Monoclonal antibodies (mAbs) represent the greater revenue source in the biopharma sector, with 68 mAbs available corresponding to $123 billion of the biopharma market [2].

Since the first biopharmaceutical – Humulin, approved in 1982 – several developments have been achieved in the upstream development (*e.g.* cell line and media upgrading) to improve product titer and quality, as well as to increase the production scale [3]. Nonetheless, the downstream processing of the biological pharmaceuticals was not able to keep up with the upstream developments, and it is currently considered to be the bottleneck in biopharmaceuticals production. Currently, the standard methods in downstream process for the purification of biological products are chromatographic techniques, mainly affinity chromatography. However, chromatography techniques represent a drawback in terms of process scalability and is many times associated with high costs [4].

New approaches rely in Anything But Chromatography (ABC) methodologies, which include magnetic separation, membrane processes, liquid-liquid extraction, precipitation and crystallization techniques. ABC techniques aim to overcome some drawbacks of the already implemented chromatographic techniques. Such drawbacks come from the process scalability and inability to cope with high volumes, since the costs associated with chromatographic techniques scale with the upstream volume (*e.g.* protein A affinity resin: 5000-14,000 €/L resin). ABC techniques are generally associated with lower costs (*e.g.* crystallization/precipitation process:15-140 €/L precipitant) [5].

From the ABC technologies, crystallization/precipitation has attracted a significant attention in the development of downstream processes. These techniques are currently being developed for protein purification once they are linked to low operation costs, can cope with the process scales and titers in the upstream and comply with the single-use technologies [6,7]. The use of ABC technologies to purify proteins with therapeutic market value is already implemented in the downstream train of proteins such as insulin (crystallization) [8], human serum albumin [9] or erythropoietin (precipitation) [10]. Crystallization, due to its characteristics, is successfully used as a polishing step, to improve both protein purity and concentration. As for precipitation, it can be used in an initial purification step, to precipitate the target protein or contaminants, or as a final step to further protein purification and concentration.

Currently, crystallization is a challenging technique and research on its application in the purification of other high added value proteins, such as mAbs, has been conducted [11].

Concomitantly, magnetic separation has shown potential to be used as an alternative to the traditional separation techniques [12]. Furthermore, magnetic separation has been successfully integrated in aqueous-two phase systems improving the process performance in terms of protein purity and final yield [13]. Implementing the crystallization or precipitation step in any process requires the high-throughput screening with different combination of precipitants, salts and/or polymers at different conditions (*e.g.* temperature and pH), followed by its scale-up and optimization. For protein purification process development, the great impact and innovation comes from the possibility of adding additives to the precipitant conditions.

This PhD thesis aimed to develop a new crystallization method using magnetic particles. The new method, named as “Magnetic Precipitation”, finds potential applications as a platform to improve crystal quality for X-ray diffraction or as a step in the final protein purification pipeline. The great novelty in this work is the combination of the crystallization concept with magnetic particles, that are coated and functionalized in a tailor-made fashion towards the protein of interest.

Chapter 1

The role of crystallization and precipitation in biopharmaceuticals purification

Publication in peer-review paper

dos Santos, R, Carvalho AL, Roque ACA. Renaissance of protein crystallization and precipitation in biopharmaceuticals purification. Biotechnol. Adv. 35 (2017) 41-50, https://doi.org/10.1016/j.biotechadv.2016.11.0

Authors contributions:

The literature review and manuscript preparation were conducted by RS. ALC and ACAR revised the manuscript.

Abstract

The current chromatographic approaches used in protein purification are not keeping pace with the increasing biopharmaceutical market demand. With the upstream improvements, the bottleneck shifted towards the downstream process. New approaches rely in Anything But Chromatography (ABC) methodologies and revisiting former techniques with a bioprocess perspective. Protein crystallization and precipitation methods are already implemented in the downstream process of diverse therapeutic biological macromolecules, overcoming the current chromatographic bottlenecks. Promising work is being developed in order to implement crystallization and precipitation in the purification pipeline of high value therapeutic molecules. This review focuses in the role of these two methodologies in current industrial purification processes and highlights their potential implementation in the purification pipeline of high value therapeutic molecules, overcoming chromatographic holdups.

1.1. The new trend: anything but chromatography

Recent developments in more efficient fermentation and cell culture technologies led to an improvement in biopharmaceutical product titers from an average of 0.2 g/L in 1985 to 2.56 g/L in 2014, although monoclonal antibodies (mAbs) titers can reach 27 g/L [3]. This improvement in the upstream of biopharmaceuticals production led to a shift in the manufacturing bottleneck towards the downstream processing (DSP), which can weight up to 70% of the total production costs [4]. Currently, DSP face several challenges, namely the need to (i) deal with the high upstream titers and production volumes, (ii) accomplish high purities and yields with a reduced number of unit operations through process integration and intensification and (iii) comply with the trend of single-use technology DSP [6,7].

For biopharmaceutical products with high added value, DSP design aims to achieve high quality, concentration, productivity and yield. DSP trains of biological products usually comprises four main steps: recovery, isolation, capture and polishing [4]. The capture and polishing steps are frequently based on chromatographic operations with high costs associated with resin price (e.g. 5,000-14,000 €/L [5]) and operation costs (e.g. high buffer consumption of 300,000-2,000,000 L/batch). The development of new and more efficient upstream processes, leading to higher protein titers, constrains the chromatographic process of the capturing step [14]. As a result, new approaches to DSP design are being considered, due to the high costs associated. High-throughput (HTP) screenings are used in combination with statistically planned experiments (Design of Experiments, DoE) to recognize the influence of different factors, thus narrowing down the experimental conditions to be tested. In addition, Quality by Design (QbD) can also be

implemented with HTP or DoE [15,16], combining in this way the manufacturing process with product quality, while improving process robustness and productivity.

Considering mAbs DSP, the conserved domains of mAbs led many companies to define a general purification process based on a common sequence of unit operations. The heart of the process is the protein A chromatography capture step usually followed by two polishing steps composed by ion exchange chromatography. Although stable, reliable, and reproducible, protein A chromatography is considered to be a productivity bottleneck, requiring several cycles per batch (e.g.1-8 cycles/batch mAb [5]), and being particularly expensive. In order to overcome the limitations demonstrated by chromatography such as high resin cost, diffusion and capacity limitations, new approaches based on Anything but Chromatography (ABC) methodologies are gaining increasing interest [17,18]. Currently, new trends in non-chromatographic methodologies for DSP include membrane processes [19], liquid – liquid phase extraction [20], magnetic separation [12,21,22], precipitation and crystallization [23]. Non-chromatographic methods aim to reduce or even replace chromatographic operations in the purification pipeline, which tends to be hampered by the already implemented chromatographic methods that can achieve high yields and purity, despite its disadvantages. On the other hand, non-chromatographic methods can cope with the high titers and volume feed produced upstream. Within the pool of non-chromatographic methods available, precipitation is being applied to the purification of some biopharmaceuticals [24–26], and protein crystallization is a new and challenging method that can overcome the current chromatographic challenges [27,28]. Although crystallization and precipitation are currently being used for the purification of commercially available proteins, such as ovalbumin [29], lipase [30], elastase [31], protease I and II [32] and lactose [33] as revised by Miranda et al., 2009, these are still not widely implemented in the industrial biopharmaceutical sector despite their potential [35].

1.2. Understanding protein precipitation and crystallization

Protein precipitation is based on the premises that a homogenous protein solution is only homogeneous up to a certain protein concentration from which a new phase, corresponding to the precipitate formation, starts to appear. By changing the environmental conditions, one expects to exceed the protein solubility limit, leading to the formation of the new solid phase. Protein crystallization is a form of precipitation in which the precipitate is formed in an ordered manner. Protein precipitation is mostly used for low value products. However, due to its advantages in DSP, research has been conducted towards high value products, such as therapeutic proteins in the biopharmaceutical industry.

Protein precipitation depends on the solubility of a protein in an aqueous media, which is deeply related with the distribution of the hydrophobic and hydrophilic amino acid residues at the protein surface [36]. In a time where proteins were considered as colloids, the first protein precipitation experiments were carried by Antoine Fourcroy in circa 1789. By this time, Fourcroy was able to precipitate gelatin by boiling various

animal by-products and albumin from egg white, blood serum and milk casein by heating, acid or alkaline precipitation [37]. The following studies focused on proteins that could be obtained in large quantities, namely from blood and egg white. The first studies using precipitation as a means for protein purification were developed by Edwin Joseph Cohn during World War II (1939 – 1945). He became famous for the separation of blood components by fractional precipitation. The Cohn fractionation process aimed at obtaining albumin to be administered to soldiers with blood loss, starting from blood plasma and taking advantage of the different solubility among the different plasma proteins [38]. This also showed that a protein purified by precipitation had biological activity. Since its discovery, protein precipitation has been used in proteins DSP, for purification and concentration purposes [39,40].

With the development of single-crystal X-ray crystallography, the crystallization of macromolecules became one of the most common methods to determine protein structures and understand fundamental biochemical pathways or even design new drugs. However, by the time the first protein was crystallized, in the first half of the 19th century, crystallization was applied as a purification and biophysical characterization method [41,42]. Nonetheless, the interest in crystallization from a purification point of view increased due to the low costs associated, the ability to cope with high volumes, and with high concentrations of the target molecule. In addition, crystallization in the DSP of biopharmaceuticals has the ability to integrate protein purification, stabilization and concentration in one single step.

Macromolecular crystallization can be performed by four different methods, namely vapor diffusion, microbatch, dialysis and free interface diffusion. In the vapor diffusion the protein sample is set to equilibrate with a reservoir solution that contains similar precipitant and buffer solution at a higher concentration. In batch crystallization, the supersaturated protein sample is mixed with the precipitants in the same mixture and then placed in a mineral oil of branched alkanes in the C20+ range allowing little to none water diffusion, in this way enabling a controlled evaporation. Crystallization by dialysis, makes use of dialysis membranes where ions can pass but not proteins or polymers, in this way slowly supersaturating the protein solution leading to crystal formation [43]. Free interface diffusion relies on carefully placing the precipitant solution on top of the protein solution in a capillary. Due to the narrow diameter of the capillary, the precipitant and protein will slowly inter-diffuse until equilibrium is reached, leading to protein supersaturation [44].

Although a rational approach might be drawn the fact is that both precipitation and crystallization experiments have a rather empirical design, mainly due to the complexity of the occurring phenomena [45]. Currently, there is no comprehensive theory behind the process in order to guide the experimental design. Furthermore, the wide range of macromolecules possible to crystallize enhances the complexity of the crystallization design. The guidelines for macromolecular crystallization involve a systematic search, changing individual parameters that can influence the crystallization process. Once found the set or multiple sets of parameters that yield the best precipitate/crystal outcome, an optimization can be performed to obtain the best possible crystals, which for crystallography purposes correspond to single, edge-shaped crystals.

Nonetheless, some theories have been proposed to understand protein behavior in an aqueous solution. Classical nucleation theory (CNT) aims to calculate the nucleation rate of a particular system, as a

theoretical model this is an approximation [46,47]. The phase diagram plots the protein concentration *versus* any adjustable parameter (e.g. temperature, precipitant concentration, salt concentration) (Figure 1.1A). These diagrams enlighten the kind of interactions occurring between proteins in a qualitative manner, but also in a quantitative way it is possible to recover the enthalpy and entropy values for the protein in the aqueous solution [48,49].

When designing a crystallization assay it is necessary to know (as well as possible) the target protein nature and the interactions which most probably enable crystal formation [11]. Protein nature, i.e. structure and amino acid composition, have a great influence in the outcome, e.g. intrinsically disordered proteins tend to have more polar or highly charged groups than hydrophobic residues. In addition, a biochemical characterization of the target protein also helps designing a target precipitation protocol [50]. Moreover, the protein purity and the purification process may also present some challenges if the main goal is X-ray diffraction for structure determination [50].

The variables that have to be considered when designing a crystallization strategy can be divided into physical, chemical and biochemical, and range from the precipitant to the environmental vibrations [51]. In general, protein concentration, temperature or temperature variation, precipitant concentration, the presence/absence of ligands and the salt/buffer used play a greater role than gravity, viscosity or electric/magnetic field.

Ion-ion, ion-dipole, dipole-dipole, salt-bridge, hydrogen bonding, and hydrophobic interactions contribute all together to protein stability [36]. Dipolar substances, as water, will compete with dipolar interactions; ions may disrupt ionic interactions, hydrophobic substances will seek for the hydrophobic core. The sum of all medium modifications, when maintained constant, will lead to a protein rearrangement into a stable conformation. Variations of temperature, pH, salt concentration, presence of organic solvents and polymers can trigger precipitation processes. For example, a rise in temperature favors the formation of hydrophobic interactions at the same time as it weakens dipolar interactions; a decrease in temperature leads to the opposite effect. Meanwhile when a protein surface does not have net charge - at its isoelectric point – it presents the least surface hydration, with the minimum solubility while in the nondenatured form. It should be noted that minimum solubility is not synonymous of insolubility/precipitation, as precipitation requires additional perturbations. The addition of salt also plays an important role in protein precipitation/crystallization. Along the years, protein precipitation/crystallization appear to follow the Hofmeister series [52]. This series ranks the ions according to their relative effect on protein solubility and structure stability in an aqueous system [53]. In general, the effect of anions is more pronounced than that of cations. The Hofmeister anion series is as follows [53,54]:

$$CO_3^{2-} > SO_4^{2-} > S_2O_3^{2-} > H_2PO_4^{-} > F^{-} > Cl^{-} > Br^{-} \sim NO_3^{-} > I^{-} > ClO_4^{-} > SCN^{-}$$

To the left of Cl^{-}, are located the kosmotropic anions, on the other side to the right are the chaotropic anions [52,53]. Kosmotrope species are referred to as ‘water structure makers’ for strengthening bulk water hydrogen bonding network, these species also stabilize and have a salting-out effect on proteins. On the other hand, chaotropic species are cited as ‘water structure breakers’ by weakening the bulk water hydrogen bonding network, unlike kosmotropes, chaotropes destabilize and tend to unfold proteins leading to a

salting-in effect [52–54]. The concentration of salt used will vary according to the protein under study and its surface net charge, size and shape. Organic solvents such as methanol, butanol, ethanol and acetone, are commonly used in precipitation studies, all containing both hydrophilic and polar domains. While the polar groups compete with water to interact with the protein polar groups, the hydrophobic domains disrupt intramolecular interactions, resulting in a solubility decrease triggering protein precipitation. Once again, the concentration of the organic solvent will vary according to the protein under study, as for salt precipitation. Nonetheless, the use of organic solvents for protein precipitation might lead to protein denaturation; in alternative, different polymers can be used. Polymers are frequently used in protein precipitation, the most commonly used being polyethylene glycol (PEG), usually 20% (w/v) of PEG with molecular weights greater than 4000 Da due to the higher efficacy. In solution, PEG not only attracts water molecules from the protein surface [55], but also has an effect in sterically exclude proteins from its hydrodynamic volume [56,57], enhancing protein-protein interactions leading to protein precipitation. Although limited by the availability and stability of the target protein, different combination of precipitants can be used in an initial screening [58,59]. Nowadays, different screenings have been developed and are commercially available (e.g. JBScreen Wizard from Jena Bioscience) and some can be developed in-house, usually by macromolecular crystallography research labs.

In biologics DSP, precipitation is presented as an alternative to the current chromatographic methods. Precipitation protocols have a low cost associated, and can be performed with high protein titers and volume. Moreover, precipitation is a scalable technique proportional to the process volume, regardless of its titer, as opposed to the current chromatographic methods that scale stoichiometrically with the reaction between molecules in solution, i.e. titer dependent [60]. Currently, precipitation can be performed in batch, tubular and continuous stirred tank reactors, giving flexibility to the pharmaceutical industry regarding the working mode (batch or continuous) [24,61,62].

Precipitation conditions can be rationalized according to the interactions predicted to occur between the target and the precipitant. However, in many cases the theory cannot be translated into practice, making this an intrinsic empirical process due to the great amount of interactions prone to occur. Nonetheless, this makes it possible to selectively target the precipitation of a specific protein. On the other hand, contrary to crystallization, a protein may precipitate and lose its activity, therefore it becomes more critical to evaluate the biological activity of the final product.

Introducing crystallization in an industrial environment, requires a crystallizer tank (Figure 1.1B), that in the pharmaceutical industry tends to work under batch conditions, and a possible pre-conditioning step (e.g. buffer exchange), as previously reported [27,28]. For HTP screening of protein crystallization conditions robotic techniques are used, namely Oryx systems (from Douglas Instruments, Ltd), mosquito systems (from TTP Labtech), Rock Maker systems (from Formulatrix) or Cobra or Phoenix Liquid Handling System (both from Art Robbins Instruments).

Nevertheless, crystallization conditions are established empirically and are not standard for proteins of the same family, which is considered a drawback in industry. Although the same interactions (e.g. hydrophobic, electrostatic) are known to play an important role in protein crystallization by promoting the

correct fold [63] and preserving the protein structure and function [64], the intricacy of all the interactions occurring in the crystallization phenomena is such that the behavior of each protein has to be considered by itself. On the other hand, this singularity can be advantageous when purifying a macromolecule - considering the specificity of the crystallographic conditions for a single protein, it would be beneficial to promote the crystallization of the target protein from the crude extract, leaving contaminants in the supernatant.

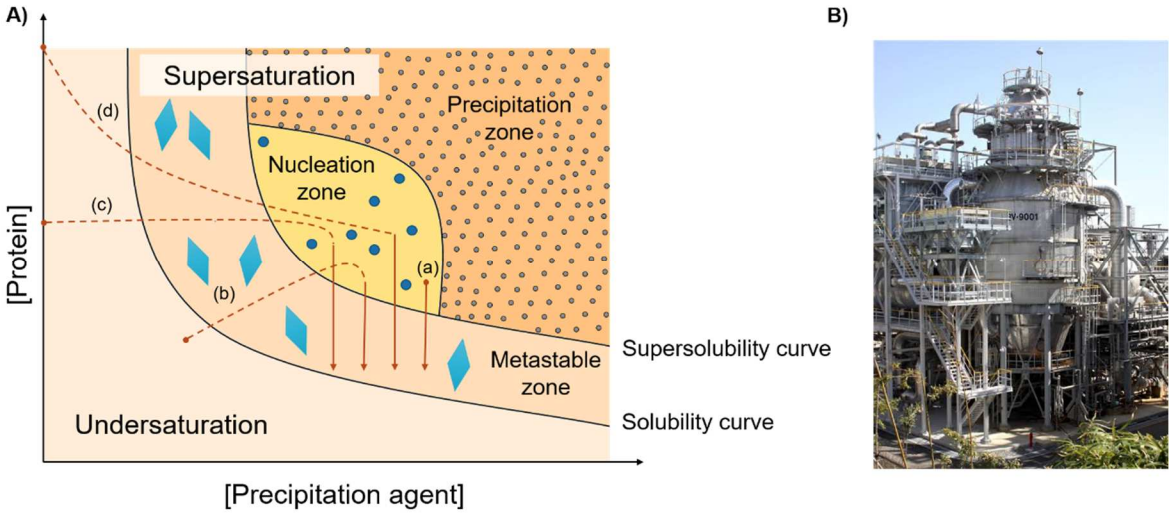

Figure 1.1. (A) Qualitative illustration of a protein crystallization phase diagram. The major paths to reach protein crystallization are represented for the four main crystallization methods: (a) microbatch, (b) vapor diffusion, (c) dialysis and (d) free interface diffusion. The solubility curve is defined as the equilibrium between crystals and protein in the solute at a certain concentration. The supersolubility curve separates the condition from which nucleation or precipitation spontaneously occur. **(B)** Industrial insulin crystallizer from GEA Group Aktiengesellschaft, kindly provided by Doctor Nadine Gerndorf.

1.3. Established purification processes

Crystallization and precipitation are two-unit operation implemented in the purification pipeline of some therapeutic proteins, due to their advantages comparing with traditional DSP unit operations (e.g. chromatography). Crystallization was the first to the employed in insulin purification, while precipitation methods are used for the purification of human serum albumin and erythropoietin.

1.3.1. Insulin

Insulin is a peptide hormone produced and stored in the pancreas by β-cells as an inactive hexamer, active only when in its monomer forms (5.8 kDa) [65]. This hormone is responsible for the uptake of glucose from the blood stream, regulating the carbohydrate and lipid metabolisms, and preventing the liver from producing glucose. Insulin in administered to patients with *diabetes mellitus*, a metabolic condition that leads

to high blood sugar levels from long fasting periods in people affected by this condition. Per year 10 tons of insulin are produced, representing a global market of $5 billion [66].

In the 1920s the source of insulin was animal pancreas, the first patient being injected with bovine insulin. The first 3-dimensional structure of insulin was unveiled in 1969 by X-ray crystallography in Dorothy Hodgkin's laboratory (PDB file: 1INS) [67]. As enlightened by Scott (1934), it is possible to crystallize insulin in conjugation with metal ions as zinc [68]. With that in mind, Petersen (1947) patented insulin purification using citrate buffer with two zinc ions per unit cell (0.34% zinc) [69]. However, only in 1969 the first patent reporting insulin crystallization from an animal source was filed by Eli Lilly, describing what turned out to be the 8.2 process, since the major yield (90-95%) was obtained with the addition of 1 M sodium hydroxide to a 0.5 M acetic acid and insulin solution, at pH 8.2. After 15 min, crystallization occurred spontaneously [70]. Only by 1978, with the development of recombinant DNA technology, Genentech scientists were able to produce human insulin in *Escherichia coli* cells. This lead to Humulin, the first biopharmaceutical molecule produced and commercialized by 1982. Since the first insulin crystallization patent at a liter scale, the industry evolved to 50,000 liter tanks used nowadays, thus demonstrating the feasibility of integrating crystallization in a biopharmaceutical bioprocess. Insulin purification process is represented in Figure 1.2A; among the different unit operation is possible to verify that crystallization plays an important role since it is introduced for three times in the DSP train. Combining this purification method with recombinant DNA technology manufacturers are nowadays able to commercialize the purest insulin formulation, with purity higher than 98% [8].

1.3.2. Human serum albumin

Human serum albumin (HSA) is present in the human plasma as a monomer (66 kDa), being the most abundant protein in the human plasma at a concentration of 30–50 g/L, and has a serum half-life of approximately 20 days [71]. Being the most abundant protein, HSA represents the determining factor in maintaining the osmotic pressure exerted by proteins in a blood vessel's plasma (oncotic pressure). In addition, due to its ligand binding capacity, HSA has not only the ability to transport (e.g. hormones or fatty acids), but also to affect the pharmacokinetics of some drugs increasing the circulation time [72]. HSA is also used as a biomarker for different diseases that include cancer, rheumatoid arthritis, ischemia and severe acute graft-versus-host disease. As therapeutic agent it is used in treating hypovolemia, shock, burns, surgical blood loss, trauma, hemorrhage, acute liver failure, cardiopulmonary bypass, hemodialysis, chronic liver disease, nutrition support, resuscitation, and hypoalbuminemia acute respiratory distress syndrome [72]. Per year 500 tons of HSA are produced, representing a global market of $1.5 billion [66].

In 1940 HSA was first purified by the Cohn fractionation process, for intravenous use as blood substitute. In this five step ethanol fractionation process, HSA was recovered in the final fraction with 40% ethanol at pH 4.8 [38]. Since then, variations of the Cohn process increased yield and purity. Due to the great interest in HSA as a therapeutic agent, many patents regarding its purification have been filed. In 1979, a patent assigned to Plasmesco AG, reported a purification process inspired in the Cohn method

using a heat ethanol/PEG process [9]. In this process a 96% recovery yield and <99% protein purity were achieved using 9% (v/v) ethanol, pH 6.5 at 68ºC. More recently, in 2014 a patent assigned to GE Healthcare Bio-Sciences for plasma proteins fractionation with polyacrylic acid precipitation was issued. In this purification scheme, polyacrylic acid precipitation in used as a capture step, prior to the chromatographic polishing step, as it is represented in Figure 1.2B. In this case HSA did not precipitate; it was maintained in the supernatant, with a recovery yield of 88%. Next, a chromatography step, affinity or ion exchange, was performed [73].

1.3.3. Erythropoietin

Erythropoietin, or EPO, is a highly glycosylated protein, it has a molecular weight of 34 kDa and is responsible for erythropoiesis in the bone marrow. In the blood, EPO has a half-life of 5 hours [74,75]. As a therapeutic agent, it is most commonly used for anemia treatment. EPO is produced by recombinant DNA (rDNA) technology, making different pharmaceutical agents with different glycosylation patterns that have been approved and are commonly named erythropoiesis-stimulating agents (ESA). Due to these modifications, ESA blood half-life may vary from the endogenous EPO, due to an increase in the protein stability [75]. Nowadays EPO represents $11 billion of the biopharmaceutical market [76].

EPO was first purified by Miyake and co-workers in 1977, in a seven-step purification process, that included ethanol precipitation [77]. The overall process consisted of (i) anion exchange chromatography , (ii) phenol treatment, (iii) ethanol precipitation, (iv) anion exchange chromatography, (v) cation exchange chromatography, (vi) gel filtration and (vii) adsorption chromatography, yielding a final recovery of 21% with 95% purity [77]. This study enabled further characterization studies, disclosing EPO amino acid sequence and coding sequence. In 1985, Lin and co-workers were able to isolate the gene encoding for EPO from a genomic phage display library, and produced it in Chinese hamster ovary cells [78]. Later in 1987, Amgen conducted a clinical trial using recombinant human EPO in 25 anemic patients with end-stage renal disease [79]. With the trade name Epogen, it was approved by the FDA in 1989 and by EMA in 2007.

The first patent in EPO purification was assigned to Genetics Institute in 1987, with an initial purification step by ethanol precipitation, followed by different chromatographic methods [10]. By 2001, a patent assigned to Sterrenbeld Biotechnologie North, regards the differential precipitation of contaminant proteins, leaving EPO in the supernatant, with 100% recovery yield, followed by a series of chromatographic methods for further purification [80].

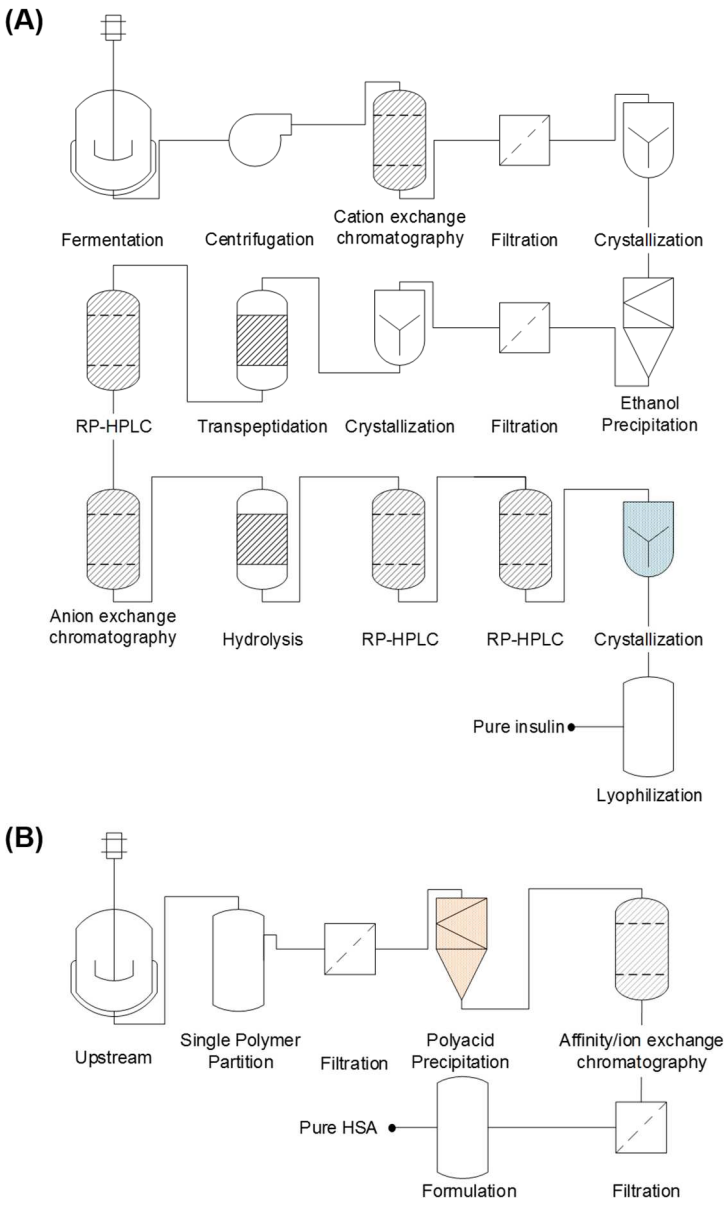

Figure 1.2. Schematic representation of the unit operations implemented in purification processes including crystallization and precipitation. **(A)** Standard insulin purification. **(B)** GE Healthcare Bio-Sciences HSA polyacrylic acid precipitation.

1.4. Purification processes under development

Crystallization and precipitation technologies can overcome some bottlenecks of current DSP unit operations, namely the capability to work with high process volume and protein titers. Several efforts are being made to evaluate their potential in replacing standard purification techniques. Currently, the use of crystallization for Apo2L purification is under development. At the same time, the development of both crystallization and precipitation techniques for mAbs purification is being intensively studied.

1.4.1. Apo2L

Apo2 ligand or tumor necrosis factor (TNF)-related apoptosis-inducing ligand (Apo2L/TRAIL), belongs to the TNF superfamily. The human full length of this transmembrane protein is composed of 281 amino acids and folds as a type II transmembrane protein, being a single-span transmembrane protein with the C-terminal exposed to the extracellular space [81,82]. The recombinant human soluble Apo2L/TRAIL, consisting of the TNF-homologous portion of the extracellular domain of the full length Apo2L/TRAIL protein, is a 168 amino acid polypeptide with 19.6 kDa [83]. Apo2L has a potential apoptotic function, identified in various cancer cell lines, but no apoptotic function was yet associated in non-cancer cells [82,83]. Therefore, Apo2L has the potential to act as a tumor repressor in tumor patients.

The first Apo2L structure was disclosed in 1999 by X-ray crystallography (PDB file: 1D4V, [81]). The small scale crystals were produced using 25% ethylene glycol with 0.1% n-octyl-β-glucoside by vapor diffusion [81]. With great potential to be used as a tumor repressing agent, and with the capability to be crystallized, in 2010 Genentech patented a new purification process for Apo2L. The crystallization was performed after a cation exchange chromatography. The eluted fraction of Apo2L, in low ionic strength solution (100 mM - 200 mM NaCl or Na_2SO_4) was cooled down to 4ºC enabling spontaneous crystallization. The crystallization occurs with or without anti-solvents (PEG, ethanol, isopropanol, dioxane or methyl pentanediol). In both conditions, the protein purity reported is at least 99% with 95% recovery yield [84].

1.4.2. mAbs

Due to their antibody-antigen interaction, mAbs are broadly employed as therapeutic agents, as diagnostic tools for *in vivo* and *in vitro* analysis, as well as in affinity purification processes [85,86]. As therapeutic agents, mAbs are mostly used in oncology and immune disorders, however they are also prescribed for infectious, neovascular, haemostasis and host-to-graft diseases [87]. Although different mAbs present a high degree of homology, the conserved domains of mAbs led many companies to define a general purification process based on a common sequence of unit operations, where the protein A chromatography capture step is central (Figure 1.3A) [88]. Even though stable, reliable, and reproducible, this methodology is considered to be a productivity bottleneck and especially expensive. The bottlenecks associated with protein A chromatography regard low elution pH (2-3) which may lead to ligand leaching and mAb precipitation. Since this is a chromatographic method, it is not able to deal with high process titers (e.g. 10 g/L) or high volumes. In addition the chromatographic process is performed under low flow-rates. On the other hand, this is a stable, reliable, and reproducible method that despite its disadvantages, continues to be preferred over other commercially available options due to the high purification achieved, great versatility and process standardization.

Even though currently mAbs crystallization is not yet a common and implemented procedure, the hope is that this approach can overcome some of the chromatography bottlenecks (Figure 1.3B and C). In order to create a rational approach, several studies try to enlighten mAbs behavior under crystallization conditions. In Table 1.1 a summary of the works reported so far in the literature for mAbs purification through

crystallization and precipitation were assembled. A systematic analysis of data available for mAb crystallization conditions, led to conclude that PEG is a common precipitating agent for crystallization at room temperature) [27,60,64,89,90]. The work of Zang and co-workers [27], first demonstrated the feasibility of having a crystallization step in the downstream process of mAbs at a µl scale. In this study, IgG4 crude extract was purified by protein A chromatography and dialyzed for buffer exchange with 20 mM Tris buffer pH 7.0 before the crystallization step. As precipitant solution, 5% (w/v) PEG 8000, 0.2 M $Ca(OAc)_2$, 0.1 M imidazole at pH 7.0 was used and crystals were obtained after 5 days at room temperature. After mAb IgG4 solubilization, the final solution showed 90% of protein purity and 31.3% recovery yield. Following this study, Smejkal and co-workers in 2013 [28] were able to crystallize an IgG1 in 1 hour using 5 mM histidine/acetate buffer, 10 mM NaCl, Tris-base up to pH 6.8 at 4ºC. Here, a scale-up from µl to L in batch conditions was successfully accomplished, with a final protein purity of 96.9% and 90% recovery yield.

Albeit precipitation is not a conventional purification step in mAbs DSP, precipitation methods are regarded as alternatives. Recent studies show the feasibility of using precipitation as a mAb purification method, resulting in a highly pure and concentrated active protein [24,61,62,91]. For example, $CaCl_2$/cold ethanol precipitation has attracted attention as it can be performed in a simple equipment as stirred tanks and centrifuges. A study from Jungbauer group, demonstrated the possibility of mAb precipitation from mammalian cell supernatant with 78% recovery yield and >99% protein purity [61]. A more recent study, improved $CaCl_2$/cold ethanol precipitation in a continuous tubular reactor achieving 92% recovery yield [24]. As in crystallization, also PEG-based precipitation systems are frequently tested with mAbs. Application of high-throughput screening to a rapid identification and selection of PEG precipitation conditions using only µl volumes of protein is usually the initial approach in these studies, since it enables a rapid selection from a wide range of different conditions [92]. A comparison between batch and continuous PEG precipitation, demonstrated that both methods lead to >90% recovery yield and >96% protein purity without changes in mAbs secondary structure [62]. Combination of $CaCl_2$/PEG precipitation for direct mAb purification from the cell culture supernatant can also be used. The $CaCl_2$ precipitation promotes the high molecular weight contaminates to precipitate, while PEG precipitation was used for mAb capture [24]. This method allowed 80-96% recovery yield. Additionally, the use of linear or branched PEG in mAb precipitation was evaluated, showing the feasibility of using both for purification purposes with recovery yield greater than 95% [93].

Other concept in purification is affinity precipitation. In this system a protein or peptide with affinity towards the mAb is placed in the cell culture supernatant and the precipitation of the complex is promoted [40,94–96]. In addition, other precipitants had been used in combination with chromatographic methods, as polishing steps for impurity removal from the elution fraction of protein A chromatography [97].

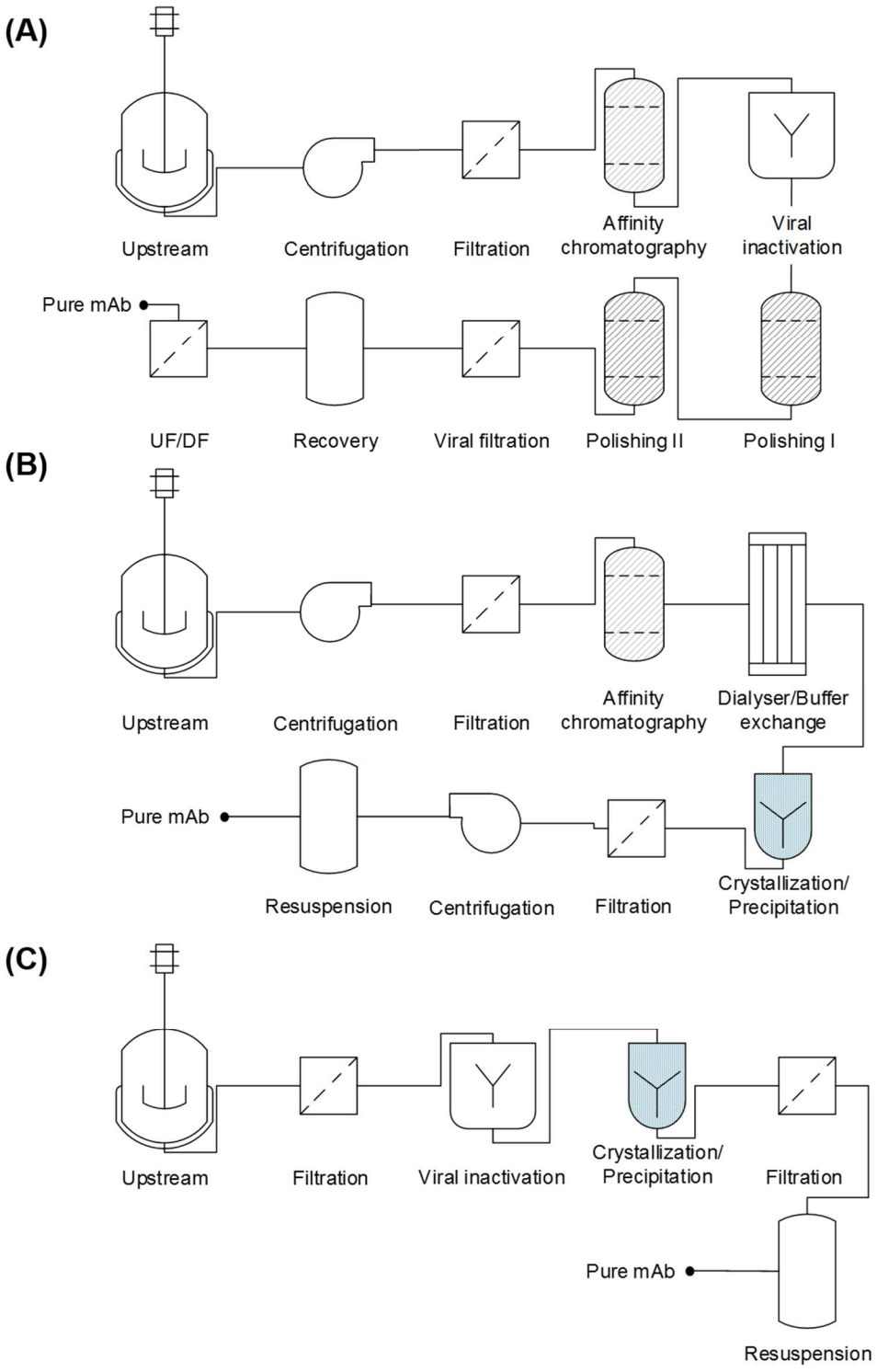

Figure 1.3. Schematic representation of different purification processes for mAbs using chromatographic supports or crystallization/precipitation techniques. **(A)** Standard mAbs purification by chromatographic methods. **(B)** mAbs purification using crystallization/precipitation techniques [27,28]. **(C)** Aimed purification process for mAbs relying on crystallization/precipitation technique.

Table 1.1. Summarized review of purification processes under development using crystallization or precipitation as unit operations in mAbs DSP. The mAb class and source where it was produced and any pre-treatment used prior to the crystallization or precipitation is discriminated. The protein purity and purification yield are described according to the crystallization or precipitation condition used for purification. ND: Not determined.

MAb class	Source	Purity[1]	Yield[2]	Crystallization/precipitation conditions	Ref.
IgG 4	CHO cell supernatant, dialyzed	90%	31%	5%(w/v) PEG 8000, 0.2M $Ca(OAc)_2$, 0.1M Imidazole, pH 7.0	[27]
IgG 1	CHO cell supernatant, dialyzed	93%	88%	5 mM histidine/acetate buffer, 10mM NaCl, pH 6.8	[28]
		97%	90%		
IgG 1	CHO cell supernatant, protein A purified	90%	96%	250 mM $CaCl_2$, PEG 20000-PEG 2000	[25]
IgG 1	CHO cell supernatant, partially purified	ND	>93%	50 mM citrate buffer, pH 6.0 with 15% (w/w) PEG 4000	[60]
IgG 1	CHO cell supernatant, protein A purified	ND	92%	250 mM $CaCl_2$, 25%(v/v) Ethanol	[62]
IgG 1	CHO cell supernatant	99%	84%	Caprylic acid precipitation: 1% caprylic acid in 100 mM sodium citrate pH 4.5 PEG precipitation: 14% (w/v) PEG 6000 pH 7.0	[91]
IgG 1		> 95%	69%	Caprylic acid precipitation: 1% caprylic acid in 100 mM sodium citrate pH 4.5 PEG precipitation: 14% (w/v) PEG 6000 pH 7.0 $CaCl_2$ precipitation: 120-150 mM $CaCl_2$, 300 mM Na_2HPO_4, 4 mM PO_4^{3-} pH 8.5 Cold ethanol precipitation: 25% (v/v) ethanol	
		> 95%	59%	$CaCl_2$ precipitation: 120-150 mM $CaCl_2$, 300 mM Na_2HPO_4, 4 mM PO_4^{3-} pH 8.5 Cold ethanol precipitation: 25% (v/v) ethanol $CaCl_2$ precipitation: 120-150 mM $CaCl_2$, 300 mM Na_2HPO_4, 4 mM PO_4^{3-} pH 8.5 Cold ethanol precipitation: 25% (v/v) ethanol	
IgG 1	CHO cell supernatant, protein A purified	70-90%	> 95%	9-10% (w/v) Branched PEG 600 or Linear PEG 4000/PEG 6000	[93]

[1] Ratio between the target protein concentration and protein concentration.
[2] Percentage of purified protein in terms of initial amount of protein.

1.5. Concluding remarks and future trends

The biopharmaceutical sector has the highest estimated growth rate for the next five years. Given this scenario, the biopharmaceutical industry will be faced with a higher production demand in the near future. Developments in the USP have already been successfully accomplished, shifting the bottleneck towards DSP. Although progresses in better performance of cell culture and growth conditions should continue to occur, DSP must explore alternative methods. Crystallization and precipitation have the great advantage of scaling-up with the process volume, instead of the process titers as in chromatography processes. In Table 1.2 a comparison between protein A chromatography and crystallization/precipitation in terms of scaling-up and purification criteria were gathered.

The implementation of protein crystallization or precipitation in purification processes will include, the high-throughput screening of different precipitants, polymers and salts, at different conditions (e.g. pH and temperature), followed by a scaling-up of the optimized methods. The great innovation in this field of purification may arise from the integration of different and new additives enhancing the crystallization efficiency and decreasing the process time [58,59] or the integration of affinity molecules to target the biopharmaceutical and promote its selective precipitation [94,95].

Crystallization and precipitation are two-unit operations already implemented in the downstream pipeline of therapeutic proteins. Indeed, crystallization is successfully used as a final polishing step, enabling at the same time greater protein purity and concentration [70]. On the other hand, precipitation can be performed as an initial capture step, either precipitating the target protein or contaminants, or as a final purification and concentration step [73,80].

In order to be considered as alternatives to the current and well implemented chromatographic steps in therapeutic protein purification, a method has to be able to handle high volume and protein titer, be scalable, and economically viable at an industrial scale. In this regard, both techniques are able to cope with the biopharmaceutical industry demands.

Table 1.2. Comparison between protein A chromatography and crystallization/precipitation unit operation in mAbs DSP regarding scaling-up and purification criteria.

	Protein A chromatography	**Crystallization/Precipitation**
Capacity	40-60 g IgG/L resin	Up to 150 g IgG/L precipitant
Scale-up	Process volume	Stoichiometrically
Cost	5,000-14,000 €/L resin	15-140 €/L precipitant
Yield	>95%	>90%
Purity	>95%	>95%
Industrial equipment	Chromatographic column	Stirred tank

Chapter 2

Designed affinity ligands to capture human serum albumin

Publication in peer-review paper

dos Santos, R, Figueiredo, C, Viecinski, AC, Pina, AS, Barbosa, AJM, Roque ACA. Designed affinity ligands to capture human serum albumin. J. Chromatogr. A. 1583 (2019) 88-97, https://doi.org/10.1016/j.chroma.2018.11.021

Authors contributions:

ACAR designed the work. The experiments were conducted by CF, ACV, ASP, RS and AJMB. RS, ASP, AJMB and ACAR prepared and revised the manuscript.

Abstract

Human serum albumin (HSA) in an important therapeutic agent and disease biomarker, with an increasing market demand. By proteins and drugs that bind to HSA as inspiration, a combinatorial library of 64 triazine-based ligands was rationally designed and screened for HSA binding at physiological conditions. Two triazine-based lead ligands (A3A2 and A6A5), presenting more than 50% HSA bound and high enrichment factors, were selected for further studies. Binding and elution conditions for HSA purification from human plasma were optimized for both ligands. The A6A5 adsorbent yielded a purified HSA sample with 98% purity at 100% recovery yield under mild binding and elution conditions.

2.1. Introduction

Human serum albumin (HSA) is the most abundant protein in the human plasma (30–50 g/l), with a serum half-life of approximately 20 days [71]. HSA plays a role in maintaining the osmotic pressure exerted by plasma proteins in a blood vessel, and in acting as carrier of several compounds, namely hormones or fatty acids. It also behaves as a drug carrier influencing drug pharmacokinetics by increasing the circulation time [72]. As a therapeutic agent, HSA is used to treat several conditions such as hypovolemia, shock, surgical blood loss and trauma. HSA can also be used as a disease biomarker for cancer or severe acute graft-versus-host disease [72]. HSA has an enormous biopharmaceutical potential, and it can be found alone [98], fused or in complex with other relevant proteins [99,100]. HSA market is about 15% of the global plasma protein market, which reaches over 20$ Billion [101].

Currently, HSA purification requires multiple unit operation steps, which may include precipitation [73], heat-shock fractionation [102], and chromatography (*e.g.* ion-exchange chromatography and hydrophobic interaction chromatography) [103,104]. The first reported HSA purification scheme was the Cohn fractionation process in 1940, to produce a blood substitute for patients with blood loss [38]. Nonetheless, affinity chromatography is still a method of choice for protein purification. There are several commercially available affinity-based resins for HSA capture. The first available resin for HSA purification was the Cibacron Blue F3G-A, an adsorbent based on a sulfonated triazine dye [105], which yields heterogeneous samples with low purity [106,107]. The use of triazine scaffold, an analogue of the blue dye, attracted attention in the late 80´s. It provides an effective strategy to develop novel adsorbents for specific targets as they are inexpensive, stable and customized [108,109]. In fact, different triazine based synthetic ligands have been so far developed for different targets including immunoglobulins [22,110], insulin [111], and viral particles [112].

In this work, a rationally designed solid-phase combinatorial library based on triazine scaffold was *de novo* designed and assessed for the discovery of new affinity adsorbents towards HSA capture and purification.

2.2. Materials and methods

2.2.1. Chemicals

All used chemicals were at least 98% pure and solvents were pro-analysis grade. The chromatographic materials, cross-linked agarose (Sepharose™ CL-6B) acquired from GE Healthcare (Uppsala, Sweden), Captiva 96-well filtration block and empty columns (0.8 cm x 6.5 cm) from Agilent Technologies (California, USA), 96-well UV-star® half area microplates from Greiner (Kremsmünster, Austria) and 96-well transparent microplates flat-bottom from Sarstedt (Nümbrecht, Germany).

2.2.2. Synthesis of the combinatorial libraries

For the synthesis of the triazine combinatorial library, Sepharose™ CL-6B was epoxyactivated and aminated as described in [113], yielding 20 µmol of epoxy/g of moist agarose. The amine content was quantified by the Kaiser test yielding 10 µmol of NH_2/g of moist agarose [22]. The combinatorial library comprised a total of 64 ligands, each ligand was obtained by nucleophilic substitution of triazine chlorine atoms by different amines [109,114]. Every ligand consisted of a different combination of the amines as presented in Table 2.1.

2.2.3. Combinatorial library screening with HSA

The screening of the combinatorial library started with the regeneration and equilibration of the resins in 96-well filtration blocks (250 mg of resin/well). Resins were regenerated with 250 µl of regeneration buffer (0.1 M NaOH in 30% (v/v) isopropanol) followed by 3 x 750 µl of distillated water per well. The equilibration step was conducted by adding 15 x 750 µl of equilibration buffer (10 mM sodium phosphate, 150 mM sodium chloride (PBS), pH 7.4) per well, until the absorbance measured at 280 nm was lower than 0.005. Once equilibrated, 250 µl of pure 0.25 mg/ml HSA (Sigma-Aldrich) solution in PBS at pH 7.4 or pH 6.0, was loaded into each well of the blocks, and incubated for 1 hour at 25 ºC with orbital shaking (200 RPM). The functionalized resins were then washed with the corresponding buffer, PBS at pH 7.4 or at pH 6.0 (8 x 250 µl). Total protein quantification was performed using QuantiPro™ BCA assay kit (Sigma-Aldrich) and the HSA binding percentage to each adsorbent calculated according to Equation 2.1:

$$\%\ \text{Binding (w/w)} = \frac{\mu g\ \text{HSA bound}}{\mu g\ \text{HSA loaded}} \times 100 \qquad \text{Equation 2.1}$$

The same procedure was repeated for the re-screening of the most promising ligands. The best ligands were re-synthesized and tested for binding to human IgG (hIgG) (product name: Gammanorm®, Octapharma) and HSA, both loaded at 0.25 mg/ml in each well and tested in triplicates. For the adsorbents, the enrichment factor was calculated according to Equation 2.2:

$$\text{Enrichment factor} = \frac{\%\ \text{HSA bound}}{\%\ \text{hIgG bound}} \qquad \text{Equation 2.2}$$

Table 2.1. List of amine compounds used in the triazine library for the solid-phase combinatorial library, with the respective chemical name and structure.

Amine	Chemical name	Structure	Amino acid mimicked
A1	Tyramine	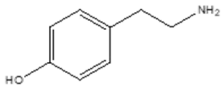	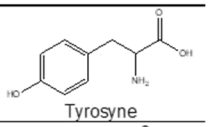 Tyrosyne
A2	Isopentylamine	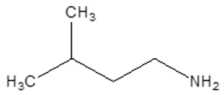	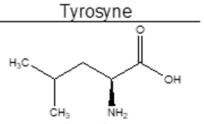 Leucine
A3	3,4-Dimethylaniline	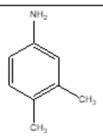	
A4	1,4-Diaminobutane	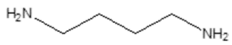	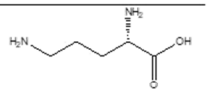 Lysine
A5	Phenethylamine	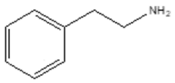	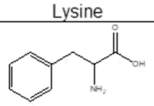 Phenylalanine
A6	Sulfisoxazole	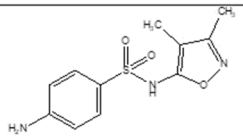	
A7	Amino-2-propanol	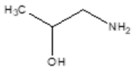	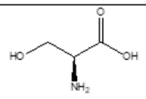 Serine
A8	2-Aminopentane	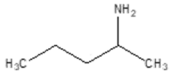	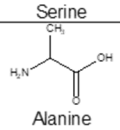 Alanine

2.2.4. On-column binding studies with triazine lead ligands

Two triazine lead ligands, A3A2 and A6A5, were re-synthesized and 0.5 g of moist functionalized agarose (1 ml of 50% (w/v) slurry) was packed into a 3 ml column (0.8 cm x 6.5 cm). The resins were regenerated, washed and equilibrated as previously described (see 2.2.3). The equilibration step was performed with different binding buffers (Table 2.2): (B1) 10 mM sodium phosphate, 150 mM sodium chloride, pH 7.4 at 20-25 ºC, (B2) 10 mM sodium phosphate, 150 mM sodium chloride, pH 7.4 at 0-4 ºC, (B3) 10 mM Tris-HCl, 150 mM sodium chloride, pH 8.0, (B4) 50 mM citrate buffer, pH 5.0, (B5) 10 mM Tris-HCl, 300 mM sodium chloride, pH 8.0 or (B6) 50 mM citrate buffer, 300 mM sodium chloride, pH 5.0. A 0.5 ml sample of protein solution (0.5 mg/ml HSA or hIgG) in the respective binding buffer was loaded into the columns. The flow-through and washes with the corresponding binding buffer (5 x 500 µl) were collected in 1.5 ml centrifuge tubes under gravitational flow. After screening the resins were washed, regenerated and

stored as previously described (see 2.2.3). Total protein quantification of all samples was performed using bicinchoninic acid (BCA) assay reagent (Sigma-Aldrich).

Table 2.2. Selected binding buffers for the optimization of HSA binding towards the triazine-based ligands A3A2 and A6A5.

Binding buffer	Buffer composition
B1	10 mM Sodium phosphate, 150 mM sodium chloride, pH 7.4, 20-25 ºC
B2	10 mM Sodium phosphate, 150 mM sodium chloride, pH 7.4, 0-4 ºC
B3	10 mM Tris-HCl, 150 mM sodium chloride, pH 8.0
B4	50 mM Citrate buffer, pH 5.0
B5	10 mM Tris-HCl, 300 mM sodium chloride, pH 8.0
B6	50 mM Citrate buffer, 300 mM sodium chloride, pH 5.0

2.2.5. Elution screening with two triazine lead ligands

The two lead ligands from the triazine-based library (A3A2 and A6A5) were re-synthesized, regenerated, equilibrated and a 0.25 mg/ml HSA or hIgG solution in PBS at pH 7.4 was loaded in a 96-well filtration block (n=3), as previously described (see 2.2.4). The elution buffers tested were (Table 2.3): (E1) 100 mM glycine-HCl, pH 3.0, (E2) 25 mM sodium phosphate, 150 mM sodium chloride, 30 mM sodium caprylate, pH 6.0, (E3) 10 mM sodium phosphate, 1 M sodium chloride, pH 7.4, (E4) 50 mM sodium phosphate, 1.5 M potassium chloride, pH 6.0, (E5) 100 mM glycine-NaOH, pH 10.0, (E6) 150 mM ammonium acetate, 10 mM sodium caprylate, pH 6.0, (E7) 10 mM sodium phosphate, 150 mM sodium chloride at pH 7.4 in 50% (v/v) ethylene glycol, (E8) 10 mM sodium phosphate, 2 M magnesium chloride, pH 7.4, (E9) 25 mM sodium phosphate, pH 6.0 and (E10) 25 mM sodium phosphate, 30 mM sodium caprylate, pH 6.0. After screening, the resins were washed, regenerated and stored as previously described (see 2.2.3). Total protein quantification of all samples was performed using QuantiPro™ BCA assay kit (Sigma-Aldrich). The binding percentage was calculated according to Equation 2.1. For the elution buffers that interfered with the quantification assay (E7 and E8), a previous dialyses step was performed for buffer exchange with PBS.

2.2.6. On-column purification of HSA from human plasma with A3A2 and A6A5 ligands

Adsorbents A3A2 and A6A5 were re-synthesized and 0.5 g of moist functionalized agarose (1 ml of 50% (w/v) slurry) was packed into a 3 ml column (0.8 cm x 6.5 cm) (n=3). The resins were regenerated, washed and equilibrated as previously described (see 2.2.3). A 0.5 ml sample of human plasma (Sigma-Aldrich) with a total protein concentration of 0.7 mg/ml was loaded into the columns. The flow-through, washes with the optimized binding buffer (5 x 500 µl) and elution with the optimized elution buffer (5 x 500 µl) were collected in 1.5 ml centrifuge tubes under gravitational flow. For ligand A3A2, the optimized binding buffer was 10 mM sodium phosphate, 150 mM sodium chloride at pH 7.4 at 20-25 ºC and the optimal elution buffer

10 mM sodium phosphate, 150 mM sodium chloride at pH 7.4 in 50% (v/v) ethylene glycol. For ligand A6A5 the best binding buffer was 50 mM citrate buffer, 300 mM sodium chloride at pH 5.0 and as elution buffer 25 mM sodium phosphate, 30 mM sodium caprylate at pH 6.0. The resins were then washed, regenerated and stored as previously described (see 2.2.3). The adsorbent A6A5 was re-synthesized and 1.5 g of moist functionalized agarose (3 ml of 50% (w/v) slurry) was packed into a 3 ml column (0.8 cm x 6.5 cm) (n=6). The resins were regenerated, washed and equilibrated as previously described (see 2.2.3). Samples of human plasma (0.25 ml; Sigma-Aldrich), with total protein concentrations of 5 mg/ml and 14 mg/ml, were loaded into the columns. The flow-through, washes (5 x 1.5 ml) and elution (5 x 1.5 ml) with the buffers described above, were collected in 2 ml centrifuge tubes under gravitational flow. Assays with human plasma were performed in triplicates (n=3). The determination of total protein concentration was performed using bicinchoninic acid (BCA) assay reagent (Sigma-Aldrich). Sodium dodecyl sulfate–polyacrylamide gel electrophoresis (SDS–PAGE) was performed to evaluate the samples purity. Samples were applied in a 12.5% acrylamide gel and ran at 90 mV. Images were acquired with Gel Doc™ XR+ System with Image Lab™ software from Bio-Rad and analyzed with ImageJ software.

Table 2.3. Selected elution buffers for the optimization of HSA elution from the triazine-based ligands A3A2 and A6A5.

Elution buffer	Buffer composition
E1	100 mM Glycine-HCl, pH 3.0
E2	25 mM Sodium phosphate, 150 mM sodium chloride, 30 mM sodium caprylate, pH 6.0
E3	10 mM Sodium phosphate, 1 M sodium chloride, pH 7.4
E4	50 mM Sodium phosphate, 1.5 M potassium chloride, pH 6.0
E5	100 mM Glycine-NaOH, pH 10.0
E6	150 mM Ammonium acetate, 10 mM sodium caprylate, pH 6.0
E7	10 mM Sodium phosphate, 150 mM sodium chloride, pH 7.4 in 50% (v/v) ethylene glycol
E8	10 mM Sodium phosphate, 2 M magnesium chloride, pH 7.4
E9	25 mM Sodium phosphate, pH 6.0
E10	25 mM Sodium phosphate, 30 mM sodium caprylate, pH 6.0

2.2.7. Molecular Docking

The crystal structure of HSA in complex with warfarin (PDB ID: 2BXD) [115] was selected for molecular docking calculations using AutoDock 4.0 [116]. The ligands A6A5 and sulfisoxazole were designed using ChemDraw® Professional 16.0.1.4, and submitted to the ProDrg server [117] for AutoDock format parametrization. Being synthesized in solid-phase, the A6A5 was truncated with a methyl group in the triazine amine used to experimentally bind the ligand to the solid support. After visual inspection and validation of ligands' structures and parameters, they were submitted to a docking protocol using Autodock's

Lamarckian Genetic Algorithm with a population of 150 individuals, during 100 runs for 27000 generations, and 25 million energy evaluations. Docking results were analyzed with AutodockTools [116].

2.3. Results and discussion

2.3.1. Design, synthesis and screening of combinatorial libraries of ligands

Human serum albumin (HSA) has a globular heart-shape form with three structurally homologous domains (I, II and III), each one divided into two sub-domains (A and B). Domains IIA and IIIA are also known as Drug site I and II, respectively, since exogenous molecules usually bind in one of these sites [118,119]. Drug molecules such as 3,5-diiodosalicylic acid, indomethacin [115], sulfisoxazole [120] and aspirin [72] are known to interact with the HSA domain II, whereas ibuprofen, diazepam and propofol interact with HSA domain III [115].

HSA protein binders including protein H from *Streptococcus pyogenes* [121], protein G from *Streptococcal* group C or G [122], protein MAG (binding α2-macroglobulin, albumin and IgG) from *Streptococcus dysgalactiae* [123], protein ZAG (binding α2-macroglobulin, albumin and IgG) from *Streptococcus zooepidemicus* [124], and protein PAB (*peptostreptococcal* albumin-binding) from *Peptostreptococcus magnus* naturally bind to domain II [125]. Protein PAB is known to bind HSA domain II though PAB residues Phe27, Leu44, Lys36, Ser25, Tyr28 and Ala31,35 [125]. Neonatal Fc receptor (FcRn), is also a natural HSA binder responsible for IgG and HSA regulation in mammalians. This receptor is known to bind to domains I and III of HSA in a pH-dependent mode (binding occurs at pH 6.0 and dissociation is observed at pH 7.4) [126–128]. Evidence showed that conjugation of HSA or IgG to other proteins or peptides with poor bioavailability or exhibiting rapid clearance, can increase their pharmacokinetics due to the FcRn mediated recycling and transport [129].

A combinatorial library of synthetic ligands based on triazine scaffold was rationally designed focusing on the mode of interaction between domain II of HSA and its natural binders, leaving HSA domains I and III free for possible interaction with FcRn. As a consequence, eight different amines were selected to incorporate into the triazine scaffold. Here, one chlorine is reacted with the aminated solid-phase and the remaining two chlorines are replaced by amine compounds in a step-wise temperature dependent process, generating bi-substituted ligands. A library of 64 adsorbents was prepared by a mix-and-split combinatorial chemistry approach in 96-well filtration blocks. The screening of the solid-phase library towards HSA binding was performed by micro-scale chromatography at two distinct pH values, pH 6.0 and 7.4. The idea behind these pH values was to ensure the binding of the chosen ligands mimicking HSA domain II natural binders at pH 7.4, and concomitantly mimicking the pH-dependent interaction of FcRn with HSA evaluating the ligands binding stability at pH 6.0. As such, a synthetic triazine library, able to capture HSA from a complex media and to potentially work as a spacer between HSA and a drug to increase its pharmacokinetics properties, was rationally designed. Ligands AxAy and AyAx displayed nearly identical screening results for

the binding to HSA (in 64 ligands only 3 pairs AxAy/AyAx presented a difference higher than 15%; Figure 2.1.). This suggests a controlled synthesis of the adsorbents which yielded a symmetric library.

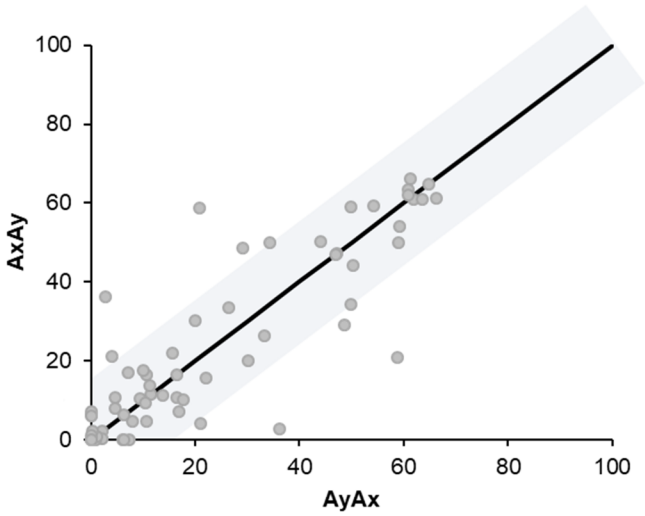

Figure 2.1. Triazine AxAy/AyAx symmetry plot. Experimental data are in ● and difference of 15% between AxAy/AyAx is represented in grey.

The results obtained from the library screening revealed 23 triazine-based ligands with more than 50% of HSA bound at both pH values (**Figure 2.2.** Screening of the combinatorial triazine-based library towards HSA binding at (**A**) pH 6.0 and (**B**) 7.4.**Figure 2.2**). These were selected to proceed with further studies.

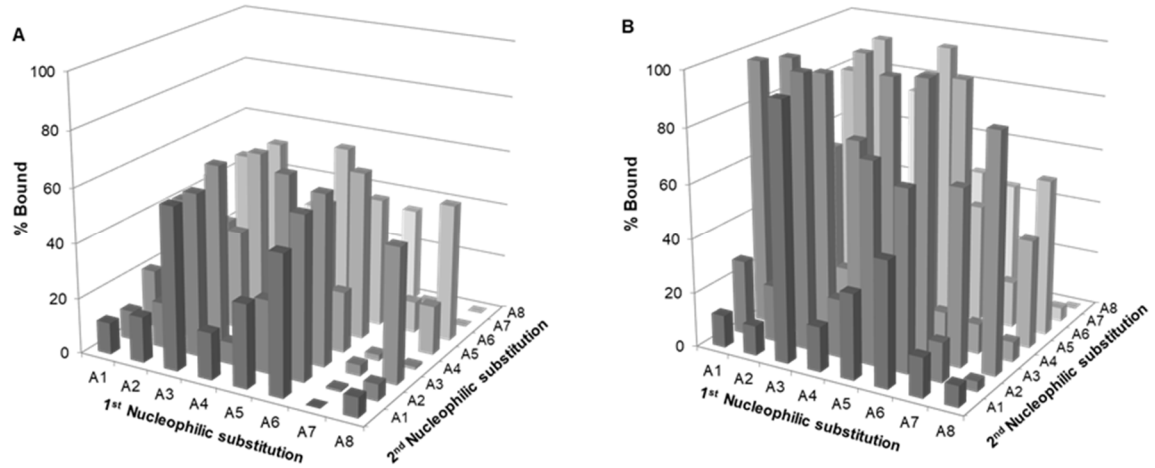

Figure 2.2. Screening of the combinatorial triazine-based library towards HSA binding at (**A**) pH 6.0 and (**B**) 7.4.

The ligands were re-synthetized in 96-well filtration blocks and re-screened for HSA. At this stage, the binding of these ligands towards human IgG (hIgG) at pH 7.4 (Figure 2.3) was also assessed as hIgG is the

second most abundant protein in the human serum. The re-screening results obtained revealed that lead ligands bound with higher percentages to HSA when comparing with hIgG binding.

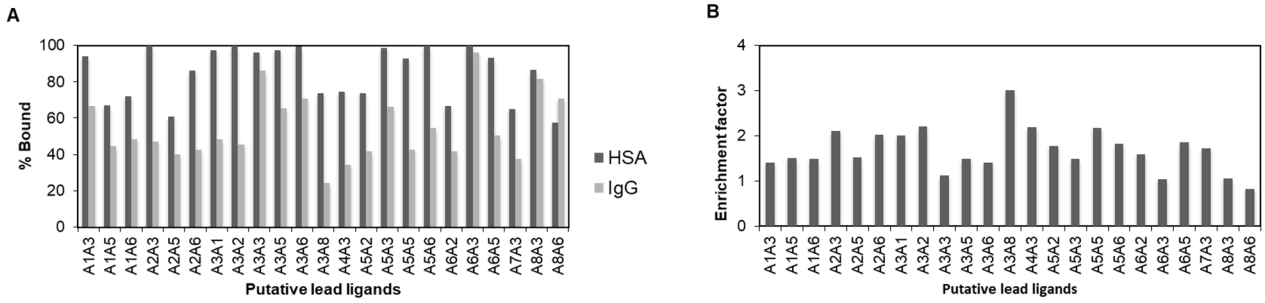

Figure 2.3. Results for the re-screening of the 23 putative lead ligands for binding (**A**) HSA and hIgG, and (**B**) enrichment for HSA during the binding process.

The lead ligands were then selected having as the basis the following criteria of selection: (i) more than 50% of HSA bound and (ii) an enrichment factor higher than 1.7 (Figure 2.4), corresponding to half of the maximum enrichment factor observed. In this way, 8 putative lead ligands for HSA were selected, of those ligands A3A2 and A6A5 were the most promising due to the higher enrichment factor, 3.1 ± 0.4 and 2.2 ± 0.2 respectively (Figure 2.4B).

Ligand A3A2 is composed by 3,4-dimethylaniline as amine R1 and isopentylamine, mimicking leucine amino acid, as amine R2. Ligand A6A5 is composed by sulfisoxazole as amine R1, a typical drug found to bind to HSA, and phenethylamine, mimicking phenylalanine amino acid, as amine R2. Both ligands present aromatic ring in their constitution leading to believe that hydrophobic interaction might play a role in HSA-ligand recognition.

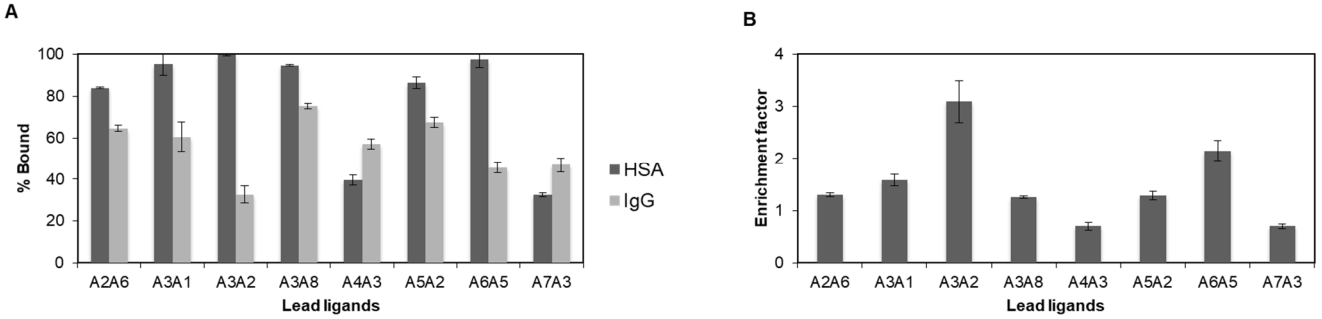

Figure 2.4. Screening of the triazine lead ligands towards HSA and hIgG binding and HSA enrichment, data are presented as means ± SEM (n=3). (**A**) Percentage of bound HSA and hIgG in PBS at pH 7.4 and (**B**) HSA enrichment factor.

2.3.2. Optimization studies with lead ligands

In order to optimize the lead ligands performance as promising adsorbents, the binding and elution conditions were optimized. According to the previous screening assays, the binding conditions used were PBS (10 mM sodium phosphate, 150 mM sodium chloride at pH 7.4) presenting 99% HSA binding to A3A2

and 100% to A6A5. Although these binding percentages seemed to be promising, these ligands also revealed great binding percentage towards hIgG (59% to A3A2 and 61% to A6A5). In this way, the first attempt of optimization was to improve the specificity of these ligands towards HSA.

The first step dealt with the optimization of the binding buffer to selectively bind HSA, using adsorbent comprising ligands A3A2 and A6A5. For the adsorbent A3A2, all binding buffers presented more than 85% HSA bound, and binding buffer B3 promoted unspecific interactions as it bound 100% of both HSA and hIgG (Figure 2.5A). The temperature showed no impact in the binding specificity (B1 (PBS at 20-25 ºC) *vs* B2 (PBS at 0-4 ºC)) and citrate buffer at pH 5.0 (B4) presented lower HSA binding (Figure 2.5A). The results are compatible with the hypotheses that hydrophobic interactions play the major role in HSA binding as the hydrogen phosphate ion has a more kosmotrope effect than citrate, enhancing hydrophobic interactions. By the present study, PBS pH 7.4 at 20-25 ºC was the best binding condition of the HSA-A3A2 ligand pair.

Using the adsorbent A6A5, all the binding buffers tested presented 100% binding to HSA. Temperature showed no impact in the binding specificity (B1 (PBS at 20-25 ºC) *vs* B2 (PBS at 0-4 ºC)) (Figure 4B and S4B). B3 and B4 binding buffers did not provide any selectivity towards HSA (Figure 2.5B). Since hydrophobic interactions may play a role in the binding of both proteins to the ligand, the next approach was to increase the sodium chloride concentration (buffers B5 and B6). The sodium chloride increment decreased hIgG binding by 2-fold when comparing B3 *vs* B5 and B4 *vs* B6. By the results, buffers B5 and B6, presented promising HSA selective binding for the HSA-A6A5 ligand pair (Figure 2.5B).

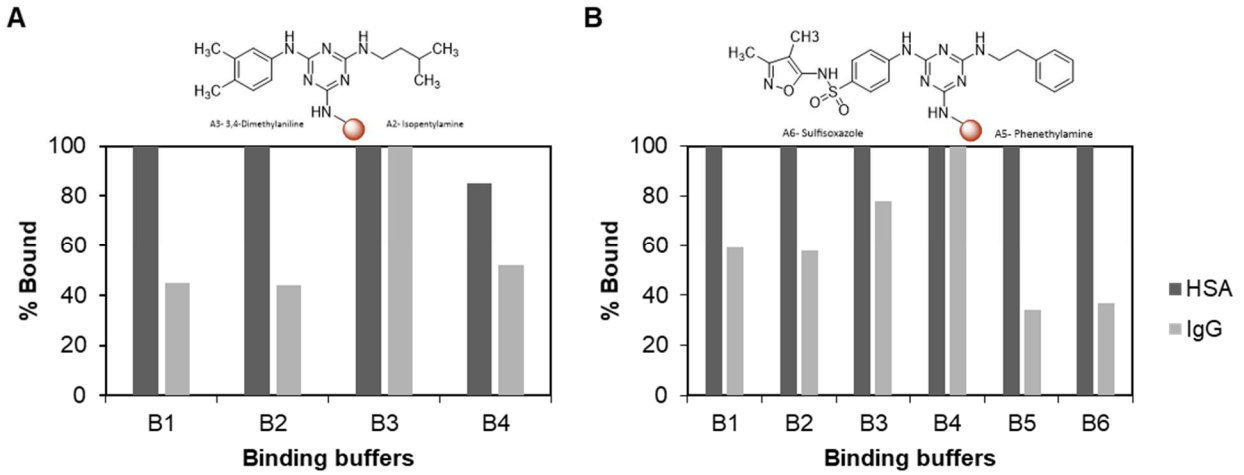

Figure 2.5. Binding buffer optimization for HSA purification using adsorbents (**A**) A3A2 and (**B**) A6A5, with the respective expected ligand chemical structure. **Legend**: **B1**: 10 mM sodium phosphate, 150 mM sodium chloride, pH 7.4, 20-25 ºC; **B2**: 10 mM sodium phosphate, 150 mM sodium chloride, pH 7.4, 0-4 ºC; **B3**: 10 mM Tris-HCl, 150 mM sodium chloride, pH 8.0; **B4**: 50 mM citrate buffer, pH 5.0; **B5**: 10 mM Tris-HCl, 300 mM sodium chloride, pH 8.0; **B6**: 50 mM citrate buffer, 300 mM sodium chloride, pH 5.0.

Secondly, the best elution conditions were selected using pure proteins. Considering the structure of the ligands, these are expected to promote hydrophobic interactions (due to aromatic compounds) and hydrogen bonds. Considering the ligands' structure and the commercially available HSA triazine-based purification schemes, eight different elution buffers were screened for HSA elution. Due to the diversity of possible interactions, buffers with different pH, ionic strength and the presence of an organic compound were tested. The elution studies were performed for HSA and hIgG, to assess a selective elution profile.

For both triazine-based ligands A3A2 and A6A5, it was possible to achieve a differential HSA selective elution (Figure 2.6). For A3A2, the glycine buffers (E1 and E5) and E2 favored hIgG elution (Figure 5A and S5A). The high concentration of salt with monovalent ions (E3, E4 and E6) showed to have no impact in the elution profile, whereas a high concentration of a salt with a divalent ion (E8) favored HSA elution. According to the Hofmeister cation series, while K^+ and Na^+ lead to "salting-out" effects that strengthen hydrophobic interactions, Mg^{2+} leads to a "salting-in" effect which weakens hydrophobic interactions (Figure 2.6A). Nonetheless, for A3A2 the best elution condition was 10 mM sodium phosphate, 150 mM sodium chloride at pH 7.4 in 50% (v/v) ethylene glycol which will likely interfere and disrupt the hydrophobic interactions between HSA and A3A2 ligand (Figure 2.6A; Table 2.4). The same elution buffers were tested under the same conditions for A6A5 ligand (Figure 2.6B). The high pH glycine-NaOH buffer (pH 10.0) (E5) was the only buffer favoring hIgG elution, while a low pH buffer (pH 3.0) (E1) favored HSA elution (Figure 2.6B). Regarding the salt effect in the elution profile, the same behavior was observed for A6A5 ligand (Figure 2.6B). The elution buffer E7, with ethylene glycol, also presented a high percentage of HSA eluted (Figure 2.6B). However, for A6A5 the best elution condition (54% HSA eluted *vs* 0% hIgG eluted) was 25 mM sodium phosphate, 150 mM sodium chloride, 30 mM sodium caprylate at pH 6.0 (E2) (Figure 2.6B). To further improve the elution conditions of A6A5 ligand, an additional optimization of the elution buffer was performed for a differential HSA/hIgG elution having as basis 25 mM sodium phosphate, 150 mM sodium chloride, 30 mM sodium caprylate at pH 6.0 (E2). Two elution buffers at pH 6 were tested: E9, where sodium chloride and sodium caprylate were depleted; and E10, where only the sodium chloride was depleted. When using only sodium phosphate, no protein eluted, whereas using sodium phosphate and sodium caprylate HSA elution increased and hIgG elution decreased (Table 2.4), showing the importance of caprylate in HSA elution step. Caprylic acid is many times used as HSA stabilizing agent used in treatment of hypoalbuminemia [130], moreover caprylic acid binds to HSA domain II by hydrogen bonding and hydrophobic interactions [131]. Nevertheless, for A6A5, the best results were obtained using as binding buffer 50 mM citrate buffer, 300 mM sodium chloride at pH 5.0 (B6) and as elution buffer 25 mM sodium phosphate, 30 mM sodium caprylate at pH 6.0 (E10) (Table 2.4).

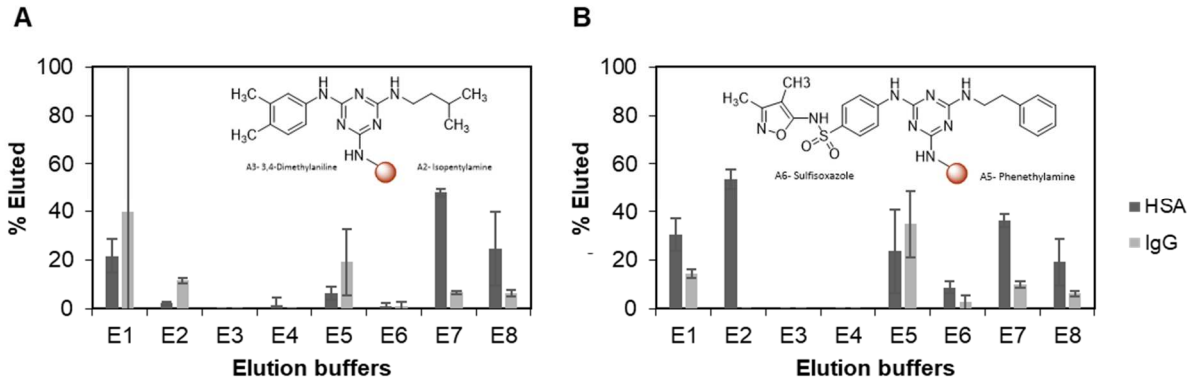

Figure 2.6. Elution buffer optimization for HSA purification using adsorbents **(A)** A3A2 and **(B)** A6A5, with the respective expected ligand chemical structure, data are presented as means ± SEM (n=3). **Legend: E1:** 100 mM glycine-HCl, pH 3.0; **E2:** 25 mM sodium phosphate, 150 mM sodium chloride, 30 mM sodium caprylate, pH 6.0; **E3:** 10 mM sodium phosphate, 1 M sodium chloride, pH 7.4; **E4:** 50 mM sodium phosphate, 1.5 M potassium chloride, pH 6.0; **E5:** 100 mM glycine-NaOH, pH 10.0; **E6:** 150 mM ammonium acetate, 10 mM sodium caprylate, pH 6.0; **E7:** 10 mM sodium phosphate, 150 mM sodium chloride at pH 7.4 in 50% (v/v) ethylene glycol; **E8:** 10 mM sodium phosphate, 2 M magnesium chloride, pH 7.4.

Table 2.4. Percentage of HSA and hIgG bound and eluted from triazine-based ligands A3A2 and A6A5 with the respective binding and elution buffers. Highlighted in grey are the best binding and elution conditions for both A3A2 and A6A5 ligands. Data are presented as means ± SEM (n=3).

Ligand	Binding buffer Elution buffer	% HSA	% hIgG
A3A2	**B1:** 10 mM Sodium phosphate, 150 mM sodium chloride, pH 7.4 **E7:** 10 mM Sodium phosphate, 150 mM sodium chloride, pH 7.4 in 50% (v/v) ethylene glycol	**99** **48**	**59** **7**
A6A5	**B5:** 10 mM Tris-HCl, 300 mM sodium chloride, pH 8.0 **E9:** 25 mM Sodium phosphate, pH 6.0	97 0	68 2
	B5: 10 mM Tris-HCl, 300 mM sodium chloride, pH 8.0 **E10:** 25 mM Sodium phosphate, 30 mM sodium caprylate, pH 6.0	97 74	68 2
	B6: 50 mM Citrate buffer, 300 mM sodium chloride, pH 5.0 **E9:** 25 mM Sodium phosphate, pH 6.0	99 0%	96 0%
	B6: 50 mM Citrate buffer, 300 mM sodium chloride, pH 5.0 **E10:** 25 mM Sodium phosphate, 30 mM sodium caprylate, pH 6.0	**99%** **100%**	**96%** **0%**

2.3.3. HSA purification from human plasma

Purification of HSA from human plasma was performed using adsorbents modified with both lead ligands, A3A2 and A6A5, and the optimized conditions for binding and elution. Firstly, 0.4 mg of total protein were loaded in 0.5 g of packed bed adsorbents A3A2 and A6A5. In the elution fractions from A3A2 adsorbent, it was observed the co-elution of hIgG with HSA (Figure 2.7A). The adsorbent A6A5 presented a better compromise between purity and recovery (Figure 2.7B; Table 2.5) with a recovery yield of 88% and protein purity of 93% (estimated by densitometric analysis using ImageJ software). Adsorbents with A6A5 ligand (1.5g of resin) were also loaded with higher protein titers (9 mg and 36 mg), increasing in this way the ratio total protein loaded/resin. The SDS-PAGE analyses showed selective HSA elution. The best results were found for the higher protein loading with 98% purity and 100% recovery (estimated by densitometric analysis using ImageJ software) (Figure 2.8; Table 2.6). These results demonstrate the feasibility to use A6A5 adsorbent for HSA purification from a complex crude extract as human plasma.

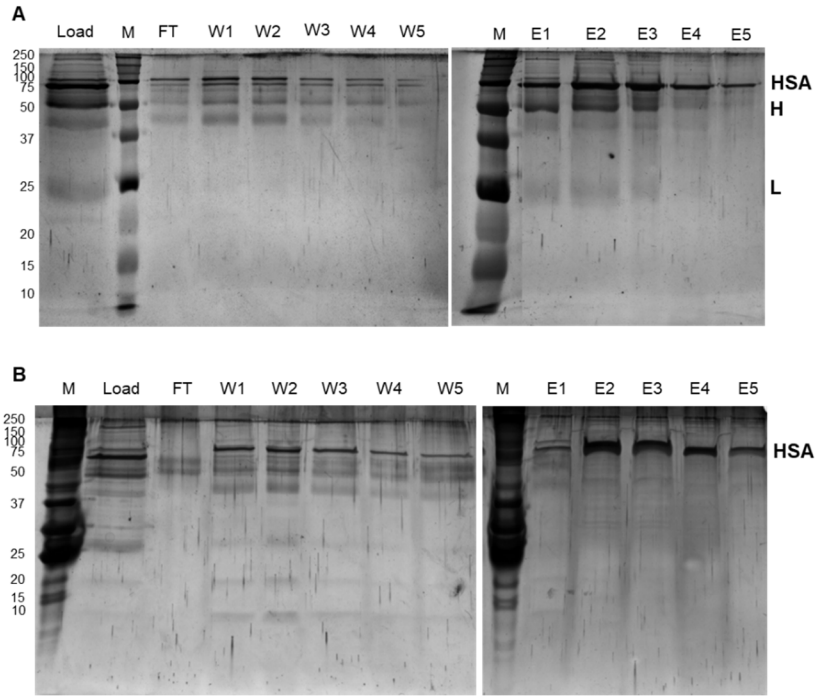

Figure 2.7. Purification performance of **(A)** A3A2 and **(B)** A6A5 for HSA purification from human plasma. Silver stained SDS-PAGE gel (12.5% acrylamide) in reducing conditions. As purification conditions for **(A)** the binding buffer used was 10 mM sodium phosphate, 150 mM sodium chloride at pH 7.4 (B1) and as elution buffer 10 mM sodium phosphate, 150 mM sodium chloride at pH 7.4 in 50% (v/v) ethylene glycol (E7) was used, for **(B)** as binding buffer 50 mM citrate buffer, 300 mM sodium chloride at pH 5.0 (B6) and as elution buffer 25 mM sodium phosphate, 30 mM sodium caprylate at pH 6.0 (E10) were used. **Lanes ID: M:** Precision Plus Protein™ Dual Color Standards (molecular weight in kDa); **Load:** human plasma; **FT:** flow-through; **W1:** first wash; **W2:** second wash; **W3:** third wash; **W4:** fourth wash**; W5:** fifth wash**; E1:** first elution; **E2:** second elution; **E3:** third elution; **E4:** fourth elution; **E5:** fifth elution (all fractions with the same protein quantity (1200 ng/well)). Position of **HSA** (66 kDa) and hIgG heavy (**H**) (50 kDa) and light (**L**) (25 kDa) chains are indicated in the right side of the gel.

Table 2.5. HSA purity assessment from its purification from human plasma with a total protein concentration of 0.7 mg/ml, with triazine-based ligands A3A2 and A6A5 with the respective optimal binding and elution conditions.

Ligand	Binding buffer Elution buffer	HSA purity (%)	Recovery yield (%)
A3A2	**B1:** 10 mM Sodium phosphate, 150 mM sodium chloride, pH 7.4 **E7:** 10 mM Sodium phosphate, 150 mM sodium chloride, pH 7.4 in 50% (v/v) ethylene glycol	**37**	**100**
A6A5	**B6:** 50 mM Citrate buffer, 300 mM sodium chloride, pH 5.0 **E10:** 25 mM Sodium phosphate, 30 mM sodium caprylate, pH 6.0	**93**	**88**

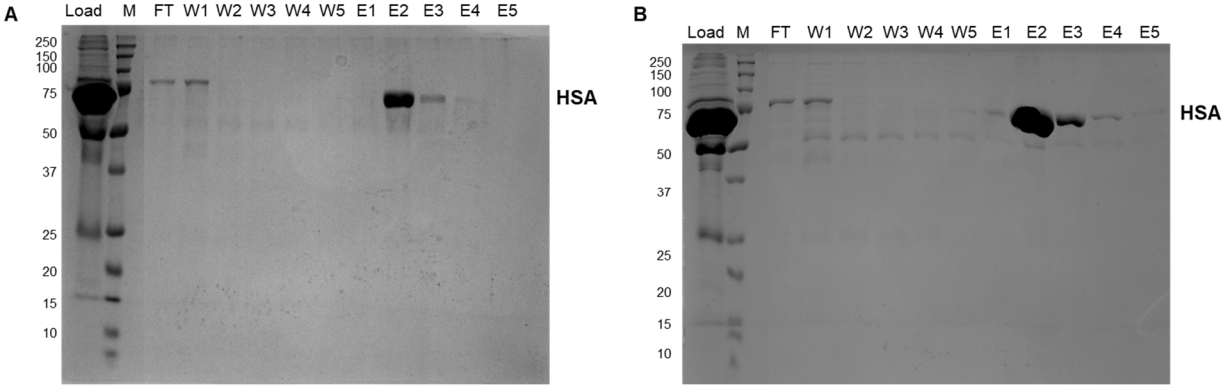

Figure 2.8. Purification performance of HSA from human serum plasma with 8.9 mg **(A)** and 36 mg **(B)** total protein loading using as binding buffer 50 mM citrate buffer, 300 mM sodium chloride at pH 5.0 (B6) and as elution buffer 25 mM sodium phosphate, 30 mM sodium caprylate at pH 6.0 (E10). Coomassie stained SDS-PAGE gel (12.5% acrylamide) in reducing conditions. **Lanes ID: M:** Precision Plus Protein™ Dual Color Standards (molecular weight in kDa); **Load:** human plasma; **FT:** flow-through; **W1:** first wash; **W2:** second wash; **W3:** third wash; **W4:** fourth wash**; W5:** fifth wash**; E1:** first elution; **E2:** second elution; **E3:** third elution; **E4:** fourth elution; **E5:** fifth elution (Load sample diluted 10 times and sample fractions diluted 2 times). Position of **HSA** (66 kDa) is indicated in the right side of the gel.

Table 2.6. HSA purity assessment from its purification from human plasma with a total protein concentration of 8.9 mg and 36 mg, with triazine-based ligand A6A5 using as binding buffer 50 mM Citrate buffer, 300 mM sodium chloride at pH 5.0 and as elution buffer 25 mM Sodium phosphate, 30 mM sodium caprylate at pH 6.0.

Loading (mg total protein)	mg Total protein bound/ g support	mg HSA recovered/ g support	HSA purity (%)	Recovery yield (%)	Purification factor [a]
0.4	3.23 ± 0.17	0.31 ± 0.02	89 ± 4.3	98 ± 3.4	$1.93 \pm 0.19/2.15$
9.0	5.84 ± 0.02	0.53 ± 0.08	92 ± 8.7	93 ± 19	$1.74 \pm 0.33/1.88$
36	5.88 ± 0.04	1.81 ± 0.34	98 ± 1.2	100 ±10	$2.09 \pm 0.41/2.13$

[a] Ratio between final and initial protein purity. As different loadings were used in the several runs the maximum purification factor is given after SEM.

2.3.4. Modeling of A6A5 binding to HSA

As sulfisoxazole has an identical allosteric behavior as drugs like warfarin and azapropazone in human serum albumin (HSA), it is assumed that it binds to Drug site I (Figure 2.9A), as already described for the latter drugs [115,120].

To analyze the putative binding mode of ligand A6A5 to HSA, molecular docking studies were performed. The docking grid covered all domain II residues, including the key residues for PAB protein interaction with HSA: Phe228, Ala229, Ala322, Val325, Phe326, and Met329 [125]. As ligand A6A5 has a sulfisoxazole substituent in the triazine based compound, the molecular docking of sulfisoxazole was also performed as no crystallographic structure for sulfizoxazole bound to albumin has been reported. When comparing sulfisoxazole docking position to the crystal structure of HSA-warfarin complex (Figure 2.9B and 8D), similar interactions are observed [115]. The Drug Site I residue Lys199, performs a cation-π interaction with six-carbon aromatic rings in both drugs; His242 also acts as a hydrogen bond donor to the warfarin's hydroxyl group and sulfisoxazole sulfone; and Tyr150 interacts with both ligands donating a hydrogen bond to sulfisoxazole and as a hydrogen bond acceptor of the warfarin's hydroxyl group (Figure 8B; D). Additionally, the sulfisoxazole binding mode presents: three extra hydrogen bonds, one with the sidechain of Arg257 and two with the sidechain and backbone carbonyl of Ser192; and two residues with hydrophobic interactions, Leu260 and Ala291. Overall, the binding mode proposed from the docking calculation for sulfisoxazole is in agreement with the canonical residue interactions with described HSA-drug structures [115].

The positive docking result for sulfisoxazole for the domain II located in Drug site I, should restrain the docking result position for ligand A6A5, as this drug is part of the synthesized affinity ligand. However, the increased molecular size with the addition of a triazine ring and the phenethylamine substituent, and the fact that the affinity ligand is immobilized, should not allow it to bind to HSA's Drug Site I, as observed for sulfisoxazole alone. Therefore, the position of A6A5 after its docking to HSA's domain II, is in agreement with the presented statements and located outside the Drug Site I, at the end of the surface of domain II in the vicinity of domain I, (Figure 2.9A; C). Furthermore, this binding mode presents the anchoring point towards the solvent, revealing that ligand A6A5 could be immobilized onto a solid support in that position. The main interactions present in A6A5 binding mode to HSA are three hydrogen bonds and hydrophobic interactions with two residues. Two triazine substituted amines act as hydrogen bond donors toward the side chains of Glu244 and Glu252, the additional hydrogen bond is between His247 side chain and the oxygen atom in the isoxazole group of the synthesized ligand. The hydrophobic interactions are close the isoxazole methyl group, Leu203, and the phenethylamine's phenyl group, Leu66 (Figure 2.9C). These interactions are in agreement with the best binding condition obtained for A6A5-HSA binding since citrate, present in the binding buffer, presents a kosmotropic effect promoting ligand-protein hydrogen bonding as well as hydrophobic interactions, both observed in the docking results.

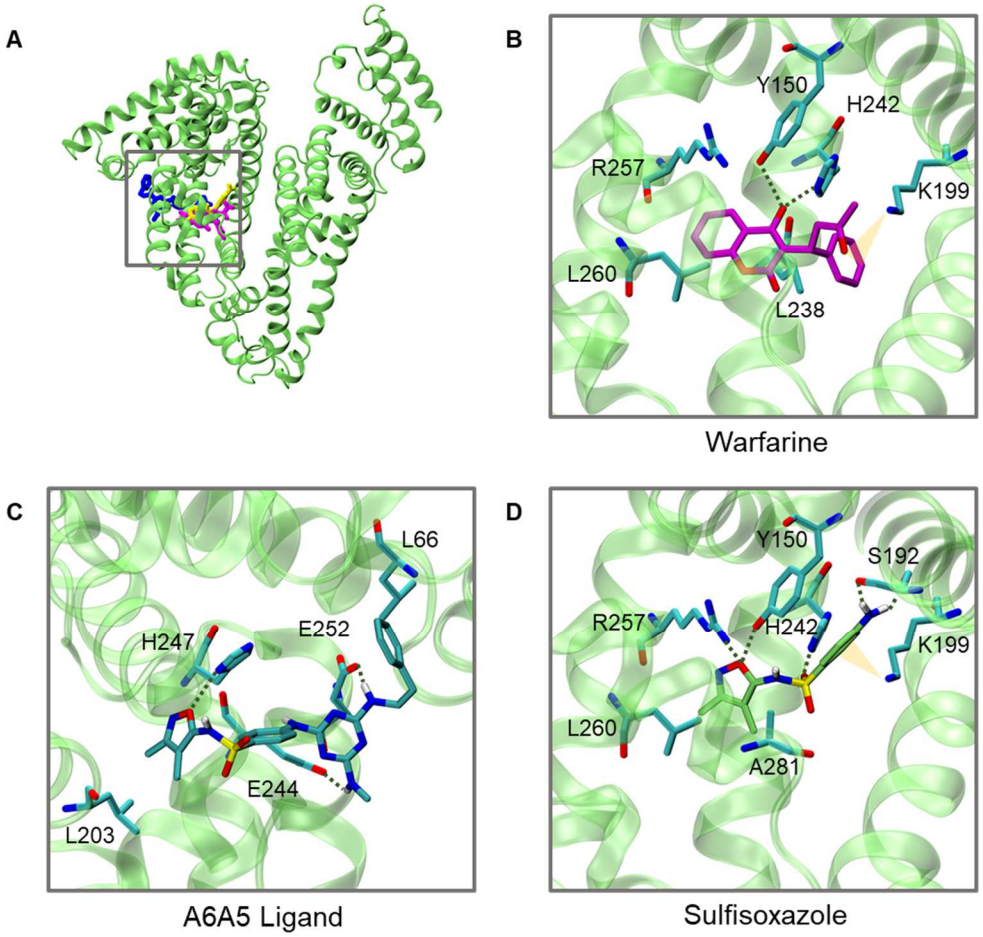

Figure 2.9. (**A**) Location of HSA ligands, warfarine (magenta), A6A5 ligand (blue) and sulfisoxazole (yellow), in its 3-dimentional structure. (**B**) Interaction details of warfarine and HSA from the complex crystallographic structure (PDB ID: 2BXD). Binding mode results for the docking of (**C**) A6A5 and (**D**) sulfisoxazole in HSA crystallographic structure (PDB ID: 2BXD) (hydrogen bonds in dotted green lines, cation-π interactions in yellow triangles).

2.4. Conclusion

HSA is an important biopharmaceutical with a wide variety of applications, ranging from its capacity to carry diverse molecules and increase their circulation half-life time, to be a biomarker in many diseases (e.g. cancer and rheumatoid arthritis). Due to its high market value, different chromatographic and non-conventional approaches for HSA purification have been explored. In this work, a library based on the triazine skeleton was rationally developed based on amino acids of the PAB protein and synthetic drugs known to bind HSA domain II. The triazine scaffold yields ligands with interesting properties for the purification of biopharmaceuticals namely potential low toxicity in process leachates [132], and capability to generate adsorbents with high resistance to conventional cleaning-in-place and sterilization-in-place

procedures [17,133–136]. Of the 64 ligands screened, 2 triazine ligands showed promising results for HSA purification, ligands A3A2 and A6A5. After optimization studies for HSA binding and elution, it was possible to purify HSA from human plasma with a purity of 98% and 100% of recovery yield using adsorbents modified with the triazine ligand A6A5. The best binding and elution conditions for HSA recovery using A6A5 adsorbent are similar to those reported for commercial kits (AlbuPure® from ProMetic BioSciences). Still, the 50 mM ammonium acetate salt used to elute HSA from AlbuPure® were replaced in our case by 25 mM sodium phosphate, thus deriving milder and less toxic elution conditions (Table 2.7).

Our preliminary data show that the binding of A6A5 to HSA is stable at physiological conditions (PBS buffer) at pH 7.4 and 6 (100% and 63%, respectively). Moreover, as the present ligand was rationally designed to bind HSA domain II (possibility confirmed by docking results), it opens the possibility to improve in the future the pharmacokinetics of HSA fusions via FcRn binding.

Table 2.7. Comparison of commercial (AlbuPure®) and in-house developed absorbents for HSA purification. N/A: Not available**.**

Ligand	Structure	Binding	Elution	HSA purity[a] (%)	Recovery yield[a] (%)	Company
AlbuPure®	**N/A**	50 mM Sodium citrate, pH 5.5	50 mM Ammonium acetate, 10 mM caprylate pH 7 (or) 50 mM sodium carbonate, pH 10	**N/A**	**N/A**	Prometic Bioseparations
A6A5	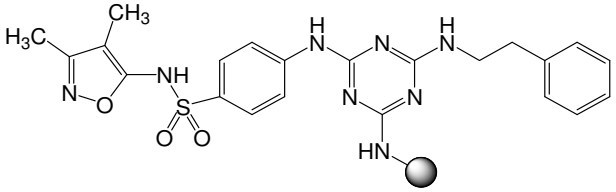	50 mM Citrate buffer, 300 mM sodium chloride, pH 5.0	25 mM Sodium phosphate, 30 mM sodium caprylate, pH 6.0	98[a]	100[a]	-
A3A2	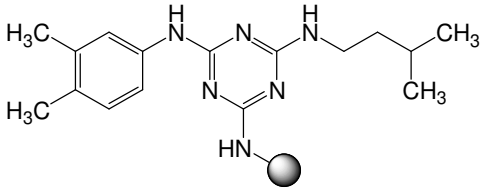	10 mM Sodium phosphate, 150 mM sodium chloride, pH 7.4	10 mM Sodium phosphate, 150 mM sodium chloride, pH 7.4 in 50% (v/v) ethylene glycol	37[b]	100[b]	-

[a] With a total protein loading of 36 mg from human serum plasma.
[b] With a total protein loading of 0.4 mg from human serum plasma.

Chapter 3

Affitins for protein purification by affinity magnetic fishing

Publication in peer-review paper

dos Santos, R, Fernandes, CSM, Ottengy, S, Viecinski, AC, Béhar, G, Mouratou, B, Pecorari, F, Roque, ACA. Affitins for protein purification by affinity magnetic fishing. J. Chromatogr. A. 1457 (2016) 50-58, http://dx.doi.org/10.1016/j.chroma.2016.06.020

Authors contributions:

GB, BM, FP and ACAR, designed the work. The experiments were conducted by RS, CSMF, SO and ACV. Manuscript preparation and revision were conducted by RS, CSMF and ACAR.

Abstract

Currently most economical and technological bottlenecks in protein production are placed in the downstream processes. With the aim of increasing the efficiency and reducing the associated costs, various affinity ligands have been developed. Affitins are small, yet robust and easy to produce, proteins derived from the archaeal extremophilic "7 kDa DNA-binding" protein family. By means of combinatorial protein engineering and ribosome display selection techniques, Affitins have shown to bind a diversity of targets. In this work, two previously developed Affitins (anti-lysozyme and anti-IgG) were immobilized onto magnetic particles to assess their potential for protein purification by magnetic fishing. The optimal lysozyme and human IgG binding conditions yielded 58 mg lysozyme/g support and 165 mg IgG/g support, respectively. The recovery of proteins was possible in high yield (≥ 95%) and with high purity, namely ≥ 95% and 81%, when recovering lysozyme from *E.coli* supernatant and IgG from human plasma, respectively. Static binding studies indicated affinity constants of 5.0×10^{4} M^{-1} and 9.3×10^{5} M^{-1} for the anti-lysozyme and anti-IgG magnetic supports. This work demonstrated that Affitins, which can be virtually evolved for any protein of interest, can be coupled onto magnetic particles creating novel affinity adsorbents for purification by magnetic fishing.

3.1. Introduction

Affinity-based separations are extremely efficient tools in protein production. Still, production costs of biopharmaceutical proteins are now mostly associated with the downstream processing steps [137], [138]. Historically, antibodies were explored as affinity biological ligands in purification as they combine a tailored high specificity for a diversity of targets [137]. However, they are prone to degradation, modification, aggregation and/or denaturation [137], their complex structure results in high production costs [139] and they have low shelf-life [140]. These properties limited their widespread use for cost effective affinity purification schemes.

Alternative biological affinity ligands have been gathering advantages over classical full-length monoclonal antibodies, namely enhanced stability and reduced molecular size [139]. These alternative ligands include smaller versions of antibodies, as single-chain variable fragments and antigen-binding fragments [137,141] or engineered binding proteins based on different scaffolds [142]. An optimal scaffold should ideally combine a few key characteristics: it must be small and stable, lack disulfide bridges, be easily produced at high levels [143], have low background binding and must be highly soluble in aqueous solutions [144].

Members from the archaeal "7 kDa DNA binding" protein family [145], such as Sac7d from the extremophilic *Sulfolobus acidocaldarius* [146] were described as alternative scaffolds [143,147] to obtain

affinity reagents called Affitins [148]. Using combinatorial libraries and ribosome display selections, Affitins were isolated for a diversity of protein targets. Affitins have been shown to be chemically and thermally stable and resistant to extreme acidic and alkaline pH [142–144,149]. Among the targeted proteins, CelD and lysozyme are two endo-glycosidases, for which Affitins present inhibition constants in the nanomolar range. In addition, the structures of the complexes formed have been solved to decipher their modes of action [142]. Affitins designed from Sac7d scaffold and engineered in a Sso7d protein scaffold, were also targeted against human Immunoglobulin G (IgG) and shown to withstand extreme pH conditions with a dissociation constant in the micro to nanomolar range [144,149]. This study has shown that Affitins can recognize discontinuous epitopes which could explain why in general Affitins are highly specific of their cognate targets [142–144]. This additional property of high specificity of Affitins resulted in potent purification tools for affinity chromatography once covalently immobilized on agarose resin [150].

Magnetic particles (MPs) are an alternative to standard chromatographic media for protein purification [151]. The superparamagnetic properties of MPs allow their easy and selective removal from viscous biological solutions [152]. Magnetic particles have highly accessible surface areas and are non-porous supports, therefore bioseparations are not limited by pore diffusion [22,151]. Furthermore, magnetic separation is easy to use without the need of sophisticated apparatus, enabling operation in a wide range of conditions. To be suitable for protein purification, MPs should be hydrophilic and inert, should allow further functionalization [22], be stable during binding, elution and regeneration conditions, possess large surface areas and be responsive to external magnetic fields [153]. Similarly to chromatographic affinity separations, various biological molecules have been used to functionalize magnetic particles [152,153].

In this work, we explored for the first time the use of magnetic particles functionalized with Affitins for the selective capture of proteins. As a proof-of-concept, two Affitins previously evolved against lysozyme and IgG were immobilized onto magnetic particles and assessed for protein capture and recovery. Our data shows that Affitin-functionalized magnetic particles can be an alternative for protein purification. In addition, and considering the versatility of the Affitins platform, new affinity magnetic adsorbents can be developed against any target of interest.

3.2. Materials and Methods

3.2.1. Magnetic particles synthesis, coating and amination

Bare magnetic particles were synthesized by the co-precipitation method. A solution of 25% ammonium hydroxide in deionized water (200 ml) was purged with N_2 gas. A freshly prepared iron solution ($FeCl_3$ and $FeCl_2$ salts (Sigma) with a molar ratio of Fe^{2+}/Fe^{3+} of 0.5, 25ml) was added in a dropwise manner. The reaction continued for 2h. The resulting MPs were washed with distilled water (10-times) with aid of magnetic separation. The particles (10 mg/ml) were sonicated (Elmasoni S30, Elma, 37 kHz) for 15 minutes and a solution of sodium metasilicate pentahydrate (Sigma) was added (2.28 g in 80 ml ethanol/water 50%). The

mixture was incubated (40°C, 2 hours with orbital shaking (200 RPM)). Afterwards the support was washed with distilled water (10-times). The supernatant was removed and the particles were resuspended in 80 ml of ethanol/water (5:1). The solution was sonicated for 10 min and 25% ammonium hydroxide (3 ml) and tetraethyl orthosilicate (TEOS) (1.5 ml, Sigma) were added dropwise during sonication. The mixture was incubated (40°C, 2 hours with orbital shaking, 200 RPM). Afterwards the particles were washed with distilled water (10-times). The particles were resuspended in 175 ml of distilled water and sonicated for 10 minutes. A solution of dextran (2 g in 25 ml of water) was added dropwise to the particle solution and the mixture was incubated (60°C, 2 hours with orbital shaking, 200 RPM). The particle amination protocol has been described elsewhere [22]. The amount of amines was assessed by the Kaiser Test as 212.8 ± 17.3 µmol NH_2/g support. All produced magnetic supports were characterized by dynamic light scattering (DLS) and by zeta potential (0.05 mg/ml solution in deionized water, pH 5.80) using a Dynamic Zetasizer NanoZS from Malvern instruments. Magnetic particles samples were prepared by evaporating dilute suspensions which were grounded and mixed with KBr (1:100). The Fourier Transform Infrared (FT-IR) spectra were recorded on a Tensor 27 from Bruker.

3.2.2. Affitin production

The sequence of the Affitin H4 (anti-lysozyme) and Affitin D1Sso7d-DM (anti-IgG) have been previously reported [142] and [149], respectively. In this study, we inserted a cysteine at the C-terminus by directed mutagenesis to allow coupling via thiol chemistry.

The resulting Affitin H4-Ct has thus the following sequence: MRGSHHHHHHGSVKVKFFWNGEEKEVDTSKIVWVKRAGKSVLFIYDDNGKNGYGDVTEKDAPKELLDM LARAEREKKG**C**. As for Affitin D1Sso7d-DM-Ct, it has the following sequence: MRGSHHHHHHGSATVKFKYKGEELEVDISKIKKVWRDRLAAVFTYDLGGGKTGYGWVFTKDAPKELLQM LEKQKKLN**C**. The resulting Affitins were expressed in *Escherichia coli* DH5α Iq strain and purified by immobilized metal ion affinity chromatography and gel filtration as described previously [142]. The Affitins were supplied in buffer 137 mM NaCl, 2.7 mM KCl, 10 mM Na_2HPO_4, 2 mM KH_2PO_4, pH 7.4.

3.2.3. Optimization of support functionalization

For the optimization of the functionalization conditions different conditions were varied: (i) magnetic particle concentration, (ii) presence of reduction agent and (iii) NH_2:Affitin ratio. The compound sulfosuccinimidyl-4-(*N*-maleimidomethyl)cyclohexane-1-carboxylate (sulfo-SMCC) (Pierce Biotechnology) was used as an amine-to-sulfhydryl crosslinker. The magnetic support was washed 5-times with conjugation buffer (10 mM phosphate, 0.15 M NaCl, 1 mM EDTA, pH 7.2 purged with N_2). Five-molar excess of sulfo-SMCC to the amines of the support in distilled water was added to the support and incubated (30 minutes, 25°C with orbital shaking, 200 RPM). The support was washed 5-times with conjugation buffer with aid of an external magnet. The protein was then added to the mixture and incubated (1 hour, 25°C with orbital shaking, 200 RPM). The support was washed with conjugation buffer and supernatants were collected and

analyzed for protein content using a microplate reader Tecan Infinite F200 (λexcitation = 280 nm and λemission = 340 nm). A solution of 100 mM cysteine was added to the particle slurry and the mixture was incubated (1 hour at 25°C, with orbital shaking, 200 RPM) and washed 10-times with conjugation buffer. The magnetic support functionalized with affitin anti-lysozyme was named MP-H4-Ct, whereas that functionalized with the affitin anti-IgG was named MP-D1Sso7d-DM-Ct.

3.2.4. Testing magnetic supports with protein samples – optimization of binding and elution conditions

Functionalized and non-functionalized magnetic particles were tested for protein binding. The supports were previously washed with 0.2 M NaOH in 50% isopropanol, deionized water and equilibrated with phosphate buffer (PBS; 10 mM sodium phosphate, 0.15 M NaCl, pH 7.4). For the optimization of the binding conditions the following parameters were varied: (i) magnetic particle concentration (2.5, 5 and 10 mg/ml), (ii) incubation temperature (0-8°C and 25°C), and (iii) lysozyme:Affitin molar ratio (1:1, 1:1.5 and 1:3). The lysozyme solution (500 µl) was loaded and incubated for 30 minutes with functionalized magnetic support (500 µl), for final volume of 1 ml. The supports were washed with PBS by means of centrifugation (5 minutes, 1850 *×g*) and with aid of an external permanent magnet and all supernatants and loading solutions were collected and analyzed by fluorescence (λex = 280 nm and λem = 340 nm).

For the optimization of the elution conditions, 500 µl of magnetic particles (2.5 mg MP-H4-Ct/ml) were incubated with 500 µl of lysozyme solution (1:3 lysozyme to Affitin molar ratio), varying: (i) pH, (ii) salt concentration and (iii) ethylene glycol percentage of the elution buffer. Target proteins bound to magnetic supports, were recovered with the different elution buffers and all supernatants and loading solutions were collected and analyzed by fluorescence intensity (λex = 280 nm and λem = 340 nm) using a microplate reader (Tecan Infinite F200). Different calibration curves were performed for each elution buffer tested.

3.2.5. Protein purification from crude extracts

For lysozyme purification, an *E. coli* crude extract was spiked with 40% (w/v) lysozyme from chicken egg white (Sigma-Aldrich) at a final concentration of 2.1 mg total protein/ml, 500 µl of this solution were incubated with 200 µl of 2.5 mg MP-H4-Ct/ml in PBS and incubated for 30 minutes at 0-8°C. Afterwards, the support was washed with PBS and the bound protein was eluted with 100 mM glycine-HCl buffer, 0.15 M NaCl, pH 2.5. Human IgG was purified from human serum samples (Sigma-Aldrich), 250 µl of solution with 1.2 ± 0.2 mg total protein/ml was loaded into 250 µl of 2.5 mg MP-D1Sso7d-DM-Ct/ml in PBS. The mixture was incubated for 30 minutes at 25°C. The weakly bound proteins were washed using PBS and the bound proteins were eluted with 100 mM glycine-HCl with 0.15 M NaCl at pH 2.5. The quantification of proteins was performed by the Bradford method using bicinchoninic acid (BCA) assay reagent provided by Thermo Scientific Pierce. The protein standard used was bovine serum albumin (BSA) from Pierce. Absorbance was measured at 562 nm in microplate reader Tecan Infinite F200. Sodium dodecyl sulfate–polyacrylamide

gel electrophoresis (SDS–PAGE) was performed to evaluate the samples purity. The buffer sample composition was 0.15 M Tris–HCl, pH 6.8, 6% SDS, 0.025% bromophenol blue, 12.5% glycerol and as reducing agent β-mercaptoethanol was used. Prior to loading in the gel all the samples were denaturated at 100°C for 5 minutes. Samples were applied in a 12% or 15% acrylamide gel, prepared from 41% or 49.5% acrylamide/bis stock solution (30:1) from Bio-Rad, respectively, and ran at 90 mV using as running buffer 192 mM glycine, 25 mM Tris-HCl and 0.1% SDS, pH 8.3. Gels were stained using Bio-Rad silver staining kit. Images were acquired with Gel Doc™ XR+ System with Image Lab™ software from Bio-Rad, and analyzed with ImageJ software.

3.2.6. Determination of the binding constants by static partition experiments

The functionalized supports were regenerated with 0.2 M NaOH in 50% isopropanol and distilled water and equilibrated with PBS. Different concentrations of lysozyme (0.5 to 3.4 mg lysozyme/ml) or IgG (0.2 to 3.5 mg IgG/ml) were incubated with the 2.5 mg/ml of functionalized magnetic particles in a total volume of 500 µl and 250 µl, respectively. The interaction was promoted over 12 hours at 4°C and 25°C, respectively for lysozyme and IgG, to achieve chemical equilibrium. The supernatants were collected and the fluorescence intensity was measured. The adsorption phenomenon followed a Langmuir isotherm and the experimental data was fitted using OriginPro (v8.5.1).

3.3. Results and Discussion

3.3.1. Affitin immobilization onto magnetic supports

The best conditions for Affitin anti-lysozyme functionalization onto magnetic particles were determined by (i) tuning magnetic particle concentration, (ii) usage of reduction agent and (iii) ratio of Affitin to amines on the support (Figure 3.1). Two different magnetic particle concentrations were tested during the immobilization protocol (2.5 and 10 mg/ml) with a 1:0.05 NH_2 to Affitin molar ratio. Both conditions yielded similar results, and a 2.5 mg/ml concentration of MP was fixed for further studies. The immobilization of Affitin was promoted through sulfo-SMCC, a crosslinker between the amine groups of the support and the sulfhydryl group of the Affitin H4-Ct. In solution, Affitin molecules can form dimers and potentially decrease the immobilization yield. However, pre-incubation with tris(2-carboxyethyl)phosphine (TCEP), a sulfhydryl group reducing agent, showed a decrease in the immobilization yield (Figure 3.1A). The results obtained in the presence of dithiothreitol (DTT) or with no-reducing agent added were comparable. However, to avoid the addition of chemicals and for more reproducible results, no reducing agent was used in the upcoming experiments. The ratio between amines in the support and moles of Affitin (NH_2:Affitin) was also tested (Figure 3.1B). Reducing the molar amount of Affitin contributed to a decrease of the Affitin immobilized (Figure 3.1B). However a higher amount of Affitin to the support amines would not be suitable due to the

large size difference between the particles and Affitin, which would not allow a 1:1 ratio as usually used with peptides [154]. Therefore, and considering that unreacted free amines are further blocked with cysteine residues, the intermediate condition was selected. To summarize, the best immobilization conditions have been determined as using 2.5 mg/ml of MP, the non-usage of a reducing agent in prior incubation step and a ratio of 1:0.1 of NH_2:Affitin, resulting in a final immobilization of 14.5 ± 4.1 µmol Affitin H4-Ct/g support (101 ± 29 mg Affitin H4-Ct/g support).

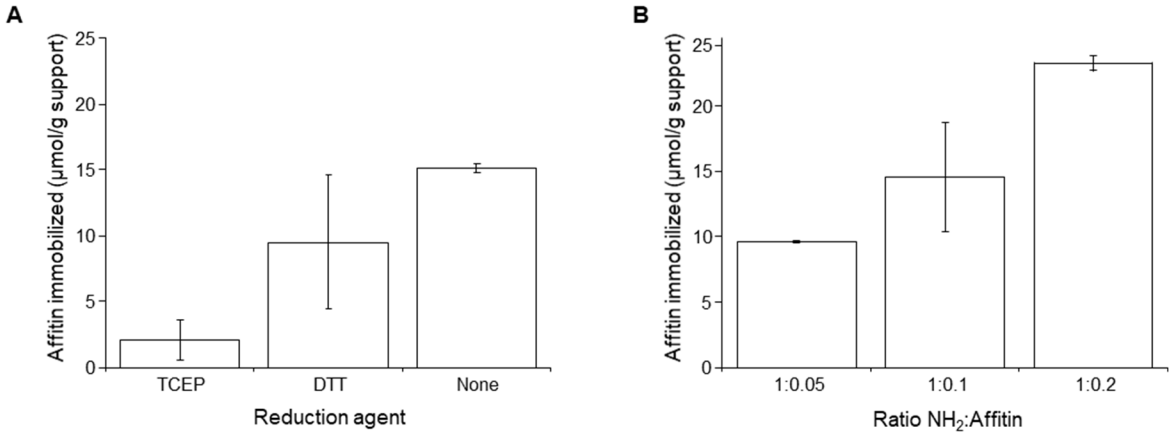

Figure 3.1. Optimization of Affitin H4-Ct immobilization (n=3) in 2.5 mg MP/ml using Sulfo-SMCC as cross linker agent by changing (**A**) reduction agent, and (**B**) ratio NH2 of the support to Affitin.

3.3.2. Magnetic particles characterization

To confirm the surface modification of magnetic particles and further immobilization of Affitins, Fourier transform infrared (FT-IR) spectroscopy was employed (Figure 3.2A). The FT-IR spectra of Affitin H4-Ct alone (Figure 3.2A; spectra a) shows a band at 1620 – 1640 cm^{-1} that corresponds to amide I (C=O stretching) and is centered in the region which has been assigned to β-sheets in protein structures [155]; this is correlated with the presence of five β-sheets in the three-dimensional structure of Affitin H4 (PDB ID: 4CJ2 [142]).

The FT-IR spectra obtained for the magnetic particle samples before Affitin immobilization (Figure 3.2A; spectra c) show bands in the region 400 - 600 cm^{-1}, typical for the Fe-O bond vibrations in the structure of magnetite [156]; a signal at 1168 cm^{-1} typical of tetraethyl orthosilicate [157]; a broad peak at 3434 cm^{-1} typical for the hydroxyl stretching vibration of dextran [158]. The main characteristic bands for dextran are superimposed in a broader peak at 1020-1146 cm^{-1} resultant of the deformation vibrations of the CCH and HCO bonds and valent vibrations of C-O and C-C bonds [158]. Affitin immobilization is confirmed in the final functionalized particles (Figure 3.2A; spectra b) by an extra band at 1550 cm^{-1}.

The magnetic particles were further analyzed by Dynamic Light Scattering (DLS). The hydrodynamic diameter (Figure 3.2B) indicates the formation of 2 µm agglomerates of the bare particles due to low stability rendered by the lack of coating [159]. The successive coatings with silica confer stability and hydrophilicity to the particles [160], which contribute to a decrease in the hydrodynamic diameter. The coating with the

polymer dextran contributed to a smaller hydrodynamic diameter. The amination reagent, (3-Aminopropyl)triethoxysilane, can crosslink and contribute for the increase of the particles' diameter. The zeta potential values (Figure 3.2C) corroborate the successive surface modification with different functionalities. Magnetite displays negative zeta potential values at pH 5.80 and a decrease towards more negative values upon silica coating was observed. The neutral polymer dextran contributes for the neutral charge of the dextran-coated particles. The zeta potential moves towards positive values after particle amination and little difference was observed after Affitin functionalization due to the isoelectric point of 8.8 and 9.6, for H4-Ct and D1Sso7d-DM-Ct, respectively.

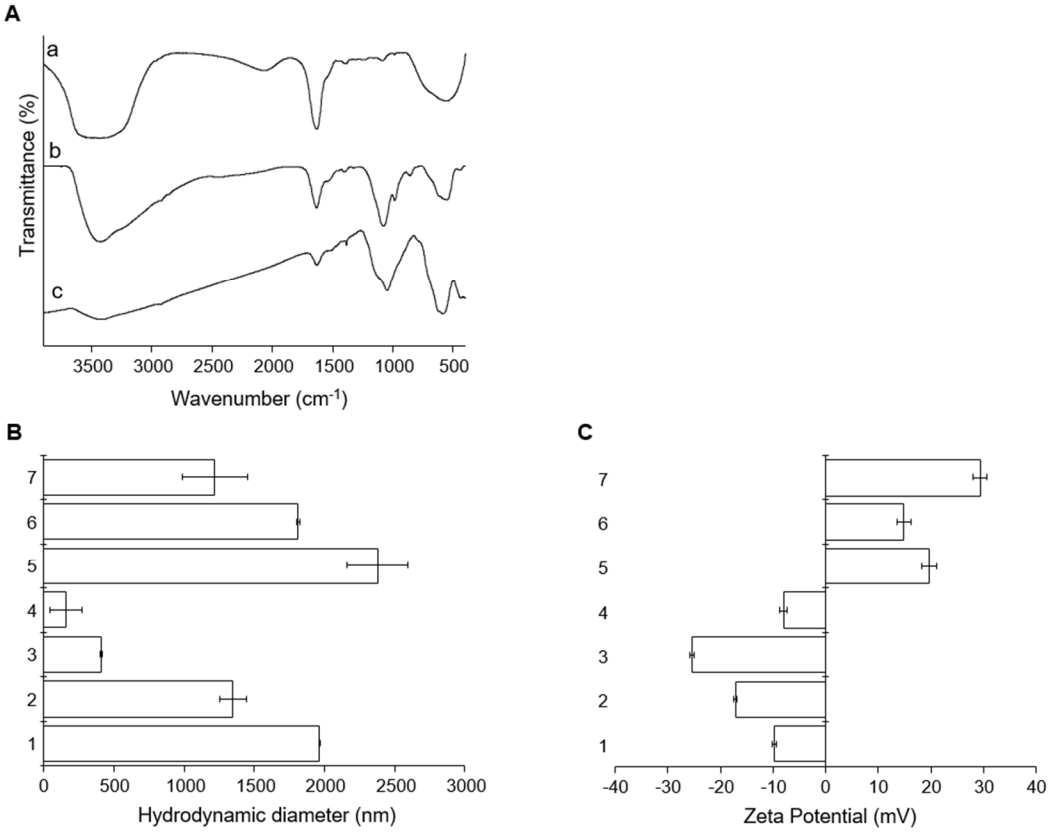

Figure 3.2. Sample characterization by (**A**) FT-IR spectra for (a) Affitin H4-Ct, (b) MP-H4-Ct, (c) MP-SiO3-TEOS-DEX-NH2 and magnetic particles characterization by (**B**) DLS and (**C**) zeta potential (n=3) for (1) MP, (2) MP-SiO3, (3) MP-SiO3-TEOS, (4) MP-SiO3-TEOS-DEX, (5) MP-SiO3-TEOS-DEX-NH2, (6) MP-H4-Ct, (7) MP-D1Sso7d-DM-Ct.

3.3.3. Optimization of binding and elution conditions of anti-lysozyme particles

Prior to functionalization, aminated magnetic supports were tested for non-specific binding to lysozyme, resulting in 7.1 ± 1.8 % of lysozyme bound (when loading 0.5 mg of protein). The dextran coating renders a neutral charge to the particle surface (Figure 3.2C) and has hydroxyl functional groups which contribute for the non-specific binding, as previously reported in other works [161]. On the other hand, the isoelectric point of lysozyme is located at pH 11.0 [162], which makes lysozyme positively charged at pH 7.4 during the binding assay. The positive charge of the aminated particles decrease the binding of lysozyme, and contribute to low non-specific binding.

The best conditions for lysozyme binding were determined by tuning (i) magnetic particle concentration, (ii) lysozyme to Affitin ratio and (iii) incubation temperature (Figure 3.3). Contrary to what was observed during the immobilization step, particle concentration had a high influence on lysozyme binding (Figure 3.3A). A lower concentration (2.5 mg/ml) of particles contributed to a higher amount of lysozyme binding to the support, probably due to lower hindrance, which could allow lysozyme to better interact with the immobilized Affitin. A higher molar ratio (1:3) between Affitin and lysozyme contributed to increase the binding percentage, as a higher amount of binder increases the probability of lysozyme to bind (Figure 3.3B). Lower incubation (0-8ºC) temperature contributed to increase the percentage of lysozyme bound to the support (Figure 3.3B). Therefore the best binding conditions have been determined as follows: a particle concentration of 2.5 mg/ml, a ratio of lysozyme to Affitin of 1:3, and an incubation step at lower temperatures, which resulted in a final binding of 58.3 ± 12.6 mg lysozyme/g support.

The first approach for lysozyme recovery from the magnetic supports was determined by setting the phosphate buffer and tuning the pH and NaCl concentration (Figure 3.4A). Varying the salt concentration resulted in different elution yields, with higher yields observed at lower NaCl concentration. However, the pH of the buffer was the determinant condition for lysozyme elution. A higher elution yield (24.3 ± 5.6 mg/g support) was obtained at acidic pH 2.5, as classically observed in affinity chromatography. For example, the salt-bridge formed at neutral pH between Asp52 (pK_a = 3.9) and Lys39 of Affitin H4-Ct could be disrupted as aspartic acid is no longer negatively charged at low pH [142]. This would contribute to the dissociation of the two proteins. Higher lysozyme recoveries from magnetic supports were also observed by Chen *et al.* at lower pH values [163]. Good yields were also obtained at pH 11.0, a value closed to the isoelectric point of lysozyme, contributing for the disruption of the interaction between Affitin and lysozyme. For instance, the same Lys39 of lysozyme (pK_a = 9.74) [142] is no longer protonated at pH 11.0.

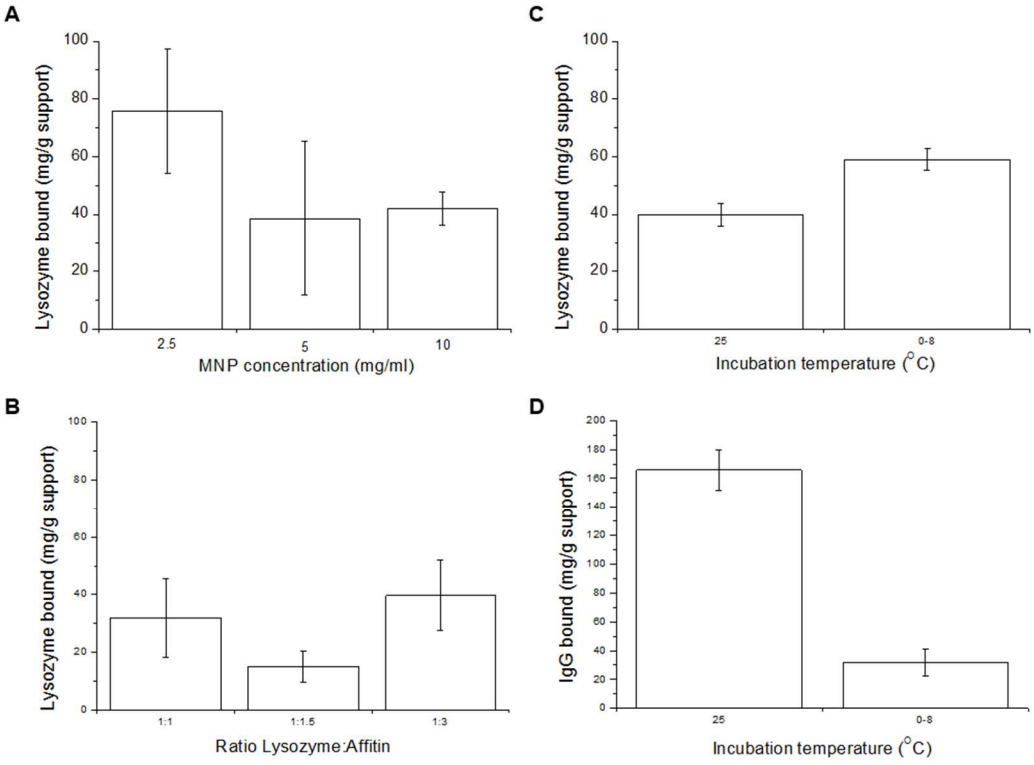

Figure 3.3. Optimization of lysozyme binding to MP-H4-Ct by changing: (A) MP concentration (mg/ml; performed at 0-8 °C), (B) ratio lysozyme to immobilized Affitin (performed at 0-8 °C) and (C) incubation temperature (°C). (D) hIgG binding to MP-D1Sso7d-DM-Ct with 2.5 mg/ml MP (performed at 0-8 °C), and a 1:3 hIgG to Affitin ratio changing the incubation temperature.

Due to its capacity to disrupt hydrophobic interactions, 50% ethylene glycol was also added to the elution buffers at pH 2.5 and pH 11.0 (data not shown). It was observed the recovery of 17.6 mg lysozyme/g support and 7.1 mg lysozyme/g support at pH 2.5 and pH 11.0, respectively, therefore showing that the presence of ethylene glycol decreased the recovery yield. The results suggest that hydrophobic contacts identified between lysozyme and the Affitin H4 do not contribute as significantly as hydrogen bonds and salt bridges [142] (Figure 3.4A).The best elution condition (0.15 M NaCl, pH 2.5) was tested with a glycine-HCl buffer, to study the influence of the buffer composition (Figure 3.4B). This resulted in recovering twice the amount of lysozyme than using a phosphate buffer for the same pH, with a total of 55.0 ± 4.1 mg lysozyme eluted/g support. Additionally, an SDS-PAGE gel analysis was performed to confirm lysozyme elution, and at the same time that the low pH does not promote Affitin leakage from the support as no band corresponding to about 9 kDa was visible on the gel (Figure 3.4C).

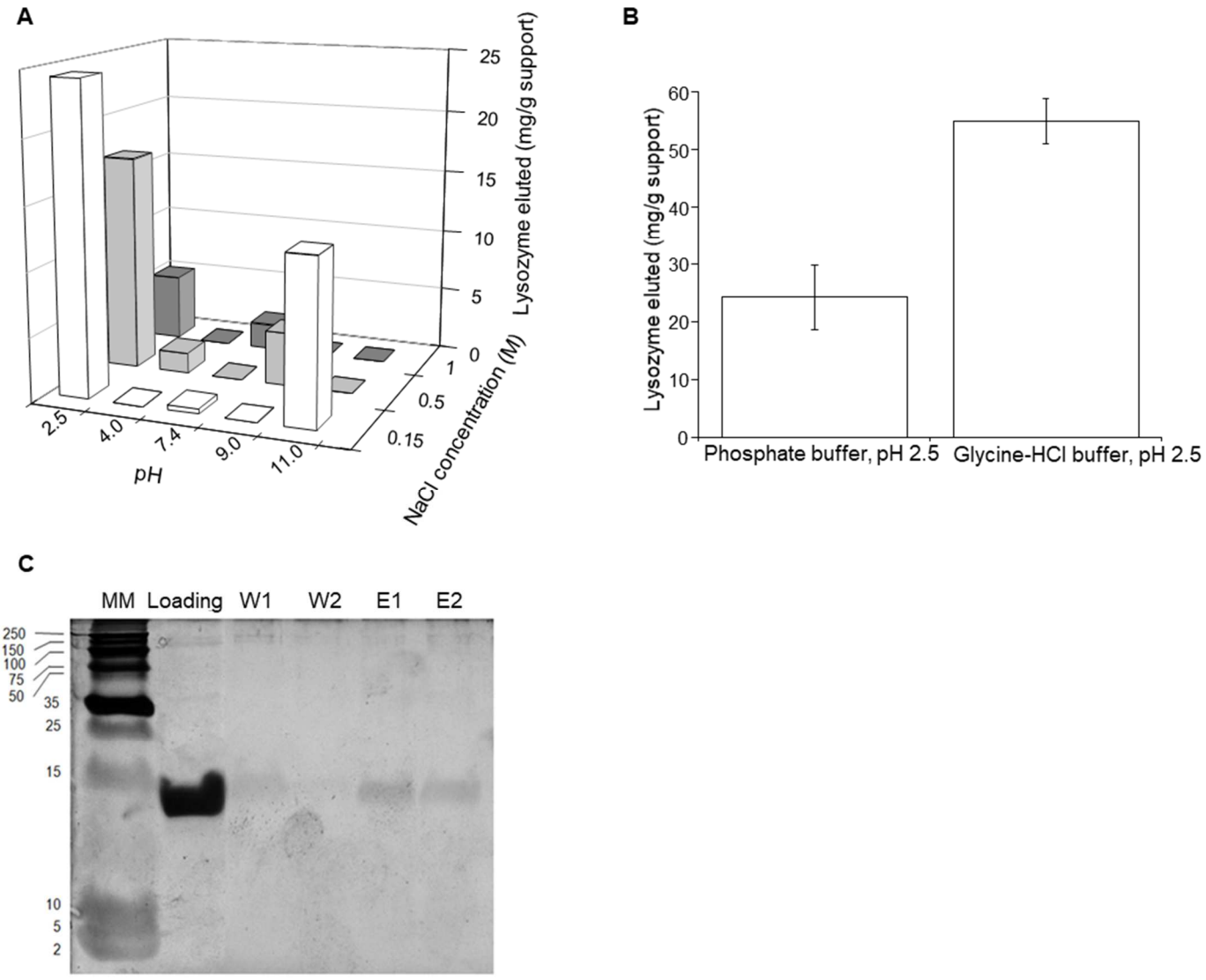

Figure 3.4. Optimization of lysozyme elution from Affitin-functionalized magnetic particles. (**A**) Using a 10 mM phosphate buffer, varying the pH conditions and NaCl concentration. (**B**) Comparing lysozyme elution using 10 mM phosphate buffer, 0.15 M NaCl, pH 2.5 and 100 mM glycine buffer, 0.15 M NaCl, pH 2.5. (**C**) Coomassie stained SDS-PAGE gel (12.5% acrylamide) in reducing conditions of purification fractions collected using pure lysozyme from chicken egg white using as purification conditions 2.5 mg/ml MP functionalized, with an incubation period of 30 minutes at 4°C, as elution buffer 100 mM glycine buffer, 0.15 M NaCl, pH 2.5 was used. Lanes ID: MM: Precision Plus ProteinTM Dual Color Standards (molecular weight in kDa); Loading: pure lysozyme from chicken egg white; W1: first wash; W2: second wash; E1: first elution; E2: second elution.

3.3.4. Application of the magnetic adsorbent for lysozyme recovery

The performance of the MP-H4-Ct support for the recovery of lysozyme from an *E. coli* crude extract was tested. A cell-free *E. coli* supernatant was spiked with 0.8 mg/ml of lysozyme for a total protein concentration of 2.1 ± 0.5 mg total protein/ml in 500 µl, and incubated with 500 µl of 2.5 mg MP-H4-Ct/ml for 30 minutes at 0-8°C. Afterwards, the support was washed with PBS and the bound protein was eluted with 100 mM glycine-HCl buffer, 0.15 M NaCl, pH 2.5. The resultant samples were analyzed by SDS-PAGE (Figure 3.5A). It was possible to confirm that most host-cell proteins were present in the flow-through (FT) and first wash, and no lysozyme was present after the third wash. The non-specific binding of host cell proteins to the magnetic support was negligible even with about seven times more concentrated crude extract proteins. A one-step elution was possible with 100 mM glycine-HCl buffer, 0.15 M NaCl, pH 2.5, with a lower concentration of lysozyme coming out in the following elution steps. It was possible to achieve a final lysozyme purity ≥95%, which is higher than the purity values described for the one-step purification of lysozyme from non-diluted egg white [164] although the protein complexity of this kind of sample is much lower than an *E. coli* crude extract.

3.3.5. Application of the magnetic adsorbent for IgG recovery

Following the optimization process using MPs functionalized with the anti-lysozyme Affitin, the best conditions were applied for the immobilization of Affitin D1Sso7d-DM-Ct (anti-IgG) on MP and for the purification of IgG. Regarding the immobilization of Affitin D1Sso7d-DM-Ct on the magnetic support, the following optimized conditions were used - 2.5 mg/ml of MP, a 1:0.1 NH_2:Affitin ratio, without any reduction agent-, resulting in a final immobilization of 15.1 ± 0.76 µmol Affitin D1Sso7d-DM-Ct/g support (133.5 ± 6.7 mg Affitin D1Sso7d-DM-Ct/g support). Regarding the optimization of the binding conditions, the MP concentration (2.5 mg/ml) and the protein:Affitin ratio (1:3) were maintained constant, changing the incubation temperature. The binding was compared at 25°C and 0-8°C, since previous studies showed binding of this Affitin to the target protein at room temperature [142,144]. Before functionalization, aminated supports were tested for non-specific binding to IgG resulting in 4.7 ± 1.6 % IgG bound (loading 0.25 mg). For the functionalized magnetic particles, the results (Figure 3.3B) showed that IgG was able to bind at both temperatures after 30 minutes incubation period. However, better results were obtained at 25°C with a 165.8 ± 14.1 mg IgG/g support binding. Bound IgG was eluted using 100 mM glycine-HCl with 0.15 M NaCl at pH 2.5, resulting in a recovery yield of 165.8 ± 9.3 mg IgG/g support, meaning 100% of the bound IgG was eluted in a one-step elution. The interaction between Affitin D1Sso7d-DM-Ct occurs in the Fc region of IgG but not in the same recognition sites as for protein A or CD64, two proteins known to bind strongly to IgG. One of the Affitin residues strongly involved in IgG recognition is Asp26 (pK_a = 3.9) [144]. Hence at low pH this negatively charge residue is no longer charged and this could contribute to disrupt the interaction between Affitin and IgG.

To assess the purification capacity of MP functionalized with anti-IgG Afftin, human serum was used as crude extract. In Figure 3.5B, it is possible to confirm the washing of most proteins in the FT fraction, although no IgG is present (50 and 25 kDa). This confirms that IgG remains bound to the affinity magnetic support. Likewise, no IgG was lost in the two following washes. Three elution steps were performed; nonetheless IgG was only eluted in the first elution enabling not only its recovery but also its concentration. At the end it was possible to achieve a final purity of 81% with an approximate final concentration of 60 mg IgG eluted/g support. Higher final purities have been reported for the isolation of antibodies from CHO cell culture (higher than 95%) [21,110,136]. However, our tests were performed with human plasma which contains a higher abundance of contaminant proteins (25 mg total protein/mg IgG) when compared to CHO cell culture supernatant (1.5 mg host cell protein/mg IgG) [165–167]. In addition, human plasma contains all Ig classes, even though it's known that D1Sso7d-DM-Ct does not interact with IgA [144], its binding to other classes in unknown, therefore the extra bands in the elution fraction may also be related to other classes of Ig with higher molecular weight, such as IgM.

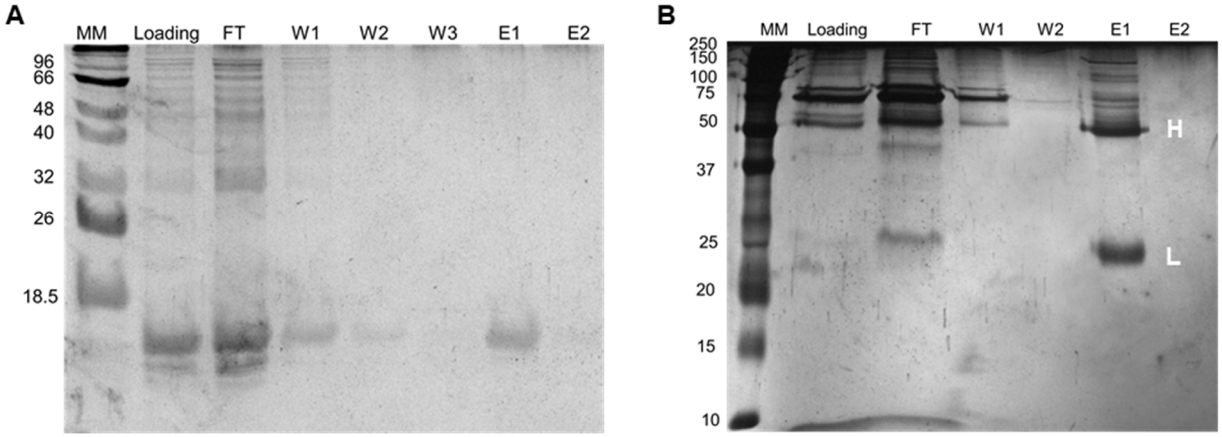

Figure 3.5. Purification performance of H4-Ct and D1Sso7d-DM-Ct for (**A**) lysozyme and (**B**) IgG. Silver stained SDS-PAGE gel (12.5% acrylamide) in reducing conditions of purification fractions collected using crude extracts from (**A**) *E.coli* supernatant and (**B**) human plasma using as purification conditions 2.5 mg/ml MP functionalized, with an incubation period of 30minutes at (**A**) 4°C and (**B**) 25°C, as elution buffer 100 mM glycine buffer, 0.15 M NaCl, pH 2.5 was used. Lanes ID: MM: (**A**) Low molecular weight Protein Marker and (**B**) Precision Plus ProteinTM Dual Color Standards (molecular weight in kDa); Loading: Crude extracts loaded: (**A**) E.coli supernatant and (**B**) human plasma; FT: flow-through; W1: first wash; W2: second wash; W3: third wash; E1: first elution; E2: second elution (all fraction with the same protein concentration (0.06 mg total protein/ml). Position of IgG heavy (**H**) (50 kDa) and light (**L**) (25 kDa) chains are indicated in the right side of the gel.

3.3.6. Determination of the binding constants by static partition experiments

The affinity constant (K_a) and Hill coefficient were determined by the application of Hill plot adjusted to data obtained from partition equilibrium studies (Figure 3.6A; B), with the maximum binding capacity of the supports (Q_{max}) estimated by the Langmuir model (Figure 3.6C; D). The obtained values are summarized in Table 3.1. Considering the estimated static Q_{max}, the value obtained for MP-H4-Ct (287 ± 41 mg lysozyme /g support or 20 ± 3 µmol lysozyme/g support) was significantly higher than the Q_{max} value obtained for other lysozyme magnetic purification systems (e.g. 70 mg lysozyme/g [168] and 138 mg/g [164]), but within the range of other works relying on ion-exchange supports with high surface area (209 mg lysozyme/g support [169]). As for the MP-D1Sso7d-DM-Ct adsorbent, a lower Q_{max} was observed (157 ± 13 mg IgG/g support or 1.1 ± 0.1 µmol IgG/g support), which might be due to steric hindrance between immobilized Affitin and the large IgG molecule. This problem could be surpassed with a longer spacer between the MP and Affitin.

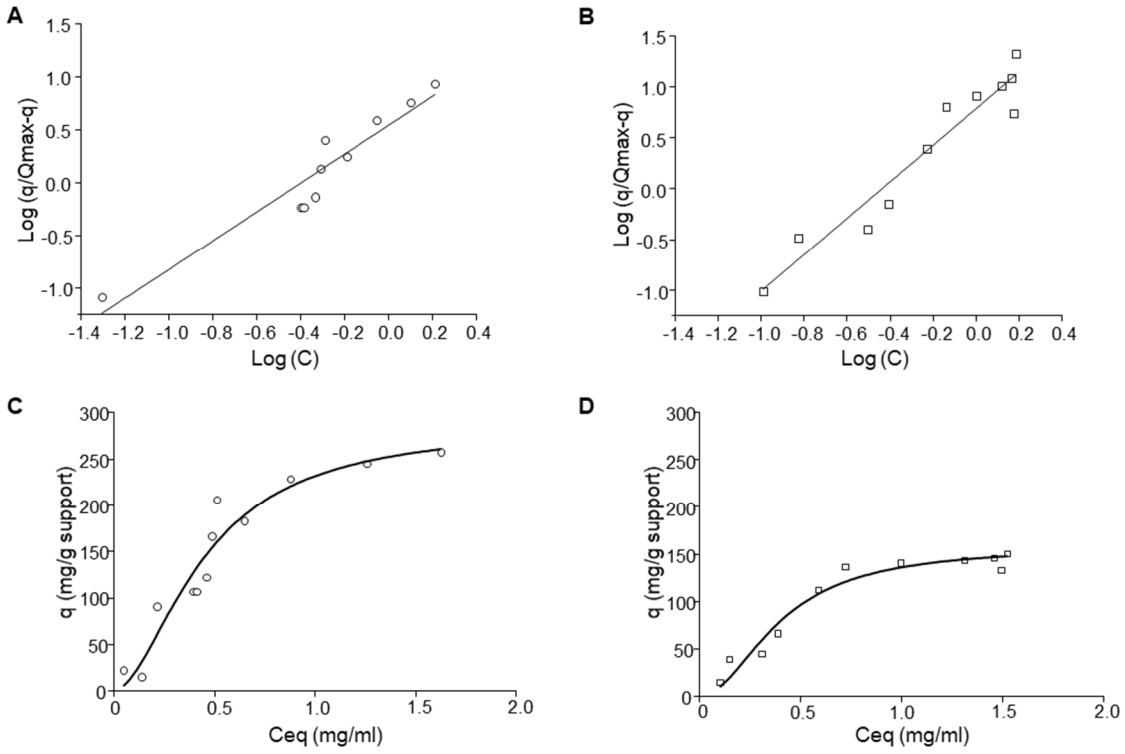

Figure 3.6. Binding isotherms for the affinity pair MP-H4-Ct and lysozyme (**A** and **C**; ○) and MP-D1Sso7d-DM-Ct and hIgG (**B** and **D**; □). The experimental results (**C** and **D**) were fitted to the Langmuir model (q= ((Qmax × Ka × C) / (1 + Ka ×C)), where q is the bound protein per mass of support (mg/g support) and C corresponds to the concentration of unbound protein in equilibrium (mg/ml) [43]. The experimental results (**A** and **B**) were fitted to the Hill plot linearization Log(q/ (Qmax-q)) = Log(Ka) + nH x Log(C), where q is the bound protein per mass of support (mg/g support) and C corresponds to the concentration of unbound protein in equilibrium (mg/ml) [41].

The K_a obtained for the MP-H4-Ct was lower than that described originally by Correa *et al.* between the free Affitin and lysozyme by isothermal titration calorimetry (5.0×10^4 M^{-1} *vs* 1.1×10^8 M^{-1}) [142]. It is commonly observed that immobilization tends to alter the binding constants due to the influence of the support and linker chemistry [170]. Still, the K_a value obtained was within the range considered suitable for purification methods (10^3-10^9 M^{-1} [171]), with K_a values between 10^4 - 10^5 M^{-1}, considered ideal for reversible binding/elution purification schemes. Regarding the MP- D1Sso7d-DM-Ct, the system also presented a K_a favorable for purification (9.3×10^5 M^{-1}), and these results are in line with previous reporting a 4×10^6 M^{-1} for this Affitin by surface plasma resonance experiments [149]. In both affinity pairs the Hill coefficient determined was higher than 1 (n>1), demonstrating a positive cooperative binding in both cases.

Table 3.1. Binding constants determined for both affinity pairs by fitting of the experimental results to Langmuir isotherm and Hill.

	Affinity pair	K_a (M^{-1})	Q_{max} (mg/g support)	Hill factor (n)	R^2	K_a reported in literature (M^{-1})
Langmuir isotherm	MP-H4-Ct/Lysozyme	$6.1\times10^4 \pm 4.5\times10^4$	287 ± 41	-	0.90	11×10^8 [6]
	MP-D1Sso7d-DM-Ct/hIgG	$9.2\times10^5 \pm 4.7\times10^5$	157 ± 13	-	0.94	4×10^6 [12]
Hill plot	MP-H4-Ct/Lysozyme	$5.0\times10^4 \pm 1.7\times10^4$	287 ± 41	1.4 ± 0.1	0.90	11×10^8 [6]
	MP-D1Sso7d-DM-Ct/hIgG	$9.3\times10^5 \pm 1.8\times10^5$	157 ± 13	1.8 ± 0.2	0.92	4×10^6 [12]

3.4. Conclusions

This work reports the first successful immobilization of Affitins on magnetic particles to yield an efficient platform for protein purification by magnetic fishing. Here, an optimization study was done in order to improve the immobilization, binding and elution conditions, which represent a critical step in any novel purification scheme. The optimal lysozyme binding conditions - particle concentration of 2.5 mg/ml, an incubation step at low temperature and a 1:3 lysozyme to Affitin ratio- resulted in 58.3 ± 12.6 mg lysozyme bound/g support, similar to what was obtained in other studies (e.g. 76.5 mg lysozyme/g support) [168]. On the other hand, IgG purification had the best results at room temperature, binding over 165.8 ± 14.1 mg IgG/g support, a higher amount than those reported using MP (51 mg IgG/g support [172] or 130 mg IgG/g support [22,136]). The binding parameters, Q_{max} and K_a for both proteins are favorable for the use of MP

with Affitins for purification purposes. All these results confirm attractive features observed previously for Affitins immobilized on agarose matrix and their use for affinity purification applications [150].

The best elution conditions were 100 mM glycine-HCl with 0.15 M NaCl at pH 2.5, allowing the recovery of 55.0 ± 4.1 mg lysozyme/g support and 157 mg IgG/g support. Using this elution condition and pure proteins, it was possible to recover 100% of lysozyme and IgG in a one-step elution. When performing the proteins purification from heterogeneous samples, crude extracts of *E.coli* for lysozyme separation, and human serum for IgG separation, it was possible to have a final purity of 100% for lysozyme and 81% for IgG.

Here we have reported two systems for protein purification using MP functionalized with Affitins. These Affitins have been proven to be highly specific for their cognate targets, robust under the extreme acidic or alkaline pH generally used for affinity separations, well produced in *E. coli* and easy to engineer [149]. All these properties might contribute to development of cost effective magnetic separation systems not only for lysozyme and IgG, but virtually for any protein of interest given the versatility of Affitins. We anticipate Affitin-MPs might find a broad panel of applications, such as research and diagnostics tools, either to quickly enrich a sample for a given target or on the contrary to deplete it from samples, and as an alternative to the traditional chromatographic systems.

Chapter 4

Magnetic crystallization as new approach for protein crystallization

Manuscript in revision for peer-review publication

dos Santos, R. Romão, MJ, Roque, ACA, Carvalho, AL. Magnetic crystallization as new approach for protein crystallization. J. Phys. Chemistry. (2020)

Authors contributions:

RS, MJR, ACAR and ALC, designed the work. The experiments and manuscript preparation were conducted by RS. Manuscript revision were conducted by ACAR and ALC.

Abstract

After more than one hundred and thirty thousand protein structures determined by X-ray crystallography, the challenge of protein crystallization for 3D structure determination remains. As new additives emerge, magnetic particles (MPs) are versatile inorganic materials, easy to use and manipulate in a wide range of biological assays. The potential of using MPs as crystallization chaperones for protein crystallization was here evaluated. MPs coated with different molecules were rationally designed to promote crystallization by affinity-triggered nucleation to enhance protein crystal growth. Hen egg white lysozyme (HEWL), trypsin and green fluorescence protein (GFP), were crystallized in the presence of MPs either bare or coated with a polysaccharide (chitin), a protein (casein) and a synthetic ligand (A4C7), respectively. The addition of MPs was characterized in terms of bound protein to the MPs, crystal morphology, time-lapse of crystal emergence, crystallization yield fold change and crystal diffraction quality for structure determination. The MPs additives have shown to bind to the respective target protein, promoted nucleation and crystal growth and, moreover, crystal morphology did not change in the presence of MPs. On the other hand, MPs addition led to faster detectable crystal emergence and an up to 13 times higher crystallization yield. Structure determination of the protein crystallized in the presence of MPs revealed that the structural characteristics of the protein remained unchanged, as shown by the superposition with PDB annotated proteins. Moreover, and unlike most reported cases, it was possible to crystallize trypsin in the absence of its inhibitor benzamidine. Instead, functionalized MPs were used to trigger crystallization, showing promising results. These inorganic materials, coated with affinity molecules to target proteins, can be used as controlled-crystallization inducers.

4.1 Introduction

High-resolution structure determination of macromolecules alone or in complex with ligands is a powerful tool in protein engineering and drug design. The structural information about a protein is one of the key steps to control or improve its function, by rationally designing small binding molecules [173] (*e.g.* agonist or antagonist drugs), or by engineering mutants with a desirable biological activity [174]. On the other hand, the three-dimensional high-resolution structure of molecular complexes can unveil macromolecule-ligand interactions enhancing its biotechnological applications in fields such as biocatalysis [175], sensing material development [176], macromolecule function redesign [177], or in the downstream processing field [178].

One of the most powerful tools for high-resolution structure determination is X-ray crystallography, providing an atomic resolution 3D structure of a single protein, protein-DNA complex, protein-protein or a protein-ligand complex. X-ray crystallography requires high-quality protein crystals for X-ray diffraction. However, the major bottleneck still lies in finding the conditions that give rise to diffraction-quality single crystals, added to reliable reproducibility. This can be overcome by developing new and more efficient

crystallization screening protocols, but also by introducing new additives that can act as nucleation agents for protein crystal growth.

Protein crystallization occurs under saturated conditions, by changing the protein environment until protein's solubility limit is exceeded, leading to nucleation and crystal growth. The supersaturating environment is most of the times determined in an empirical manner. Although classical nucleation theory and phase diagram plots may enlighten the interactions promoting protein crystallization, the fact is that protein crystallization is still a rather empirical process. The formation of a protein crystal starts with the nucleation phase in which the protein molecules, in the supersaturated solution, become arranged in a specific repetitive pattern, characteristic of the crystalline form. Then, additional protein molecules are deposited on the nucleus surface and the crystal grows in progressive layers. To overcome some of the protein crystallization challenges, with the prospect of developing a more general and straightforward crystallization process, new additives with nucleation properties are frequently tested. An additive for crystallization purposes is any compound used to facilitate nucleation events, reduce the crystal solvent content or prepare heavy atom derivatives.[179,180]. Traditional additives commonly found in the crystallization screening protocols rely mainly on surfactants, organic compounds, mono- and multivalent salts, reducing agents, amino acids or monosaccharides. New additives can be of biological source, such as DNA origami [181] and cyclic oligosaccharides [182], or of non-biological origin as small synthetic ligands [180] or nanoscale materials [59]. In particular, new nanoscale materials, namely nanoparticles made of gold, porous silicon or nanodiamonds, as well as carbon nanotubes, have already been successfully used as nucleation agents to trigger crystal growth in different protein crystallization studies for 3D structure determination [183–187].

Magnetic particles with an iron oxide (Fe_3O_4) core are another class of nanomaterials never used in the context of protein crystallization. Among the advantages of magnetic particles, they are low cost, easy to produce and handle, and able to be tailored with different coatings and functionalization. In addition, with a superparamagnetic core, these particles can be easily separated from a solution by applying an external magnetic field and reversibly resuspended back in solution [136,188,189].

Here, we aimed to study the potential of magnetic nanoparticles as additives in protein crystallization. Three proteins were selected as model case studies: hen egg white lysozyme (HEWL), bovine trypsin and green fluorescent protein (GFP) from *Aequorea victoria*. To promote the selective binding of the target protein to the surface of the magnetic nanoparticles, known affinity ligands for HEWL, trypsin and GFP were coated to the surface of the particles. The obtained protein single crystals were further evaluated in terms of X-ray diffraction quality. Our results indicate that the presence of magnetic particles as crystallization additives to improve protein nucleation caused no changes in maximum resolution limits or in unit cell parameters, maintaining crystal isomorphism when compared to native conditions. Furthermore, the addition of magnetic particles led to the increase of crystallization yield and enabled a reproducible crystallization of trypsin in the absence of its inhibitor benzamidine, commonly used in trypsin crystallization assays.

4.2. Materials and methods

4.2.1. Reagents and equipment

All chemicals were at least 98% pure and solvents pro-analysis grade. All produced magnetic supports were characterized by Fourier-transform infrared spectroscopy (FT-IR), dynamic light scattering (DLS), zeta potential and transmission electron microscopy (TEM). Infrared spectra were measured on a Tensor 27 FT-IR spectrometer from Bruker with dried MPs grounded and mixed with KBr (1:100). DLS and zeta potential (0.05 mg/ml solution in deionized water, pH 5.80, or other solution if otherwise stated) were measured on Dynamic Zetasizer NanoZS from Malvern instruments. TEM of magnetic particles samples were collected using Hitachi 8100 microscope operated with 200 kV of acceleration voltage with ThermoNoran light elements EDS detector and digital image acquisition.

4.2.2. Preparation iron oxide magnetic particles

Fe_3O_4 magnetic particles (MP-Fe_3O_4) were prepared by the chemical co-precipitation method [190]. Briefly, 0.225 M $FeCl_3 \cdot 6H_2O$ (24.33 g in 400 ml of H_2O) and 1.43 M $FeCl_2 \cdot 4H_2O$ (10.79 g in 45 ml of H_2O) were mixed under mechanical stirring until homogenization was achieved. A 25% NH_4OH solution (75 ml) was added to the mixture under constant mechanical stirring (200 RPM). The resulted mixture was vigorously stirred for 5 minutes. MP-Fe_3O_4 were separated by a magnet and washed with distilled water several times until pH 7 was reached.

A suspension of 10 mg/ml MP-Fe_3O_4 was sonicated for 15 minutes and further coated with a chitin suspension (80 mg/ml; 20 mg in 2.5 ml), added dropwise to the MP-Fe_3O_4 suspension, under sonication. The mixture was incubated for 16 hours at 60ºC with vigorous stirring (200 RPM). After this, the Fe_3O_4-chitin magnetic particles (MP-chitin) were separated by a magnet and washed (10 times) with distilled water. Chitin adsorption was measured by the anthrone method as previously described [191], with 90% adsorption achieved.

The synthesis of Fe_3O_4-casein magnetic particles (MP-casein), was adapted from Alves and co-authors protocol [192]. A solution of 10 ml of 0.225 M $FeCl_3 \cdot 6H_2O$ was added to 10 ml 1.43 M $FeCl_2 \cdot 4H_2O$ and next added to a 20 mg/ml casein (from bovine milk powder) solution in 100 mM Tris-HCl at pH 8.0. The mixture pH was adjusted to pH 11 using 25% ammonium hydroxide solution. Next, the mixture was incubated for 30 minutes at 50ºC under orbital shaking (200 RPM). MP-casein were separated by a magnet and washed with distilled water several times until pH 7 was reached. The casein bound to Fe_3O_4 magnetic core was quantified using absorption at 280nm, yielding 80% binding.

Fe_3O_4 particle solution (10 mg/ml), synthesized by the co-precipitation method, was sonicated for 15 minutes, and then added to a solution of sodium metasilicate pentahydrate (from Sigma-Aldrich) in 50% (v/v) ethanol/water (28.5 mg/ml). The reaction was stopped after 2 hours at 40ºC with orbital shaking (200 RPM) and the particles washed with distilled water (10 times). The particles were resuspended in 20% (v/v)

ethanol/water (80 ml) and sonicated for 10 min, followed by dropwise addition, still during sonication, of 25% ammonium hydroxide (3 ml) and tetraethyl orthosilicate (TEOS) (1.5 ml, Sigma-Aldrich). The reaction was stopped after 2 hours at 40ºC with orbital shaking (200 RPM), and the particles washed with distilled water (10 times). The particles were resuspended in 175 ml of distilled water and sonicated for 10 minutes and further coated with dextran (from *Leuconostoc mesenteroides* 150 kDa, Sigma-Aldrich). A dextran solution (80 mg/ml in distilled water) was added dropwise to the particle solution and the mixture incubated (60°C, 2 hours with orbital shaking, 200 RPM), after which the particles were washed 5 times with distillated water. Magnetic particles coated with dextran were further functionalized with synthetic UGI ligand A4C7 [193] (MP-A4C7). Synthetic ligands based on the UGI reaction are obtained from the reaction between the aldehyde-functionalized support, an amine, a carboxylic acid and isopropyl isocyanide. The particles were firstly aminated using (3-aminopropyl)triethoxysilane (APTES). The amine content was quantified by the Kaiser Test yielding 213.3 ± 3.8 µmol NH_2/g of dried MP. The aminated particles were resuspended in 5% (v/v) glutaraldehyde and 1 M NaOH, sonicated for 5 min and incubated for 1h at 3ºC with orbital shaking (200 RPM). After this, the particles were washed with distilled water (5 times). The first substitution was the amine (1-pyrenemethylamine hydrochloride) (5 molar excess to the amine content, in methanol). The reaction was performed under 60ºC for 2 hours with orbital shaking (200 RPM), followed by addition of the carboxylic acid (phenylacetic acid) (5 excess molar to the amines content, in methanol) and isopropyl isocyanide (5 excess molar to the amines content), and incubated for 48 hours at 60ºC with orbital shaking (200 RPM). The particles were washed with methanol (2 times), 50% (v/v) DMF (N,N-dimethylformamide)/methanol (2 times), distilled water (1 time), 0.1 M sodium hydroxide with 30% isopropanol (2 times), distilled water (5 times). Finally, the particles were resuspended in the appropriated volume of water.

4.2.3. Biological material

Pure lysozyme from chicken egg white (protein ≥90 %, ≥40,000 units/mg protein, Sigma-Aldrich), pure Trypsin from bovine pancreas (PanReac AppliChem) and recombinantly expressed green fluorescent protein (GFP) were used in the crystallization assays. For GFP expression, glycerol stocks with transformed *E. coli* cells BL21(DE3) pET-21C plasmid encoding GFP (Geneart) were used as described [194]. The pre-inoculum samples (glycerol stocks (5 µl)) were incubated in LB medium (5 ml) with ampicillin (100 µl/ml final concentration) for 6 hours at 37ºC and 220 RPM. The pre-inoculum (1 ml) was placed in 500 ml shaking flask with LB medium (100 ml) and ampicillin (100 µl/ml final concentration) for 16 hours at 37ºC and 220 RPM. For protein expression, the inoculum (20 ml) was placed in a 5000 ml shaking flask with LB medium (2000 ml) and ampicillin (100 µl/ml final concentration) at 37ºC with 220 RPM orbital shaking. At OD_{600nm}= 0.6-0.8, 3-5 hours after growth, protein expression was induced with the addition of IPTG (1 mM final concentration) and culture growth was performed for 22 hours with 220 RPM at 37ºC. Afterwards, cell harvest was done by centrifugation (4500 x*g*, 15 min, 4ºC), and the pellet resuspended in 10 mM Tris-HCl at pH 8. The resuspended pellet was subjected to three freeze/thaw cycles and cell lyses carried out in a

French Press (four passages at 1000 psi). The resulting lysates were treated with 10% (w/v) DNase I for 15 min at 4ºC, following a centrifugation (10 000 x*g*, 30 min, 4ºC) and an ultracentrifugation (22 000 x*g*, 90 min, 4ºC). The soluble fraction was further purified having as capture step the multimodal chromatography using A4C7 synthetic ligand, as described [193]. The eluted fractions were pooled and dialyzed to 20 mM Tris-HCl at pH 8. Following, a polishing step using anion exchange chromatography using MonoQ (GE Healthcare, Sweden) having as binding buffer 20 mM Tris-HCl at pH 8 and as elution buffer 1 M NaCl in 20 mM Tris-HCl pH 8. The final soluble crude extract was quantified by fluorescence (λex = 485 nm, λem = 535 nm, calibration curve [GFP] 10^6 –10^1 mg/ml; Evrogen, Russia) and bicinchoninic acid colorimetric assay (BCA, calibration curve [BSA] 0.2-1 mg/ml, Sigma–Aldrich). Purity assessment was performed with Sodium dodecyl sulfate–polyacrylamide gel electrophoresis (SDS–PAGE). The buffer sample composition was 0.15 M Tris–HCl at pH 6.8, 6% (w/v) SDS, 0.025% (w/v) bromophenol blue, 12.5% (v/v) glycerol and as reducing agent β-mercaptoethanol was used. Prior to loading in the gel, all the samples were denaturated at 100°C for 5 minutes. Samples were applied in a 12.5%, prepared from 41% acrylamide/bis stock solution (30:1) from Bio-Rad and migrated at 90 mV using as running buffer 192 mM glycine, 25 mM Tris-HCl and 0.1% SDS, pH 8.3. Gels were Coomassie stained with the staining solution of 0.5% (w/v) Coomassie Blue R-250, 7.5% (v/v) acetic acid, 45% (v/v) methanol, for 30 minutes at room temperature with orbital shaking and revealed with the distaining solution (7.5% (v/v) acetic acid, 45% (v/v) methanol) until proper protein visualization. Images were acquired with Gel Doc™ XR+ System with Image Lab™ software from Bio-Rad and analyzed with ImageJ software.

4.2.4. Static binding capacity

MP-Fe_3O_4 (0.5 mg/ml) and MP-chitin (0.5 mg/ml) in 0.5 M NaCl were separately incubated with HEWL at different concentrations (0.2 to 5 mg/ml) in 50 mM CH_3COONa at pH 4.5. 0.5 mg/ml of MP-Fe_3O_4 and MP-casein in 0.2 M $(NH_4)_2SO_4$ with 30% (w/v) PEG8000 were separately incubated with trypsin at different concentrations (0.2 to 5 mg/ml) in (a) 3 mM $CaCl_2$ with 10 mg/ml benzamidine and (b) 3 mM $CaCl_2$. The interaction was promoted over 16 h at 20ºC. The supernatants were collected, and fluorescence intensity was measured (λex = 280 nm and λem = 340 nm). The adsorption phenomena followed a Hill isotherm (Equation 4.1) and the experimental data was fitted using OriginPro (v8.5.1).

$$q=\frac{Q_{max}\times K_a\times C^{1-n}}{1+K_a\times C^{1-n}} \qquad \text{Equation 4.1}$$

Where, q is the bound protein per mass of support (mg/g support) and C corresponds to the concentration of unbound protein in equilibrium (mg/ml).

4.2.5. Binding assay

HEWL (500 µl at 25 mg/ml) in 50 mM CH_3COONa at pH 4.5 was incubated with 500 µl of 0.5 mg/ml of MP-Fe_3O_4 and MP-chitin in 0.5 M NaCl for 1 hour at 20ºC with 200 RPM orbital shaking. For trypsin, 500 µl

of 60 mg/ml of trypsin in (a) 3 mM $CaCl_2$ with 10 mg/ml benzamidine and (b) 3 mM $CaCl_2$ were incubated with 500 µl of 0.5 mg/ml of MP-Fe_3O_4 and MP-casein in 0.2 M $(NH_4)_2SO_4$ with 30% (w/v) PEG8000, for 1 hour at 20ºC with 200 RPM orbital shaking. The supernatants were collected, and fluorescence intensity was measured (λex = 280 nm and λem = 340 nm).

4.2.6. Magnetic crystallization

Crystallization assays were performed using the hanging drop method in 24-well crystallization plates. The crystallization setups were carried out at 20ºC and drop inspections were performed using an optical microscope (V81 Stereo Microscope equipped with Camera – AxioCam Erc5s (5 MP), ZEISS). HEWL in 50 mM CH_3COONa at pH 4.5 (25 mg/ml) was crystallized using the following precipitant solutions: (i) 500 µl of 0.5 M NaCl, (ii) 0.5 mg/ml MP-Fe_3O_4 in 500 µl of 0.5 M NaCl and (iii) 0.5 mg/ml MP-chitin in 500 µl of 0.5 M NaCl, in 4 µl crystallization drops with 1:1 protein-to-precipitant ratio. 60 mg/ml of trypsin from bovine pancreas in (a) 3 mM $CaCl_2$ with 10 mg/ml benzamidine and (b) 3 mM $CaCl_2$ were crystallized using the following precipitant solutions: (i) 500 µl of 0.2 M $(NH_4)_2SO_4$ with 30% (w/v) polyethylene glycol 8000 (PEG8000), (ii) 0.5 mg/ml MP-Fe_3O_4 in 500 µl of 0.2 M $(NH_4)_2SO_4$ with 30% (w/v) PEG8000 and (iii) 0.5 mg/ml MP-casein in 500 µl of 0.2 M $(NH_4)_2SO_4$ with 30% (w/v) PEG8000, in 4 µl crystallization drops with 1:1 protein to precipitant ratio. 15 mg/ml of GFP in 10 mM Tris-HCl at pH 8.0 were crystallized using the following precipitant solutions: (i) 500 µl of 0.05 M KH_2PO_4 and 20% (w/v) PEG8000 at pH 3.8, (ii) 0.5 mg/ml MP-Fe_3O_4 in 500 µl of 0.05 M KH_2PO_4 and 20% (w/v) PEG8000 at pH 3.8 and (iii) 0.5 mg/ml MP-A4C7 in 500 µl 0.05 M KH_2PO_4 and 20% (w/v) PEG8000 at pH 3.8, in 4 µl crystallization drops with 1:1 protein to precipitant ratio.

4.2.6.1. Yield fold change

The crystallized proteins were harvested from the crystallization drops using a crystallization loop, washed in harvesting solution (with 10% more of the correspondent precipitant in solution) to avoid crystal solubilization and remove precipitated protein adsorbed to the crystal or MPs. Once cleaned, the crystals were solubilized in 10 mM phosphate buffer with 150 mM NaCl at pH 7.4 and centrifuged for 10 minutes at 2000 x*g* at room temperature. The supernatant was retrieved and compared with the loading sample in terms of amount of protein. HEWL and trypsin were quantified by λex = 280 nm and λem = 340 nm, while GFP was quantified by λex = 485 nm, λem =535 nm. The fold change in crystallization yield was calculated by Equation 4.2.

$$\text{Yield fold change} = \frac{\text{mg of protein recovered from the crystallization drop}}{\text{mg of protein recovered from positive control drop}} \qquad \text{Equation 4.2}$$

4.2.7. X-ray diffraction and data processing

Data collections from all suitable protein crystals grown in the presence of different MP-Fe_3O_4 were carried out at the in-house X-ray diffraction facility using a Bruker D8 Venture Cu K_α X-ray generator coupled to a Photon 100 CMOS detector and an Oxford Cryo-Systems nitrogen stream at 100 K. All protein crystals were cryo-protected prior to flash-freezing in liquid nitrogen. HEWL and trypsin were cryo-protected using 20% glycerol added in the harvesting buffer and GFP using paratone. Data were indexed, integrated and scaled using PROTEUM3 software pipeline (Bruker AXS 2015) and converted to observed structure factors using SCALEPACK2MTZ and TRUNCATE from the CCP4 suite [195]. The structures were solved by molecular replacement using PhaserMR [196] within Phenix [197] with previously known structures of the proteins as search models (PDB 6F1L for HEWL, PDB 5MNE for trypsin and PDB 1GFL for GFP). Electron density maps were generated and analysed with COOT [198]. The output model was further refined using PHENIX.REFINE [199]. Water molecules and ions were also modelled into the structures.

4.3. Results and discussion

With the aim to overcome the current challenges that structure determination by X-ray crystallography faces, namely finding crystallization conditions and reproducing good-quality single crystals, iron oxide core magnetic particles (MP-Fe_3O_4) were used as additives. In this work, three different proteins with already known crystallization conditions, were crystallized in the presence of MPs coated or functionalized with the respective affinity ligand (Table 4.1), fomenting affinity-triggered magnetic crystallization.

Table 4.1. Affinity-triggered magnetic crystallization conditions. Proteins reported crystallization conditions and respective maximum resolutions of the X-ray crystallography structures, and the affinity ligands used in the development of the affinity-triggered magnetic crystallization assay.

Reference protein structure (PDB Code)	Molecular weight	Crystallization conditions	Spacegroup	Unit cell parameters (Å)	Matthews Coefficient (A^3/Da)	Affinity ligand
Lysozyme (PDB 6QWY)	14.4 kDa	**Protein solution:** 50 mM CH_3COONa at pH 4.5 **Precipitant solution:** 0.5 M NaCl	$P4_32_12$	*a* = 77.2 *b* = 77.2 *c* = 37.1	1.92	Chitin
Trypsin (PDB 5MNE)	23.3 kDa	**Protein solution:** 3 mM $CaCl_2$ with 10 mg/ml benzamidine **Precipitant solution:** 0.2 M $(NH_4)_2SO_4$ with 30% (w/v) PEG8000	$P2_12_12_1$	*a* = 54.7 *b* = 58.3 *c* = 66.9	2.29	Casein
GFP (PDB 5HGE)	27.0 kDa	**Protein solution:** 10 mM Tris-HCl at pH 8.0 **Precipitant solution:** 0.05 M KH_2PO_4 and 20% (w/v) PEG8000 at pH 3.8	$P2_12_12_1$	*a* = 51.2 *b* = 62.9 *c* = 69.3	2.07	A4C7 (synthetic ligand)

4.3.1. The effect of magnetic particles as additives in crystallization

Prior to the crystallization assays MPs were produced and chemically modified with affinity ligands tailoring each of the target proteins, namely MP-chitin for hen egg white lysozyme (HEWL), MP-casein for trypsin and MP-A4C7 for green fluorescent protein (GFP) assays. In brief, MPs were characterized by Fourier-transform infrared spectroscopy (FT-IR), transmission electron microscopy (TEM), dynamic light scattering (DLS) and zeta potential (Figure 4.1 and Table 4.2). Particles functionalization was confirmed by FT-IR spectra (Figure 4.1A), with spherical shape with 5 to 10 nm in diameter confirmed by TEM (Figure 4.1B). DLS and zeta potential analyses was assessed both in water and in the crystallization conditions of the respective target proteins. Overall MP-Fe_3O_4 present a smaller hydrodynamic diameter when compared with the functionalized MPs in water and in the respective crystallization conditions. Regarding the zeta potential, MP-Fe_3O_4 and functionalized MPs present the same range of stability in water and in the respective crystallization conditions (Table 4.2).

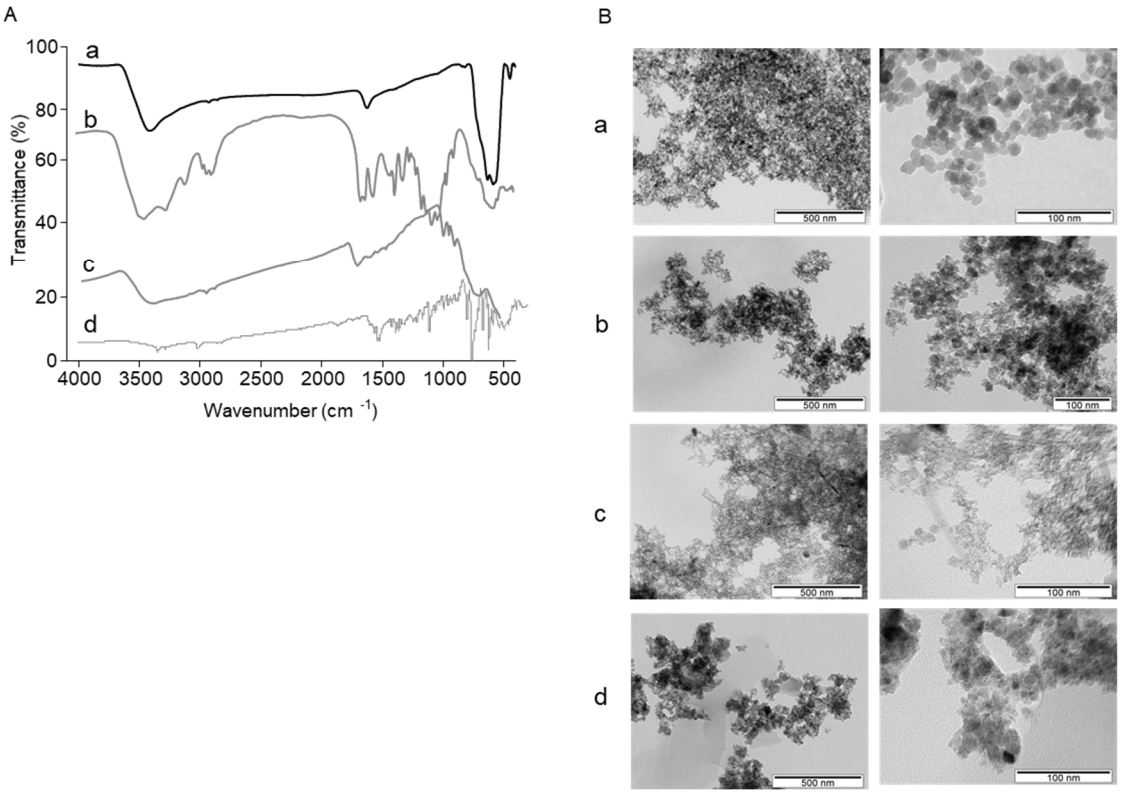

Figure 4.1. Characterization of iron oxide magnetic particles (1 mg/ml) by (**A**) FT-IR and (**B**) Transmission electron microscopy analysis. **Legend**: (**a**) MP-Fe_3O_4; (**b**) MP-chitin; (**c**) MP-casein; (**d**) MP-A4C7.

Table 4.2. Characterization of iron oxide magnetic particles (1 mg/ml) characterization by DLS and zeta potential in different crystallization conditions

	Condition \ MP	MP-Fe_3O_4	MP-chitin	MP-casein	MP-A4C7
DLS (nm)	Water	100.9 ± 0.1	245.5 ± 0.4	8243.5 ± 1579.6	6482.3 ± 784.9
	0.5 M NaCl	5134.8 ± 651.4	4102.0 ± 709.1	-	-
	3 mM $CaCl_2$ with benzamidine	95.99 ± 0.85	-	10665 ± 586	-
	3 mM $CaCl_2$	5446.7 ± 2050.8	-	10556.3 ± 1556.4	-
	20% PEG8000	231.8 ± 14.3	-	-	1331.0 ± 187.7
Zeta potential (mV)	Water	-0.6 ± 0.4	-15.8 ± 0.4	-6.9 ± 1.8	-1.5 ± 0.6
	0.5 M NaCl	10.3 ± 2.8	-13.5 ± 2.2	-	-
	3 mM $CaCl_2$ with benzamidine	23.1 ± 2.8	-	9.7 ± 1.9	-
	3 mM $CaCl_2$	-0.4 ± 0.3	-	14.1 ± 0.5	-
	20% PEG8000	-54.0 ± 1.9	-	-	-42.1 ± 3.6

Crystal growth and crystallization yield, as in yield fold change (Equation 4.2), were assessed using MP-Fe_3O_4 as nucleation agent for HEWL crystallization. Crystal size measurement was impaired by the opacity of MPs in the crystallization drop, hence this was not a reliable method to assess the influence of MPs in protein crystal growth (Figure 4.2A). Nonetheless, having MP-Fe_3O_4 as additives enhanced HEWL crystal growth in all concentrations tested, from 0.5 mg/ml up to 4 mg/ml of MPs. The yield fold change, always having as threshold the HEWL crystallization in the absence of MPs, demonstrated the positive effect (crystal yield >1) of MPs as additives by enhancing the mass of protein crystallized per assay (Figure 4.2B). The data suggested an association between the concentration of MPs added and an increase in protein crystallized. An increase from 1.5 to 1.9 in yield fold change was observed in the presence of 0.5 and 4 g/l of MP-Fe_3O_4, respectively. However, an exponential association was not observed and, for subsequent assays, 0.5 mg/ml of MPs were used as standard MPs concentration to facilitate observations at the microscope. The effect of the addition of MP-Fe_3O_4 was also assessed in the crystallization of trypsin and GFP. These additives had a notorious effect in the amount of trypsin crystallized, as seen in the major difference in yield fold change in the presence and absence of MP-Fe_3O_4 (Figure 4.2C), with up to 12 times more protein crystallized in the presence of MP-casein. The addition of MPs to the GFP crystallization conditions did not affect the crystal growth, and marginal change in the yield fold change of GPF crystallization was improved by 1.1 fold (Figure 4.2C).

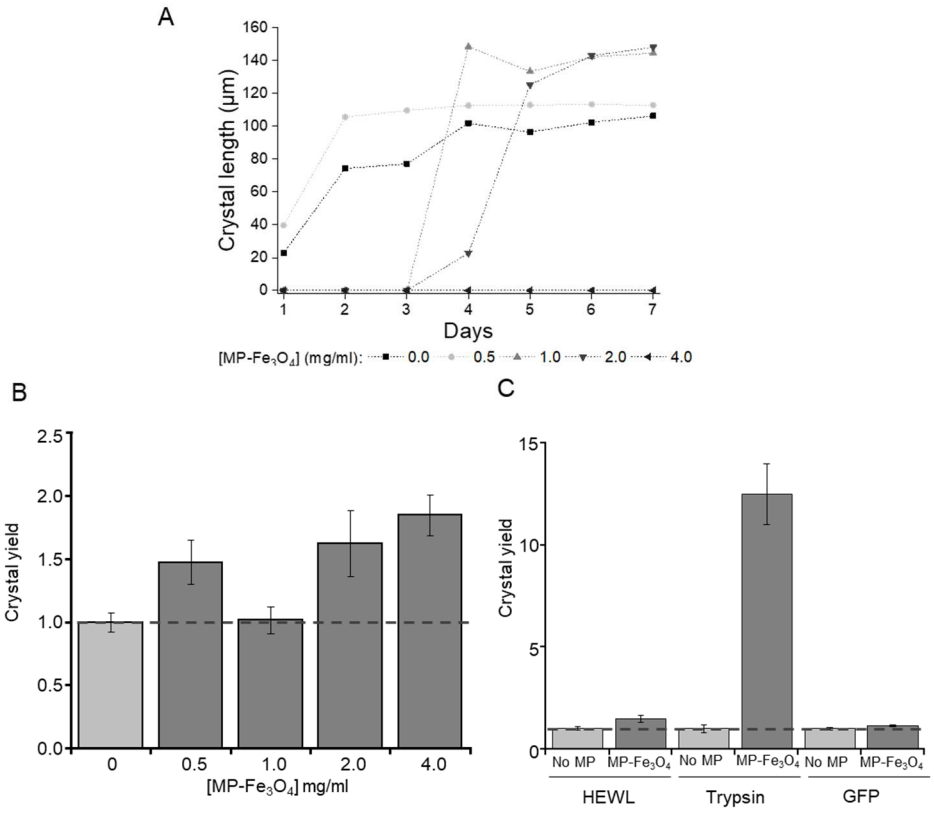

Figure 4.2. Effect of MPs in protein crystal growth (n=3). (**A**) Average crystal longest length of visual measurement of HEWL crystals over 7 days in the presence of MP-Fe_3O_4 at different concentrations: 0 mg/ml (■); 0.5 mg/ml (●); 1 mg/ml (▲); 2 mg/ml (▼) and 4 mg/ml (◄). (**B**) HEWL crystallization yield fold change between crystals grown in the presence of MP-Fe_3O_4 at different concentrations (0, 0.5, 1.0, 2.0 and 4.0 mg/ml). (**C**) HEWL (25 mg/ml), trypsin (60 mg/ml) and GFP (15 mg/ml) crystallization yield fold change between crystals grown in the presence of no MP (**light grey**); 0.5 mg/ml of MP-Fe_3O_4 (**grey**)**.**

4.3.2. The effect of affinity-triggered magnetic crystallization

As HEWL binds to chitin [200], iron oxide MPs coated with chitin (MP-chitin) were evaluated in terms of binding capacity under the HEWL crystallization conditions (Table 4.3). The binding assay of HEWL at 25 mg/ml to both particles - MP-Fe_3O_4 and MP-chitin - at 0.5 mg/ml showed yields higher than 50% (Table 4.3). In the same line, the static binding capacity data of both isotherms were fitted to the Hill plot, since it was the best model to fit the MP-chitin::HEWL binding. The summarized data is shown in Table 4.4. The static binding capacity data (Table 4.3 and Table 4.4) suggested that HEWL binds to both MP-Fe_3O_4 and MP-chitin at static conditions, as indicated by the Q_{max} calculated, K_a and Hill coefficient.

Table 4.3. HEWL adsorption to MP-Fe_3O_4 and MP-chitin (n=3) and trypsin adsorption to MP-Fe_3O_4 and MP-casein in the presence and absence of benzamidine. Binding of 25 mg/ml HEWL in 50 mM CH_3COONa at pH 4.5 to 0.5 mg/ml of MP-Fe_3O_4 and MP-chitin in 0.5 M NaCl (n=3). Binding of 60 mg/ml trypsin in 3 mM $CaCl_2$ in the presence and absence of benzamidine in the protein solution to 0.5 mg/ml of MP-Fe_3O_4 and MP-casein in 0.2 M $(NH_4)_2SO_4$, 30% (w/v) PEG8000 (n=3).

	Bound protein (g protein/g support)	
	MP-Fe_3O_4	**MP-affinity**
Lysozyme	17.8 ± 0.7	22.4 ± 1.1
Trypsin (without benzamidine)	206.4 ± 1.7	206.88 ± 2.2
Trypsin (with benzamidine)	127.7 ± 0.5	126.4 ± 2.9

Table 4.4. Affinity data for the fitting of the affinity pairs HEWL::Fe_3O_4 / HEWL::MP-chitin and trypsin::MP-Fe_3O_4 / trypsin::MP-casein in the presence and absence of benzamidine. The experimental results were fitted to the Hill isotherm $q = Q_{max} \times Ka \times C^{1-n}/(1 + Ka \times C^{1-n})$, where q is the bound protein per mass of support (mg/g support) and C corresponds to the concentration of unbound protein in equilibrium (mg/ml).

	HEWL		**Trypsin**			
	MP-Fe_3O_4	**MP-chitin**	**MP-Fe_3O_4**		**MP-casein**	
			Benzamidine	No benzamidine	Benzamidine	No benzamidine
R^2	0.96	0.95	0.92	0.94	0.95	0.91
Q_{max} (mg/g support)	16021.6 ± 24418.9	6311.7 ± 1328.1	999.6 ± 86.2	2221.1 ± 279.1	1283.6 ± 74.0	2709.5 ± 552.8
K_a (M^{-1})	1.2 x10^7	1.1 x10^7	7.9 x10^3	2.4 x10^4	4.4 x10^3	2.4 x10^4
n (Hill coefficient)	1.2 ± 0.4	1.4 ± 0.4	2.1 ± 0.7	2.5 ± 0.7	1.7 ± 0.4	1.7 ± 0.5

A crystallization period of 4 days was recorded to assess if the magnetic (MP-Fe_3O_4) and affinity-triggered magnetic (MP-chitin) crystallization had an effect in crystal growth (nucleation time and maximum dimensions). As representative, in Figure 4.3 the time course of crystal growth for 3 drops with no MPs, MP-Fe_3O_4 and MP-chitin is shown. The affinity-triggered magnetic crystallization led to an earlier visible onset of HEWL crystals, almost at its full length by day 2. The presence of MP-Fe_3O_4 did not cause such fast-triggering effect in crystal nucleation as MP-chitin, but still the HEWL appeared at day 3, one day earlier than under the crystallization conditions without MPs. The condition with no MPs, not only led to a delayed crystal visible onset, but at the same time, by day 4 the crystal was 3 times smaller than in the presence of MPs (Figure 4.3).

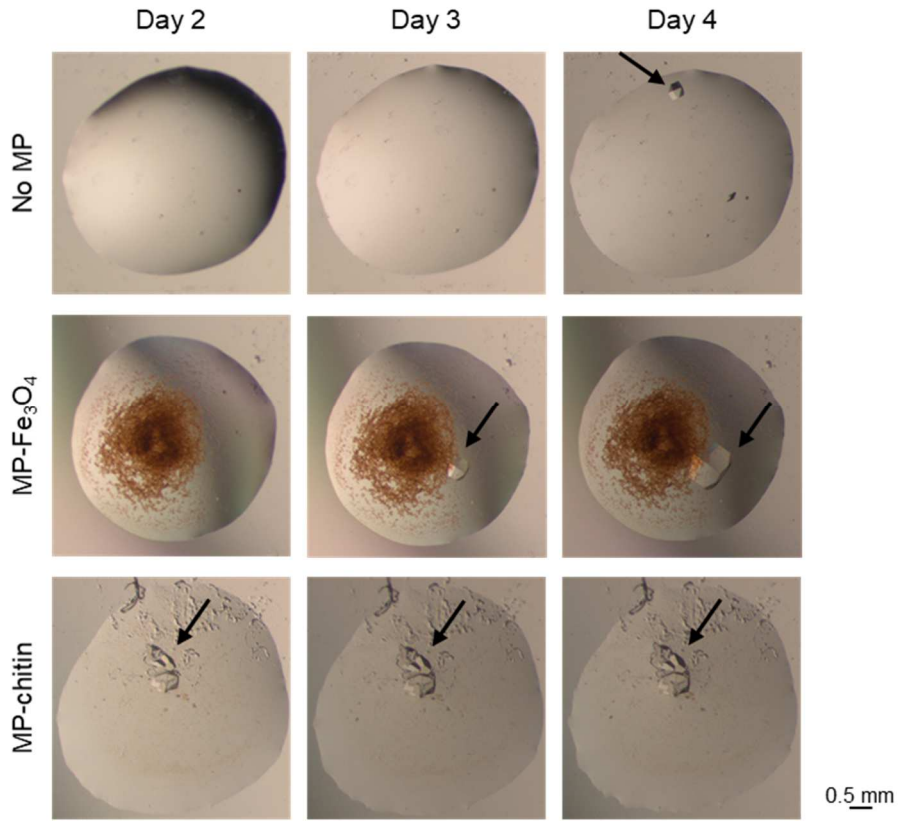

Figure 4.3. HEWL (25 mg/ml) crystallization in the absence and presence of MP-Fe_3O_4 and MP-chitin (0.5 mg/ml). Visual inspection of days 2, 3 and 4 of crystal growth. Black arrows indicate protein crystal.

Prior work demonstrated the feasibility of purifying trypsin from a complex mixture by magnetic fishing with iron oxide core MPs coated with casein [192]. The binding capacity of trypsin to MP-Fe_3O_4 and MP-casein was calculated in trypsin's crystallization conditions, and binding results were best fitted by the Hill equation (Table 4.3 and Table 4.4). Overall, the MP-casein performed better for trypsin binding than MP-Fe_3O_4 in terms of K_a and Q_{max}. Once again, the addition of MPs has a notorious effect in the amount of protein crystallized, as seen in the major difference in yield fold change in the presence and absence of MPs (Figure 4.4A), with up to 13 times more protein crystallized in the presence of MP-casein.

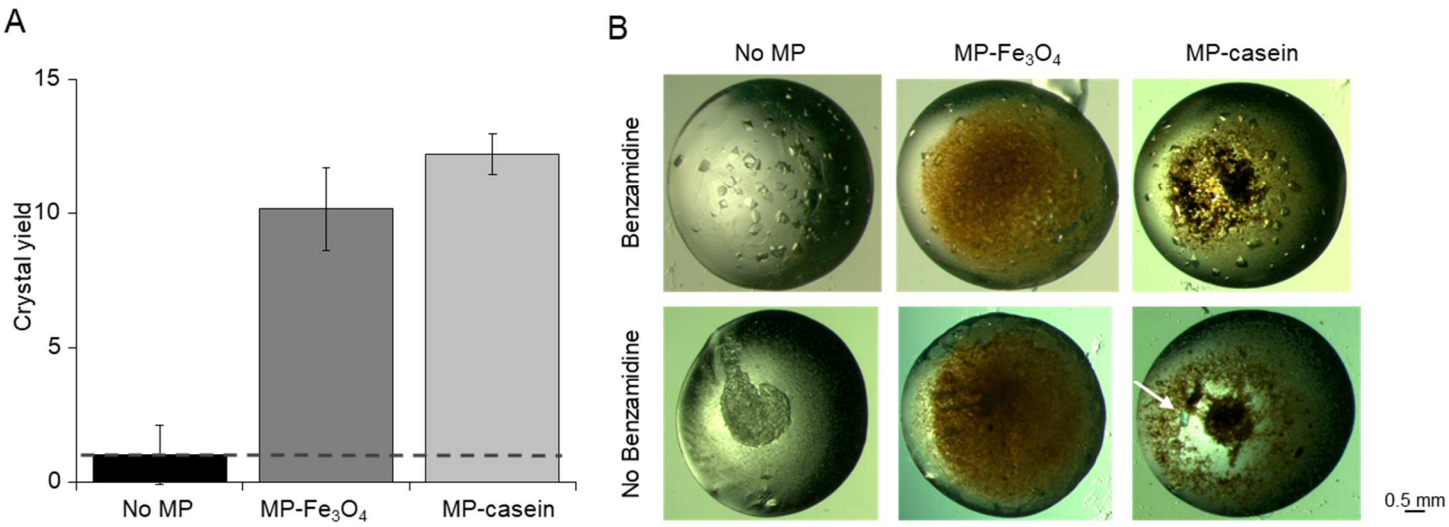

Figure 4.4. Trypsin adsorption to MP-Fe_3O_4 and MP-casein (n=3). (**A**) Trypsin (60 mg/ml) crystallization yield fold change between crystals grown in the presence of no MP (**black**); MP-Fe_3O_4 (**grey**) and MP-casein (**light grey**). (**B**) Trypsin (60 mg/ml) crystallization in the absence and presence of MP-Fe_3O_4 and MP-casein (0.5 mg/ml) in the with and without benzamidine (10 mg/ml) present in the protein solution. Visual inspection was performed at day 30 of crystal growth. White arrow indicates protein crystal.

Green fluorescent protein (GFP) has been reported as a tag protein to enhance protein crystallization in fusion with the target protein [201–203]. Its intrinsic fluorescence brings the additional advantage of easy detection of protein crystals in the precipitation solution, by visual inspection under normal light conditions. As previously described, the synthetic ligand based on the UGI reaction, named A4C7, was uncovered as a new ligand to bind and purify GFP and GFP fusion proteins from complex media [193]. As for the addition of MP-Fe_3O_4, the affinity MPs did not improve or had a great impact in crystal yield (Figure 4.5A), nonetheless it did not hamper crystal growth (Figure 4.5B).

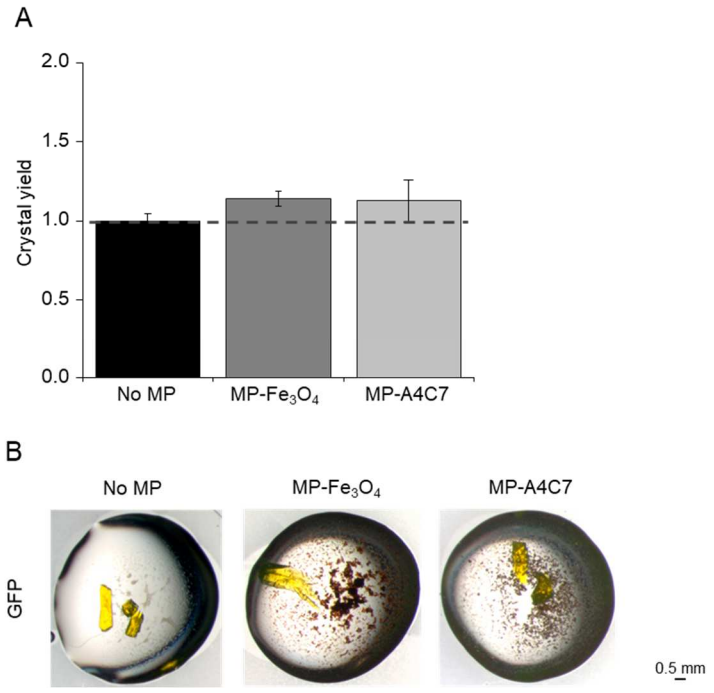

Figure 4.5. GFP adsorption to MP-Fe_3O_4 and MP-A4C7 (n=3). (**A**) GFP (15 mg/ml) crystallization yield fold change between crystals grown in the presence of; no MP (**black**); MP-Fe_3O_4 (**grey**) and MP-A4C7 (**light grey**). (**B**) GFP (15 mg/ml) crystallization in the absence and presence of MP-Fe_3O_4 and MP-A4C7 (0.5 mg/ml). Visual inspection was performed at day 10 of crystal growth.

4.3.3. Magnetic crystallization for peptidases

Trypsin, being a peptidase, is many times crystallized in the presence of benzamidine, a competitive inhibitor of trypsin, trypsin-like enzymes and serine peptidase. In this work the presence of benzamidine in the crystallization conditions was assessed in terms of trypsin's binding capacity to both MPs.

The binding capacity of trypsin to MP-Fe_3O_4 and MP-casein was determined in trypsin's crystallization conditions – in the presence and absence of benzamidine (Table 4.3 and Table 4.4). The presence of benzamidine impaired trypsin binding to both MPs (Table 4.3), as it was corroborated by the static binding capacity results (Table 4.4). This could be due to benzamidine occupying trypsin's binding site to the MPs or by benzamidine binding to the MPs. The presence of benzamidine led to lower K_a and Q_{max}, whereas the absence of benzamidine led to higher K_a, up to one order of magnitude higher (Table 4.4). The higher K_a and Q_{max} observed in the absence of benzamidine rises the hypothesis that either benzamidine and casein bind to the same trypsin residues hampering casein to bind trypsin, or some conformational change in trypsin occurs when bound to benzamidine, impeding casein to bind. Overall, the MP-casein performed better for trypsin binding than MP-Fe_3O_4 in terms of K_a and Q_{max}, (Table 4.4). Once established the effect of benzamidine in MPs binding, the effects in trypsin crystallization in the absence of MPs, presence of MP-Fe_3O_4 and MP-casein, with and without the addition of benzamidine, were assessed (Figure 4.4B). The

presence of benzamidine led to higher nucleation rate and crystal size. In contrast, the lack of benzamidine in the crystallization drop led to protein precipitation and therefore, no crystal appearance in the drops without MPs and with MP-Fe_3O_4 (Figure 4.4B). When no inhibitor was added, the only condition in which it was possible to achieve protein crystallization was in the presence of MP-casein. The affinity-triggered crystallization led to crystal growth in conditions that otherwise would result in protein precipitation. When adding MP-casein in crystallization assay without adding the inhibitor, in 2 out of 3 crystallization drops crystal growth was observed.

4.3.4. X-ray diffraction studies

To assess diffraction quality and isomorphism of the crystals obtained in the presence of MPs, in comparison to reported crystallization conditions for HEWL, trypsin and GFP, X-ray diffraction studies were performed to completion.

Primary evaluation of the effect of MPs in crystal morphology was done by comparative analysis of the indexed spacegroups, cell parameters and solvent content (Matthews coefficient, V_M) for the crystals of each protein. In the presence of the correspondent MPs, both GFP and trypsin kept their original $P2_12_12_1$ spacegroup, and the same happened with HEWL, which crystallized in spacegroup $P4_32_12$, as originally reported (see Table 4.1). Unit cell parameters for HEWL in the presence of MPs were a=b=79.0 Å, c=37.0 Å and α=β=γ=90.0°, with a calculated V_M of 1.92 A^3/Da. Unit cell parameters for bovine trypsin in the presence of MPs were a=54.2 Å, b=58.2 Å, c=66.3 Å and α=β=γ=90.0°, with a V_M of 2.29 A^3/Da. Finally, unit cell parameters for GFP in the presence of MPs were a=51.2 Å, b=62.9 Å, c=65.9 Å and α=β=γ=90.0° and the V_M was 2.07 A^3/Da. All unit cell parameters are within values comparable with the reference structures and the same was observed for the calculated V_M values (see Table 4.1). After structure solution and refinement, the 3D structures were superposed (in PyMol, Cealign) with PDB available structures from crystals grown in similar precipitant conditions, but in the absence of the additives under study.

HEWL structure obtained from crystals grown in the presence of MP-chitin was superposed and fCα atoms (Figure 4.6A). The 3D structure of trypsin obtained from a crystal grown in the presence of MP-casein and benzamidine was superposed with PDB ID: 5MNG [204], presenting an 0.26 Å r.m.s.d. for 216 Cα atoms (Figure 4.6B). The structural superposition of the GFP structure obtained from crystals grown in the presence of MPs with PDB ID: 1GFL produced an r.m.s.d. of 0.01 Å for 224 Cα atoms, with no relevant structural differences (Figure 4.6C).

The X-ray crystallography results in this study show that nanoparticles can behave as nucleating agents without changing crystal morphology or protein structure. This is in accordance with previous studies [59].

Figure 4.6. Superposition of the 3D structures obtained from crystals grown in the presence of MPs with corresponding representative structures available in the PDB (rmsd values were calculated in PyMol Cealign). (**A**) HEWL 3D structure from a crystal grown in the presence of MP-chitin and HEWL from PDB ID: 6F1L, presenting an r.m.s.d. of 0.92 Å for the matching of 120 C**α** atoms. (**B**) Trypsin 3D structure from a crystal grown in presence of MP-casein and trypsin from PDB ID: 5MNG, presenting an r.m.s.d. of 0.26 Å for the matching of 126 C**α** atoms. (C) GFP 3D structure from a crystal grown in presence of MP-A4C7 and GFP from PDB ID: 1GFL, presenting an r.m.s.d. of 0.01 Å for the matching of 224 C**α** atoms.

4.4. Conclusions

This is the first report of a rationally-designed crystallography assay based on the addition of magnetic particles, coated or functionalized with affinity molecules towards a protein of interest, with the purpose of producing single crystals for 3D structure determination. Here, after the successful characterization of all MPs – coated and functionalized, three different proteins were used to exemplify and reinforce the straightforward approach that magnetic affinity crystallization represents.

HEWL, is an extensively used protein in the search for innovative crystallization methods, and here also elected to investigate the influence of MPs as additives in protein crystallization. However, more than demonstrating the feasibility of using MPs and still be able to obtain protein crystals that diffract as optimally as the ones grown without the additives, we could witness faster onset of crystals with more protein (in mass) crystallized. This was particularly notorious when using affinity-triggered magnetic crystallization with MP-chitin.

Similarly to HEWL, bovine trypsin is also broadly used in crystallization studies as model protein. Nonetheless, as a peptidase, it is necessary to add benzamidine as an inhibitor of its proteolytic activity. Once added to the crystallization conditions, this inhibitor led to the decrease in the amount of protein bound to both MPs and to the decrease of Ka for the same MP. The depletion of benzamidine from the crystallization assays led to protein precipitation when no MP and MP-Fe_3O_4 was used as additive. However, when MP-casein was added, in 2 out of 3 crystallization drops, it was possible to achieve protein crystal growth without the need of benzamidine. Moreover, the addition of MPs led to a great increase in mass of crystallized protein, compared to the absence of MP additives, even in the presence of benzamidine.

A similar approach was designed for the crystallization of GFP. The addition of MPs as crystallization additives was evaluated in terms of yield fold change and crystal morphology. The crystallization of GFP in the presence of MPs additives, led to an increased amount of crystallized protein.

Overall, the addition of MPs to the crystallization assays led to faster onset and growth of crystals. This was more pronounced when adding MPs with affinity towards the target protein. Affinity-triggered magnetic crystallization not only reduced the crystallization time, but also enabled the removal of critical additives as benzamidine, a trypsin inhibitor, usually necessary to obtain reproducible single crystals of trypsin. In all the tested proteins, MP addition did not change the crystal diffraction quality and unit cell parameters. Moreover, this work once again reinforces the versatility of MP coating and functionalization, here coated with a polysaccharide (chitin), a protein (casein) and a synthetic ligand (A4C7). Furthermore, the use of affinity driven MPs, such as MP-casein to crystallize trypsin, allowed to exclude the peptidase inhibitor, enabling the possible screening of different inhibitors or competition assays.

Chapter 5

The use of magnetic particles as additives in polyclonal and monoclonal antibodies crystallization

Abstract

Antibodies are an important class of proteins used in a wide range of areas from fundamental research to clinical therapy. Regardless of their use, antibodies must comply with the need for high purity and concentration. The current antibody purification processes are fully dependent on chromatographic techniques which are a bottleneck in antibody production. As such, alternative non-chromatographic approaches are being explored. Given the difficulty to crystallize antibodies, new additives to the crystallization assays can be added to promote crystal nucleation. New additives include magnetic particles that already had been successfully used in the purification of antibodies from complex media. With the aim to explore the synergy between the crystallization and magnetic fishing techniques for the purification of polyclonal and monoclonal antibodies, different crystallization screens were tested for the crystallization of both proteins in the presence of magnetic particles. Using this approach, we observed spherulite crystals of polyclonal antibodies in the presence of magnetic particles coated with dextran and functionalized with an affinity synthetic ligand to capture antibodies in solution. On the other hand, no crystal growth was observed for monoclonal antibodies, although some conditions led to the precipitation of the proteins in solution. This work demonstrated the possibility of using magnetic particles as additives in antibodies crystallization and precipitation, foreseeing the synergetic use of magnetic particles in antibody precipitation for purification.

5.1. Introduction

With the ability to bind virtually any epitope, antibodies are powerful proteins ubiquitously used across a variety of scientific and therapeutic areas [205–207]. Depending on the application, polyclonal (pAbs) or monoclonal (mAbs) antibodies can be used. PAbs are able to recognize different epitopes of the same antigen, whereas mAbs are only able to recognize one epitope of a given antigen [208]. As for scientific or therapeutic applications, these proteins are required to be highly pure and at high concentrations.

The current downstream pipeline used for antibodies purification and formulation, mainly composed by chromatographic steps, comprises the major hold-up in antibody production [209]. New alternatives for antibody purification and formulation rely on anything but chromatography strategies, as is the case of crystallization [28,207,210,211]. Antibodies have a particular Y shape structure, where the two arms correspond to the Fab (fragment antigen binding) while the tail corresponds to the Fc (fragment crystallizable) regions, both linked by disulphide and noncovalent bonds, comprising a region rich in proline, threonine, and serine residues (hinge region). Such structural features make antibodies very flexible and therefore hard to crystallize [208]. Successful crystallization of antibodies for purification purposes has already been described, nonetheless it was only possible with previously purified and/or dialysed antibodies

samples [27,28,212]. New crystallization approaches depend on the addition of new materials that function as crystallization additives to act as nucleation agents in the crystallization process [59,183,213].

Magnetic particles had already been successfully used in the purification of antibodies by magnetic fishing [12,136]. Iron oxide magnetic particles (MPs) have a non-porous surface with a high surface area to volume ratio. MPs can be coated and functionalized with different polymers [214], synthetic ligands [136], proteins or peptides [12]. The synthetic triazine ligand 22/8, with affinity towards antibodies, has already been successfully synthetized on iron oxide magnetic particles for antibody purification [13,215].

We propose the hypothesis that a different coating and functionalization may foster crystal nucleation by promoting different interactions between the coated MPs and the target protein. With the main goal of retrieving antibody crystallization conditions for further use in the purification pipeline of antibodies, MPs coated with dextran and functionalized with synthetic ligand 22/8 were used as additives in the high throughput crystallization of pAbs and mAbs using commercially available crystallization screens. The crystallization screens used had polyethylene glycol as the main precipitant, as it has been reviewed as the major precipitating agent in antibody crystallization [216], the present work also confirms the role of kosmotropic cations as major influents in antibody precipitation. This work can be translated for the development of new non-chromatographic methods for antibody purification relying on MPs and selective precipitation of target proteins.

5.2. Materials and Methods

5.2.1. Materials

All used chemicals were at least 98% pure of analytical or HPLC grade.

5.2.2. Magnetic particles synthesis and characterization

Iron oxide magnetic particles were synthesized by the co-precipitation method. A solution of 25% ammonium hydroxide (200 ml) was purged with N_2 gas, and a newly iron solution ($FeCl_3$ and $FeCl_2$ salts (Sigma-Aldrich) with a 0.5 molar ratio of Fe^{2+}/Fe^{3+}, 25 ml) was added in a dropwise manner. The reaction was stopped after 2 hours, the particles were washed with distilled water (10 times), using a permanent magnet for magnetic particle separation. The particle solution (10 mg/ml) was sonicated for 15 minutes, following a solution of sodium metasilicate pentahydrate (Sigma-Aldrich) in 50% (v/v) ethanol/water (28.5 mg/ml). The reaction was stopped after 2 hours at 40ºC with orbital shaking (200 RPM)) and the particles washed with distilled water (10 times). The particles were resuspended in 20% (v/v) ethanol/water (80 ml) and sonicated for 10 min. Then, 25% ammonium hydroxide (3 ml) and tetraethyl orthosilicate (TEOS) (1.5 ml, Sigma-Aldrich) were added dropwise during sonication and the reaction was stopped after 2 hours at 40ºC with orbital shaking (200 RPM). The particles were washed with distilled water (10 times). The particles were resuspended in 175 ml of distilled water, sonicated for 10 minutes, and further coated with dextran

(from *Leuconostoc mesenteroides* 150 kDa, Sigma-Aldrich). A dextran solution (80 mg/ml in distilled water) was added dropwise to the particle solution and the mixture incubated (60°C, 2 hours with orbital shaking, 200 RPM), after which the particles were washed 5 times with distillated water. Magnetic particles coated with dextran (MP-dextran) were further functionalized with synthetic triazine ligand 22/8 (MP-22/8).

MP-dextran functionalization with synthetic ligand 22/8 (MP-22/8) was carried out through a triazine scaffold. The particles were firstly aminated using (3-aminopropyl)triethoxysilane (APTES) as previously described [22]. The amount of amines was 213.3 ± 3.8 µmol NH_2/g of dried MP, assessed by the Kaiser Test as described [22]. The aminated particles were washed 2 times with cold distilled water and 2 times with 50% (v/v) acetone/distilled water solution and suspended at a 10 mg/ml concentration. The particles were let to react with 5 molar excess of cyanuric chloride (in acetone) to the amine content on the support, for 1 hour at 0ºC with orbital shaking (200 RPM). The particles were washed with 100% acetone (2 times), 50% (v/v) acetone/distilled water (3 times) and distilled water (5 times). The first nucleophilic substitution was carried out using 3-hydroxyaniline dissolved in 50% (v/v) dimethylformamide (DMF)/distilled water with 2 molar excess to the amines in the support to a final MP concentration of 10 mg/ml, the reaction was let to occur for 24 hours at 30ºC with orbital shaking (200 RPM). Next, the particles were washed with distilled water (5 times) and the second nucleophilic substitution was carried out using 5 molar equivalents of 4-amino-1-naphthol hydrochloride, dissolved in 50% (v/v) DMF/distilled water, to a final MP concentration of 10 mg/ml. The reaction occurred for 48 hours at 80ºC with orbital shaking (200 RPM). The particles were washed with water (2 times), 0.1 M hydrochloric acid (1 time), distilled water (1 time), 0.1 M sodium hydroxide with 30% isopropanol (1 time) and distilled water (5 times). In the final step, particles were resuspended in the appropriated volume of water.

All particles were characterized by Fourier transform infrared (FT-IR), dynamic light scattering (DLS), zeta potential and transmission electron microscopy (TEM). DLS and zeta potential (0.05 mg/ml solution in MilliQ and precipitant solution (20% (w/v) PEG3350 in Tris buffer)) were measured using Dynamic Zetasizer Nano ZS from Malvern instruments. FT-IR spectra were recorded on a Spectrum Two™ spectrometer from Perkin Elmer. For that, MP samples were prepared by drying the samples overnight at 60ºC, followed by grounding and mixing with KBr (1:100) and pressing in a hydraulic press, up to 10 tones force. Analytical TEM was done in a Hitachi 8100 microscope with ThermoNoran light elements EDS detector and digital image acquisition without staining.

5.2.3. Biological material

Human polyclonal antibodies (pAbs) (product name: Gammanorm®) from Octapharma (Lachen, Switzerland) and clarified cell culture supernatant from CHO cell lines producing anti-TNFα or anti-HER2 monoclonal antibodies (mAbs) were kindly provided by João Gonçalves Laboratory from iMed.ULisboa – Research Institute for Medicines (Faculty of Pharmacy, University of Lisbon) and produced as in annex 1.

5.2.3.3. mAbs purification

The produced mAb, present in the cell supernatant was purified by Protein A affinity chromatography using 1 ml column MabSelect™ SuRe™ (GE Healthcare Life Sciences, Chicago, Illinois, EUA) in ÄKTA Pure 150 system from GE Healthcare Life Sciences. Adsorption was performed in 10 mM phosphate buffer saline (PBS) at pH 7.4 and elution in 100 mM glycine-HCl at pH 2. Before injection, the column was equilibrated with 5 CVs of adsorption buffer. The feed injection was loaded at 1 mL/min and the unbound or weakly bound samples were washed-out with 2 CVs of adsorption buffer. The elution of mAbs was achieved by changing the buffer to 100 mM glycine-HCl at pH 2 for 5 CVs. To avoid denaturation of the eluted antibodies, 1 M Tris-HCl at pH 8 was added to the elution fractions collected, to adjust the pH to 7. All the fractions were analysed by SDS-PAGE. Sodium dodecyl sulfate–polyacrylamide gel electrophoresis (SDS–PAGE) was performed to evaluate mAb recovery and purity. The buffer sample composition was 0.15 M Tris–HCl at pH 6.8, 6% (w/v) SDS, 0.025% (w/v) bromophenol blue, 12.5% (v/v) glycerol and β-mercaptoethanol was used as reducing agent. Prior to loading in the gel, all the samples were denatured at 100°C for 5 minutes. Samples were applied in a 12.5% gel, prepared from 41% acrylamide/bis stock solution (30:1) from Bio-Rad (Hercules, California, USA) and migrated at 90 mV using as running buffer 192 mM glycine, 25 mM Tris-HCl and 0.1% SDS, pH 8.3. Gels were stained using two methods: (i) Coomassie-stained with the staining solution of 0.5% (w/v) Coomassie Blue R-250, 7.5% (v/v) acetic acid, 45% (v/v) methanol, for 30 min at room temperature with orbital shaking and revealed with the distaining solution (7.5% (v/v) acetic acid, 45% (v/v) methanol) until proper protein visualization; or (ii) using Bio-Rad silver staining kit. Images were acquired with Gel Doc™ XR+ System with Image Lab™ software from Bio-Rad.

5.2.4. Crystallization assays

5.2.4.1. Polyclonal antibodies

Crystallization assays were performed using the sitting drop method in 96-well 3-drop Swissci plates. The crystallization setups were carried out at 20°C and regularly visualised using an optical microscope (V81 Stereo Microscope equipped with Camera – AxioCam Erc5s (5 MP), ZEISS). The PEG/Ion Screen™ (Molecular Dimensions, United Kingdom) was chosen to perform the crystallization assays. The crystallization experiments were performed using the automated nanodrop-dispensing robot Oryx8 (Douglas Instruments, United Kingdom), to obtain 1 µl drops. Polyclonal antibody (pAb) in 10 mM Tris-HCl at pH 7.0 (0.5 µl at 10 mg/ml) was crystallized either in the absence of MP (0.5 µl of precipitant), or in the presence of MP-dextran or MP-22/8 (0.1 µl at 1 mg/ml).

5.2.4.2. Monoclonal antibodies

Crystallization assays of the monoclonal antibodies (mAbs) were carried out at the High Throughput. Crystallization Laboratory (HTX Lab) at EMBL Grenoble, through the iNEXT extended support that enables the access to X-rays infrastructures for translational research. With the aim to speed and improve mAbs

crystallization, four different screens: (i) JCSG-plus™ HT-96 (Molecular Dimensions), (ii) PACT *premier*™ HT-96 (Molecular Dimensions), (iii) Wizard Classic 1 & 2 (Rigaku) and (iv) PEGs I Suite (Qiagen), were used for the screening of mAbs crystallization conditions. Crystallization assays were performed using the sitting drop method in CrystalDirect™ 96-well plate from MiTeGen. The crystallization setups were carried out at 293.15 K and drop inspections were performed using RockImager (Formulatrix, USA) with visible and UV light periodic inspections. The crystallization setups were prepared using the crystallization robot Cartesian PixSys 4200 (Genomic Solutions, United Kingdom), to obtain 200 nl drops. mAbs in 10 mM Tris-HCl at pH 7.0 (100 nl at 20 mg/ml) was crystallized either in the absence of MP (100 nl of precipitant) or in the presence of MP-22/8 (20 nl at 1 mg/ml) as additive.

5.3. Results and discussion

5.3.1. Magnetic particles characterization

Magnetic particle (MP) surface modifications (Figure 5.1A) including dextran coating (MP-dextran) and functionalization with the synthetic triazine ligand 22/8 (MP-22/8) were confirmed by Fourier transform infrared (FT-IR) spectroscopy (Figure 5.1B, spectrum a to c respectively). The uncoated MP (MP-Fe_3O_4) (Figure 5.1B, spectra a) present a single band corresponding to the Fe-O bond vibration, typical of magnetite, in the 400-600 cm^{-1} region [156]. The MP-dextran, presented a band in the characteristic peaks of dextran at 1146 and 1020 cm^{-1}; at 1146 cm^{-1} resulting from the valent vibrations of C-O-C and glycosidic bond, as for 1020 cm^{-1}, results from the great chain flexibility present in dextran around the glycosidic bonds [158] (Figure 5.1B, spectra b). The functionalization of MP with the triazine synthetic ligand 22/8 was confirmed by the presence of peaks between 1600 and 1400 cm^{-1} corresponding to the aromatic C-C stretching (Figure 5.1B, spectra c). The MP were further analysed in terms of hydrodynamic diameter by dynamic light scattering (DLS) and surface charge by zeta potential in three different solutions – MilliQ water, 10 mM Tris-HCl at pH 7 and 20% (w/v) PEG3350 in 10 mM Tris-HCl at pH 7 (Figure 5.1C). The stability of MPs, given by DLS and zeta-potential, was evaluated in the presence of Tris-buffer and PEG given the literature review [216] in which the PEG role in antibody was evidenced; here, the Tris buffer was chosen since it is the solution in which antibodies are before the crystallization assays. DLS results indicate that all MPs tend to aggregate in Tris buffer, however, with the addition of 20% (w/v) polyethylene glycol (PEG) 3350, the particles have a lower hydrodynamic diameter, as presented in water. The zeta potential (Figure 5.1D), as the hydrodynamic diameter, vary with the solution in which the particles are in suspension. MP-Fe_3O_4 presented a higher stability in 20% (w/v) PEG3350 than in water or Tris buffer. MP-dextran presented a higher stability in water than in Tris buffer or 20% (w/v) PEG3350. MP-22/8, as MP-dextran, also presented a higher stability in water, however, showing an overall zeta potential lower than -20 mV, these MPs can be considered to be stable in all of three solutions. Transmission electron microscopy (TEM) showed the presence of spherical magnetic cores (Figure 5.1E), and the tendency of MPs, in particular MP-dextran, to form aggregates, already assessed by DLS.

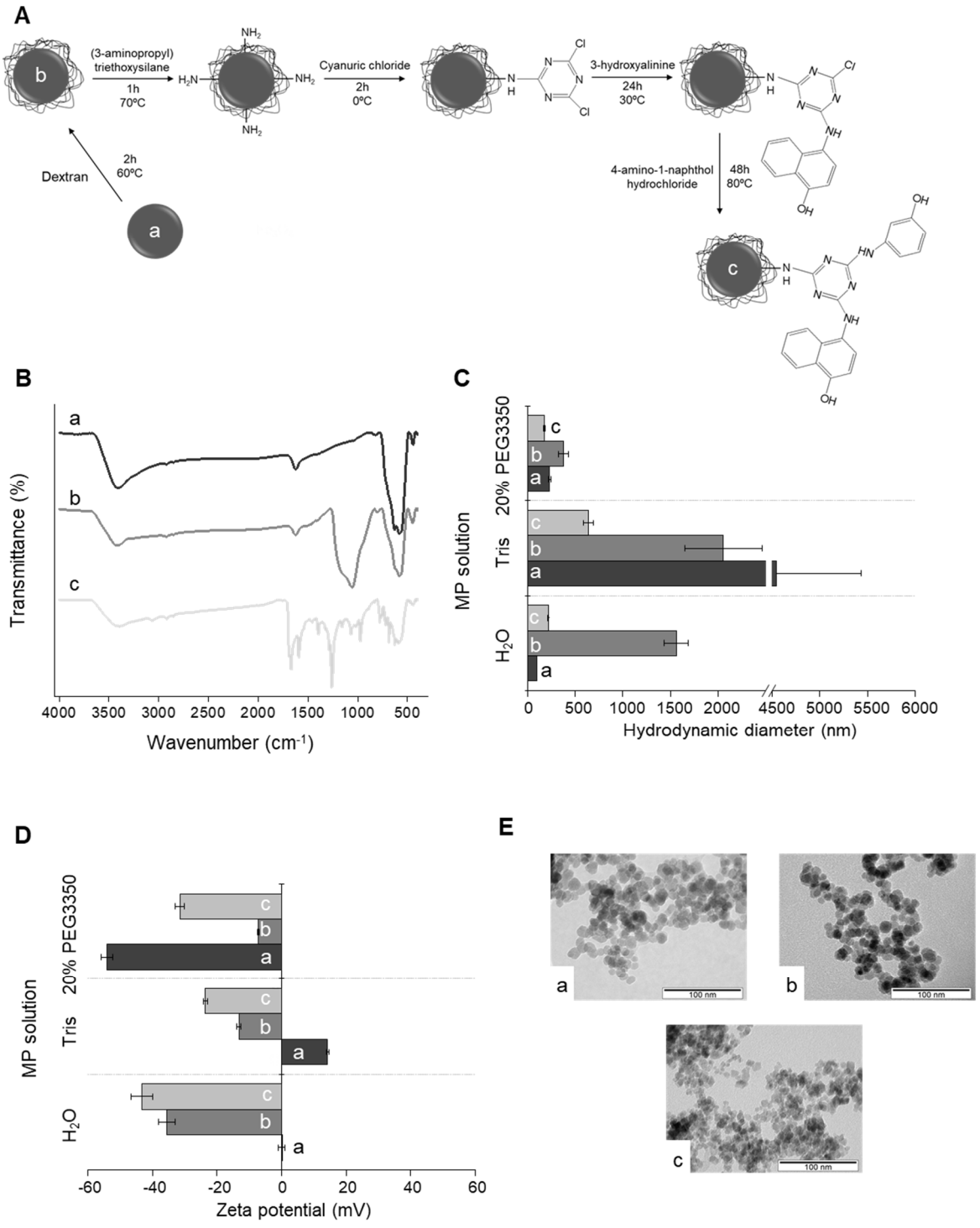

Figure 5.1. Magnetic particles (**A**) schematic synthesis and characterization by (**B**) DLS and (**C**) zeta-potential for (**a**) MP-Fe_3O_4, (**b**) MP-dextran and (**c**) MP-22/8 in MilliQ-water (H2O), buffer solution (10 mM Tris-HCl at pH 7.0) and precipitant solution (20% PEG3350) in buffer solution (n=3) and (**D**) FT-IR spectroscopy and (**E**) Transmission electron microscopy analysis of (**a**) MP-Fe_3O_4, (**b**) MP-dextran and (**c**) MP-22/8.

5.3.2. Polyclonal antibody crystallization

As reviewed that PEG plays a major role in antibody crystallization [216], the PEG/Ion Screen™ was elected for the attempts to crystallize pAbs in the presence of MP-dextran and MP-22/8 as additives. In the PEG/Ion Screen™ different salt compounds are empirically tested, keeping 20% (w/v) PEG3350 as main precipitating agent. For the designed assay, crystallization was unsuccessful in the absence of MPs as additives, demonstrating that not only PEG but also additives, as MPs, are important for antibodies crystallization. Moreover, when MPs are included as additives, crystal growth was only visible in the presence of the divalent cations' magnesium and calcium, with a major effect from magnesium, as more crystallization hits were obtained with it. According to the Hofmeister series, both Mg^{2+} and Ca^{2+} are kosmotropic cations. Kosmotrope cations tend to interact with water in solution decreasing the hydrophobic interaction while promoting protein-protein interactions. Out of six crystallization hits (Figure 5.2A and B), three are recurring to both MP-dextran and MP-22/8, being the common salts 0.2 M magnesium chloride, 0.2 M calcium acetate and 0.2 M magnesium bicarbonate all in the presence of the precipitant 20% (w/v) PEG3350. On the other hand, in the presence of MP-dextran, two additional hits were uncovered –0.2 M magnesium acetate tetrahydrate and 0.2 M magnesium sulfate in the presence of the precipitant 20% (w/v) PEG3350. As for the presence of MP-22/8, another hit – 0.2 M magnesium nitrate with 20% (w/v) PEG3350 was found.

The crystal growth conditions were monitored for 30 days for all the crystallization conditions. The average crystal size varied with the conditions as well as with the MPs used as additives (Figure 5.2C and D). Overall crystal growth is faster, and crystals tend to be bigger when MP-dextran are added, when compared with MP-22/8.

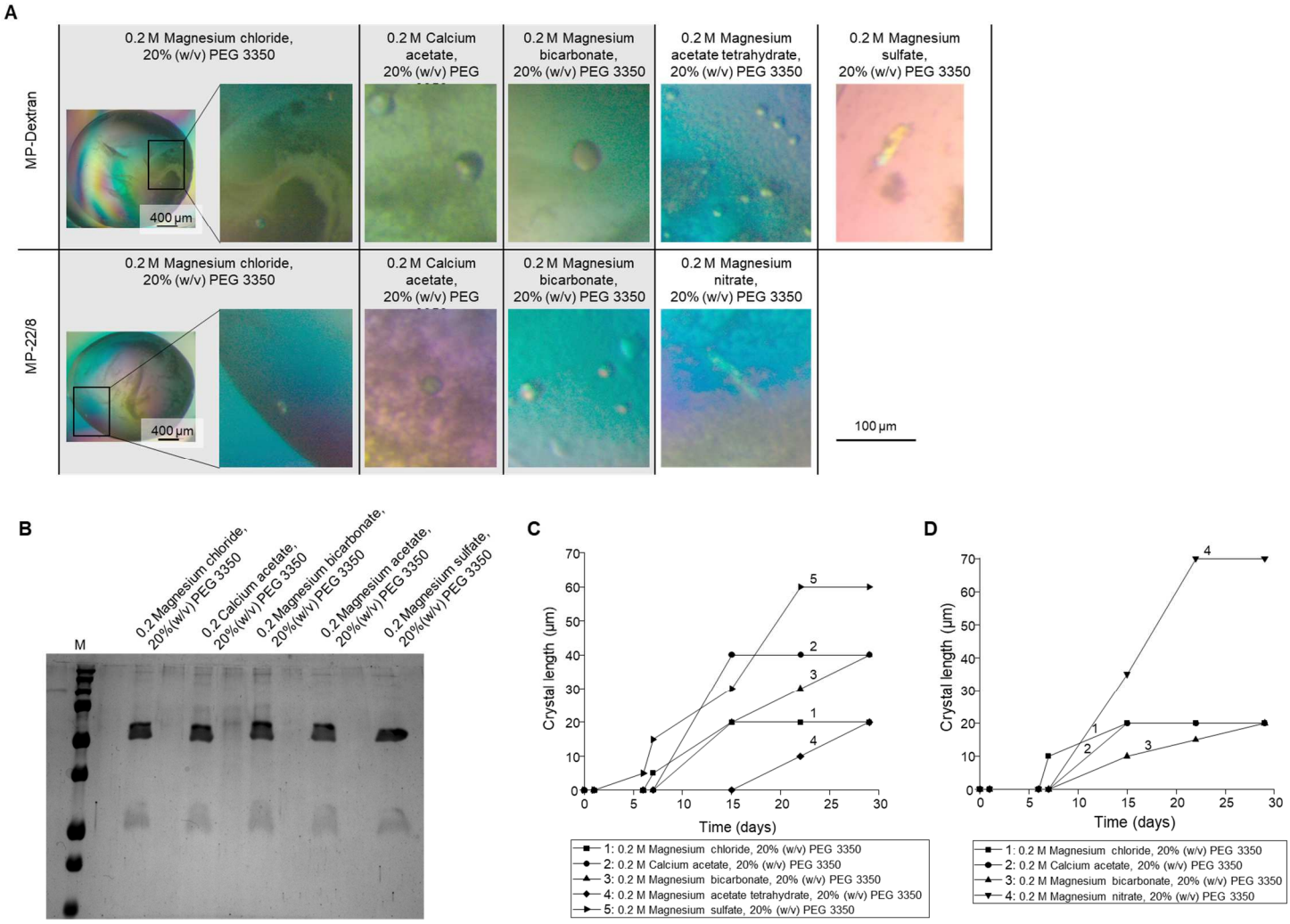

Figure 5.2. Polyclonal antibody (10 mg/ml) crystallization in the presence of MP-dextran and MP-22/8. (**A**) Visual inspection of crystallization day 30 in different crystallization conditions. (**B**) SDS-PAGE for crystals grown in the presence of MP-dextran. **Lane ID: M:** Precision Plus Protein™ Dual Color Standards (from top to bottom: 200, 150, 100, 75, 50, 37, 25 and 20 KDa) (**C**) Average crystal length of visual measurement of polyclonal antibodies crystals over 30 days in the presence of MP-dextran and (**D**) MP-22/8 in the presence of different crystallization conditions.

5.3.3. Monoclonal antibody crystallization

For the crystallization of monoclonal antibodies (mAbs), a different strategy was devised. In collaboration with the HTX Lab from EMBL (European Molecular Biology Laboratory) at Grenoble, two mAbs: anti-TNFα mAb and anti-HER2 mAb, were screened for crystallization conditions using different crystallization screens – JCSG-plus™ (Molecular dimensions); PACT premier™ (Molecular dimensions); PEGs I Suite (Qiagen) and Wizard Classic 1 & 2 (Rigaku). The crystallization screens were chosen due to their diversity in buffer, salt, ion, pH and most of the formulations include PEG as precipitant. As additives to the crystallization screens only MP-22/8 was added. Contrary to pAbs, no screened condition produced mAbs crystals, instead only protein precipitation was observed. The protein precipitation was visible by UV inspection of the crystallization drops (Table 5.1). Out of the four crystallization screens used, only the PEGs I Suite (Qiagen) did not retrieve results, either crystal or visible precipitate (Table 5.1). Of the six precipitation conditions, four had PEG in their composition, still none produced crystals of the mAb. In the same line, four of the crystallization conditions present Zn^{2+} or sodium citrate in their precipitant composition. Both Zn^{2+} and sodium citrate are in the extreme ends of the Hofmeister series as kosmotropic and chaotropic species, respectively. Whole mAbs are well known difficult proteins to crystallize due to the mobility of the interchange disulphide bond between the mAbs Fab and Fc regions. Most of the mAb structures in PDB regard the Fab region, on which stand the complementarity-determining regions (CDRs), responsible to bind the epitope of interest.

Table 5.1. Monoclonal antibody (20 mg/ml) crystallization in the presence of MP-22/8 with the corresponding precipitation condition and respective crystallization screen. UV and visible inspections of both mAbs after 90 days.

Precipitation condition	Screen	Anti-TNFα mAb In the presence of MP-22/8		Anti-HER2 mAb In the presence of MP-22/8	
		UV	Visible	UV	Visible
1.6 M Sodium citrate tribasic dihydrated, pH 6.5	JCSG-plus™ HT-96 from Molecular Dimensions			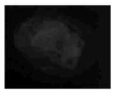	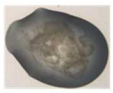
0.2 M Zinc acetate dihydrate, 0.1 M imidazole pH 8 20% (w/v) PEG 3000		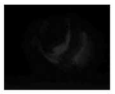	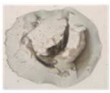		
0.002 M Zinc chloride, 0.1 M Tris-HCl pH 8, 20% (w/v) PEG 6000	PACT *premier*™ HT-96 from Molecular Dimensions		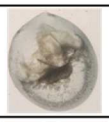		
0.1 M CHES pH 9.5, 30% (w/v) PEG 3000	Wizard Classic 1 & 2 from Rigaku		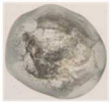		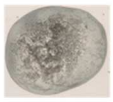
0.1 M Imidazole, 0.2 M sodium chloride, 30% (w/v) PEG 8000			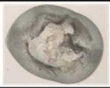		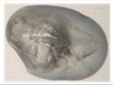
2.5 M Sodium chloride, 0.1 M imidazole, 0.2 M zinc acetate					

5.4. Conclusion

Due to antibodies' size and the flexibility of their hinge region, crystallization of a full-length antibody without leaning on stabilizing mutations is still a challenge. With the goal to overcome this difficulty, and aiming at finding antibody crystallization (or gentle precipitation) conditions fostered by the presence of MPs for purification processes, a new strategy was devised. The addition of MPs to the PEG/Ion™ crystallization screen led to the nucleation and growth of pAbs crystals with spherulite morphology. On the other hand, when no MPs were used, no crystal growth or protein precipitation was observed, reinforcing the previously confirmed role of MPs as potential nucleating agents (Chapter 4). In view of the results from the addition of MP-dextran and MP-22/8 to the crystallization conditions, it was possible to infer that kosmotropic cations, as Mg^{2+} and Ca^{2+}, in combination with PEG as precipitant, play a major role in the crystallization of antibodies. Previous knowledge supporting polyethyleneglycol as favourable precipitant for antibodies was used to choose the trial crystallization screens for mAbs anti-TNFα and anti-HER2, in the presence of MP-22/8 as additive. Nonetheless, among the different screens tested, no mAb crystals were obtained in the conditions tested. This not only confirms the inherent difficulty of crystallizing antibodies, but also that pAbs and mAbs do present different behaviours, requiring different approaches. Nonetheless, it was possible to retrieve six conditions in which both mAbs formed crystalline precipitate, as seen in the UV inspections of the crystallization drops. Here, once again, PEG was seen playing a major role in mAbs precipitation, adjuvated by the presence of Zn^{2+} and sodium citrate, respectively a cation (kosmotrope) and anion (chaotrope) from the extreme ends of the Hofmeister series.

Here, the importance of the Hofmeister series in protein precipitation was demonstrated to be a variant for antibody precipitation. Mainly kosmotropic cations are recurrent in the precipitation of pAbs and mAbs, alongside with PEG as the precipitating polymer. Further work will be developed to implement, in a criterious way, the use of the Hofmeister series in the development of a new methodology for MP-assisted purification of antibodies.

Chapter 6

Affinity magnetic precipitation: a new method for antibody purification from complex media

Manuscript accepted for peer-review publication

dos Santos, R, Iria, I, Manuel, AM, Leandro, AP, Madeira, CAC, Goncalves, J, Carvalho, AL, Roque, ACA. Magnetic precipitation: a new platform for protein purification. Biotechnol. J. (2020), DOI:10.1002/biot.202000151

Authors contributions:

RS, ACAR and ALC, designed the work. II, AMM, APL, ACAM and JG performed the analytical assays and produced the biological material. The experiments, data analysis and manuscript preparation were conducted by RS. Manuscript revision were conducted by ACAR and ALC.

Abstract

The new trend in downstream processing comprises the use of "anything-but-chromatography" methods to overcome the current downfalls of the standard packed-bed chromatography. Precipitation and magnetic separation are two techniques already proven to accomplish protein purification from complex media, yet never used in synergy. With the aim to capture antibodies directly from crude extracts, a new method combining precipitation and magnetic separation was developed – affinity magnetic precipitation. A precipitation screen based on the Hofmeister series and a commercial precipitation kit were tested with magnetic particles functionalized with a synthetic affinity ligand for antibody capture from human serum and clarified cell supernatant. The best results were obtained using PEG3350 as precipitant at 4ºC for 1h with 200 RPM orbital shaking, reaching 80% purity and 50% recovery of polyclonal antibodies from serum, and 97% recovery yield and 99% purity from anti-TNFα mAb. The synergic use of precipitation and magnetic separation can significantly influence the yield of mAbs purification processes.

6.1. Introduction

Downstream processing of biological products usually comprises four main steps: recovery, isolation, capture and polishing, and accounts for up to 60-80% of the total manufacturing costs [217]. The purification of high added value biological drugs, is mostly based on chromatographic methods [218,219]. Monoclonal antibodies (mAbs) and derived molecules are the most important players in the biopharmaceutical industry [220]. Albeit the advances in antibody engineering, antibody manufacturing still presents challenges. The development of new efficient upstream processes producing high volumes and titers (up to g/l), has added several limitations to the overall purification process mostly due to the high matrix cost, diffusion limitations and limited binding capacity [216]. To overcome these problems, anything but chromatography (ABC) approaches emerged as promising alternatives. Although most ABC approaches are not new concepts, they are not being re-adapted for the purification of biopharmaceuticals. The now-chromatographic methods include membrane separation methods [221], aqueous two-phase systems [13,20,222], magnetic separation [12,22,189], precipitation and crystallization [25,62,216,223].

Within the different methods, precipitation is mainly used for the purification of low value products [224,225]. However, this method can cope with high titers and volumes produced upstream, which scales-up with process volume, whereas chromatographic methods scale stoichiometrically with the reaction between molecules in solution [60]. Protein precipitation relies on the supersaturation of a homogenous protein solution, however, to exceed the proteins' saturation limit, changes in its environment must be introduced. Even though precipitation is a rather empirical methodology, several additives (e.g. salts or

polymers) are known to help exceed a protein's solubilization limit. However, this effect is dependent on the target protein and on the salt or polymer concentration [51]. Protein precipitation by salt addition follows frequently the Hofmeister series [52], as it ranks the anions and cations according to their relative effect on protein solubility [53,54]. Kosmotropic agents are referred as "water structure makers" that promote the salting-out of proteins; chaotropic agents are defined as "water structure breakers" that promote the salting-in effect. On the other hand, polymers such as polyethylene glycol (PEG), with a molecular weight usually higher than 4000 Da, are often associated with protein precipitation. PEG captures the water molecules from the proteins' surface, enabling the establishment of protein-protein interactions that lead to protein precipitation [55–57]. Other parameters, mainly pH and temperature, also play a role in protein precipitation by interfering in interprotein interactions. Precipitation methods have been attempted for mAbs purification, although many times the precipitated crude extract samples were previously conditioned, either purified by affinity chromatography or dialyzed in a more suitable buffer for precipitation, nonetheless the recent studies prove to be possible to precipitate mAbs maintaining its structural and functional characteristics [25,27,28,91].

The magnetic separation of proteins directly from crude extracts through the use of magnetic adsorbents is another known ABC alternative [12,136,151]. Due to their superparamagnetic properties, iron oxide magnetic particles (MPs) can be used in viscous solutions to separate a target protein, presenting a high surface area to volume ratio. Given the virtual infinite surface modifications that can be made at the particles surface, different coatings and functionalizations can be performed to target a protein from a complex crude extract [226]. From the different functionalization strategies, small affinity synthetic ligands rationally designed towards a target protein represent a low cost and viable option. For mAbs, the triazine synthetic ligand 22/8 was designed to capture antibodies from complex crude extracts [227], and its functionalization in MPs accomplished and optimized [136]. There are examples of MPs alone (magnetic fishing) or in combination with other unit operations [13,17].

Even if many times used in separate, precipitation and magnetic separation were never explored in synergy for antibody purification from complex media. The potential to use a hybrid system based on precipitation and magnetic fishing with affinity towards protein purification was explored here and enables its selective capture and concentration in a single step unit operation. In this work, different extracts – human serum and clarified cell supernatant – were used for the capture of antibodies with a new and straightforward method – affinity magnetic precipitation.

6.2. Materials and methods

6.2.1. Material

All used chemicals were at least 98% pure of analytical or HPLC grade.

The 96-well UV-star® half area microplates from Greiner (Kremsmünster, Austria) and 96-well transparent microplates flat-bottom from Sarstedt (Nümbrecht, Germany).

6.2.2. Biological material

Clarified cell culture supernatant from CHO cell lines producing anti-TNFα or anti-HER2 monoclonal antibodies (mAbs) were kindly provided by João Gonçalves laboratory from iMed.ULisboa – Research Institute for Medicines (Faculty of Pharmacy, University of Lisbon) and produced as in annex 1.

6.2.3. Production and characterization of magnetic particles

Iron oxide magnetic particles were synthesized by the co-precipitation method. A solution of 8% ammonium hydroxide (175 ml) was purged with N_2 gas, and a freshly prepared iron solution ($FeCl_3$ and $FeCl_2$ salts (from Sigma-Aldrich) with a molar ratio of Fe^{2+}/Fe^{3+} of 0.5, 25 ml) was added in a dropwise manner. The reaction was stopped after 2 hours, the particles were washed with distilled water (10 times), with a permanent magnet for magnetic particle separation. The particle solution (10 mg/ml) was sonicated for 15 minutes, followed by addition of a solution of sodium metasilicate pentahydrate (from Sigma-Aldrich) in 50% (v/v) ethanol/water (28.5 mg/ml). The reaction was stopped after 2 hours at 40ºC with orbital shaking (200 RPM)) and the particles washed with distilled water (10 times). The particles were resuspended in 20% (v/v) ethanol/water (80 ml) and sonicated for 10 minutes. Then, 25% ammonium hydroxide (3 ml) and tetraethyl orthosilicate (TEOS) (1.5 ml, Sigma-Aldrich) were added dropwise during sonication. The reaction was stopped after 2 hours at 40ºC with orbital shaking (200 RPM)), and the particles were washed with distilled water (10 times). The particles were resuspended in 175 ml of distilled water (10 mg/ml), sonicated for 10 minutes, and further coated with dextran (from *Leuconostoc mesenteroides* 150kDa, Sigma-Aldrich). A dextran solution (80 mg/ml in distilled water) was added dropwise to the particle solution (10 mg/ml) and the mixture was incubated (60°C, 2 hours with orbital agitation, 200 RPM). The particles were then washed 5 times with distilled water. Magnetic particles coated with dextran (MP-Dextran) were further functionalized with synthetic triazine ligand 22/8 (MP-22/8).

MP-Dextran functionalization with synthetic ligand 22/8 (MP-22/8) was then carried out. The particles were firstly aminated using (3-aminopropyl)triethoxysilane (APTES) as previously described [22]. The amount of amines was 213.3 ± 3.8 µmol NH_2/g of dried MP, assessed by the Kaiser Test [22]. The aminated particles were washed 2 times with cold distilled water and 2 times with 50% (v/v) acetone/distilled water solution and suspended at a 10 mg/ml concentration. The particles were let to react with 5 molar excess of cyanuric chloride (in acetone) to the amine content on the support, for 1 hour at 0ºC with orbital shaking

(200 RPM). The particles were washed with 100% acetone (2 times), 50% (v/v) acetone/distilled water (3 times) and distilled water (5 times). The first nucleophilic substitution was carried out using 3-hydroxyaniline dissolved in 50% (v/v) dimethylformamide (DMF)/distilled water with 2 molar excess to the amines in the support to a final MP concentration of 10 mg/ml, the reaction was left for 24 hours at 30ºC with orbital shaking (200 RPM). The particles were then washed with distilled water (5 times) and the second nucleophilic substitution was carried out using 5 molar equivalents of 4-amino-1-naphthol hydrochloride, dissolved in 50% (v/v) DMF/distilled water, to a final MP concentration of 10 mg/ml. The reaction occurred for 48 hours at 80ºC with orbital shaking (200 RPM). The particles were washed with water (2 times), 0.1 M hydrochloric acid (1 time), distilled water (1 time), 0.1 M sodium hydroxide with 30% isopropanol (1 time), distilled water (5 times). Finally, the particles were resuspended in the appropriated volume of water.

All particles were characterized by Fourier transform infrared (FT-IR), dynamic light scattering (DLS), zeta potential and transmission electron microscopy (TEM). DLS and zeta potential (0.05 mg/ml solution in MilliQ and precipitant solution (20% PEG3350)) were measured using Dynamic Zetasizer Nano ZS from Malvern Instruments. FT-IR spectra were recorded on a Spectrum Two™ spectrometer from Perkin Elmer. MP samples were prepared drying the samples overnight at 60ºC, then grounding and mixing with KBr (1:100) and finally pressing in a hydraulic press, up to 10 tones force. Analytical TEM was done in a Hitachi 8100 microscope with ThermoNoran light elements EDS detector and digital image acquisition without staining.

6.2.4. Antibody purification

6.2.4.1. Precipitation

A screen of precipitation conditions (Table 6.1) based on the Hofmeister series were tested for antibody precipitation using pure human pAb (product name: Gammanorm ®, from Octapharma (Lachen, Switzerland)) at 2 and 20 mg/ml and human serum (Sigma-Aldrich) at 0.5 mg/ml of total protein. Simultaneously, crystallization experiments using mAbs were carried out at the High Throughput Crystallization Laboratory (EMBL Grenoble), using the following crystallization screens PEGs-I (from Qiagen), PACT *premier*™ HT-96 (from Molecular Dimensions), JCSG-plus™ HT-96 (from Molecular Dimensions) and Wizard Classic 1 & 2 (from Rigaku). From the conditions tested, two additional precipitation conditions for antibody precipitation were unveiled – 20% PEG3350 and 2.5 M NaCl (Table 6.1). The precipitation assays were carried out at 20ºC for 1h with 200 RPM orbital shaking with a 1:1 crude extract to precipitant volumetric ratio, at a 1 ml scale. The separation of supernatant and precipitant was performed by centrifugation (5000 *xg*, 15min at 15ºC). The supernatant was removed, and the precipitate solubilized in 10 mM sodium phosphate, 150 mM sodium chloride at pH 7.4 (PBS). Protein quantification of pAb supernatant and precipitate for the different precipitant conditions were performed by measuring

absorbance at 280 nm in UV-star® half area microplates from Greiner. The pAb precipitation yield was calculated as in Equation 6.1:

$$\text{Precipitation yield (\%)} = = \frac{\mu g \text{ pAb precipitated}}{\mu g \text{ pAb loaded}} \times 100 \qquad \text{Equation 6.1}$$

For serum samples, total protein quantification was performed using bicinchoninic acid (BCA) assay reagent (Sigma-Aldrich). Sodium dodecyl sulfate–polyacrylamide gel electrophoresis (SDS–PAGE) was performed to evaluate the samples Immunoglobulin (Ig) recovery and purity. Samples were applied in a 12.5% acrylamide gel and migrated at 90 mV. Images were acquired with Gel Doc™ XR+ System with Image Lab™ software from Bio-Rad and analyzed with ImageJ software. The total protein precipitation yield was calculated as in Equation 6.2:

$$\text{Precipitation yield (\%)} = = \frac{\mu g \text{ total protein precipitated}}{\mu g \text{ total protein loaded}} \times 100 \qquad \text{Equation 6.2}$$

Table 6.1. List of the precipitants for antibody precipitation, based on the Hofmeister series, unless otherwise stated. All precipitants were used at a 300 mM concentration at its given pH or at pH 7, adjusted by 10 mM Tris-HCl pH 8, unless otherwise stated.

Precipitant	Source
KCl	Hofmeister series
KCl @pH7	Hofmeister series
K_2SO_4	Hofmeister series
NaCl	Hofmeister series
NaCl @pH7	Hofmeister series
Na_2SO_4	Hofmeister series
Na_2SO_4 @pH7	Hofmeister series
$Na_3C_6H_5O_7$	Hofmeister series
$Na_3C_6H_5O_7$ @pH7	Hofmeister series
LiCl	Hofmeister series
LiCl @pH7	Hofmeister series
Li_2SO_4	Hofmeister series
Li_2SO_4 @pH7	Hofmeister series
$CaCl_2$	Hofmeister series
$CaCl_2$ @pH7	Hofmeister series
$MgCl_2$	Hofmeister series
$MgCl_2$ @pH7	Hofmeister series
$MgSO_4$	Hofmeister series
$MgSO_4$ @pH7	Hofmeister series
20% (w/v) PEG3350	HTX Lab@ EMBL Grenoble
2.5 M NaCl	HTX Lab@ EMBL Grenoble

6.2.4.2. Affinity magnetic precipitation

The four best performing precipitant conditions - 300 mM $LiSO_4$, 300 mM $CaCl_2$, 20% PEG3350 and 2.5 M NaCl - were tested for the affinity magnetic precipitation of antibodies having 0.5 mg/ml MP-Dextran (control) or MP-22/8. Affinity magnetic precipitation was carried out at a 1 ml scale with a 1:1 crude extract to precipitant volumetric ratio. Prior to incubation with the crude extract, all MP solutions were sonicated and homogenized for 10 minutes. The crude extract and magnetic precipitant incubation were optimized in terms of orbital shaking (200 *vs* 0 RPM), temperature (4º *vs* 20ºC) and time (1h *vs* 24h). The best incubation parameters were 200 RPM at 4ºC for 1h. Crude extract and magnetic precipitant were incubated, and the MPs separated by the application of an external magnetic field for 15 min, generating the magnetic supernatant and magnetic precipitate. The magnetic supernatant was further centrifuged (5000 *xg*, 15min at 15ºC), the supernatant harvested, and the precipitate resuspended in PBS and the bound proteins eluted. MPs were recovered from solution by the application of an external magnetic field for 15 minutes and the eluted proteins were harvested in the soluble fraction. The magnetic precipitation yield was calculated as in Equation 6.3:

$$\text{Magnetic precipitation yield (\%)} = = \frac{\mu g \text{ total protein recovered}}{\mu g \text{ total protein loaded}} \times 100 \qquad \text{Equation 6.3}$$

This pipeline was performed for antibody capture from human serum (0.5 mg/ml total protein), anti-TNFα monoclonal antibody (Infliximab) and anti-HER2 monoclonal antibody (Trastuzumab) (10 mg/ml total protein). As controls, the magnetic precipitation was performed with PBS as precipitant with and without MP. Total protein quantification was performed using BCA assay reagent (Sigma-Aldrich). SDS–PAGE was performed to evaluate the samples Ig recovery and purity. Samples were applied in a 12.5% acrylamide gel and migrated at 90 mV. Images were acquired with Gel Doc™ XR+ System with Image Lab™ software from Bio-Rad and analyzed with ImageJ software. The antibody recovery yield was calculated by densitometry as in Equation 6.4 and purity as in Equation 6.5:

$$\text{Antibody recovery yield (\%)} = = \frac{\text{Area of heavy and light chains of antibody recovered}}{\text{Area of heavy and light chains of antibody loaded}} \times 100 \qquad \text{Equation 6.4}$$

$$\text{Antibody purity (\%)} = = \frac{\text{Area of heavy and light chains of antibody recovered}}{\text{Area total of protein recovered}} \times 100 \qquad \text{Equation 6.5}$$

6.2.5. Analytics

6.2.5.1. Total protein quantification

Protein quantification was performed using bicinchoninic acid (BCA) assay reagent (Sigma-Aldrich). The protein standard used was bovine serum albumin (BSA) from Sigma-Aldrich. The assay was performed in 96-well transparent microplates flat-bottom from Sarstedt. Absorbance was measured at 560 nm in Tecan Infinite F200 microplate reader. Precipitation yield was determined by dividing the total protein concentration in the precipitate fraction by the total protein content in the crude extract.

6.2.5.2. Protein gel electrophoresis

Sodium dodecyl sulfate–polyacrylamide gel electrophoresis (SDS–PAGE) was performed to evaluate the samples' Ig recovery and purity. The buffer sample composition was 0.15 M Tris–HCl at pH 6.8, 6% (w/v) SDS, 0.025% (w/v) bromophenol blue, 12.5% (v/v) glycerol and as reducing agent β-mercaptoethanol was used. Prior to loading in the gel, all the samples were denatured at 100°C for 5 minutes. Samples were applied in a 12.5% gel, prepared from 41% acrylamide/bis stock solution (30:1) from Bio-Rad and migrated at 90 mV using as running buffer 192 mM glycine, 25 mM Tris-HCl and 0.1% SDS, pH 8.3. Gels were stained using two methods: (i) Coomassie stained with the staining solution of 0.5% (w/v) Coomassie Blue R-250, 7.5% (v/v) acetic acid, 45% (v/v) methanol, for 30 min at room temperature with orbital shaking and revealed with the distaining solution (7.5% (v/v) acetic acid, 45% (v/v) methanol) until proper protein visualization; or (ii) using Bio-Rad silver staining kit. Images were acquired with Gel Doc™ XR+ System with Image Lab™ software from Bio-Rad and analyzed with ImageJ software.

6.2.5.3. High performance size-exclusion chromatography

High performance size-exclusion chromatography was performed to assess IgG aggregation and HPLC purity resulting from the precipitation strategy developed for antibody purification. The samples were loaded (20 µl) undiluted and migrated in isocratic mode in a Yarra Sec-3000 column (300x7.8 mm, particle size 3 µm, pore size 290 Å) from Phenomenex at 0.5 mL/min for 30 min with PBS and UV detection at 280 nm. The area of antibody aggregation in each precipitation condition was compared with the area of antibody aggregation from the crude extract sample. HPLC purity was calculated by the ratio between the IgG peak area and the total area of the chromatogram.

6.2.5.4. mAb activity

6.2.5.4.1. Indirect enzyme linked immunosorbent assay – Anti-TNFα mAbs

To evaluate the biological activity of anti-TNFα monoclonal antibodies after purification by precipitation, an indirect enzyme linked immunosorbent assay (ELISA) was performed, 96-well half-area microplates (Corning Costar, USA) were coated with human TNFα (200 ng/well) in PBS and incubated overnight at 4ºC. The plate was then aspirated and washed once with 150 µl PBST (PBS with 0.05% (v/v) Tween® 20). Nonspecific binding sites were blocked with 3% (w/v) BSA in PBST for 1h at 37°C. Afterwards, the plate was washed as previously above. 50 µl of the purified anti-TNFα mAb samples (0.1 µl/ml) and calibration curve (Infliximab, Remicade® 10 mg/ml at 0; 0.01; 0.03; 0.05; 0.1; 0.2; 0.3 µg/ml in 1% (w/v) BSA in PBST) were added and incubated for 1h at 24ºC. Subsequently, the plate was washed 3 times as previously described. Detection was performed with the addition of 50 µl of secondary antibody anti-Human Kappa Light Chain-horseradish peroxidase antibody from goat (RRID: AB_ 2535630, Invitrogen) diluted 1:50,000 (0.02 ng/ml) in 1% (w/v) BSA in PBST. The secondary antibody was incubated for 30 min at 24ºC, and the plate was washed 3 times as previously described. The reaction was developed with 50 µl TMB (3,3',5,5'-Tetramethylbenzidine, Merk, Germany) substrate for 30 min at 24ºC in the dark and stopped with 2 M H_2SO_4 (Merck) for 30 min at 24ºC in the dark. Absorbances were registered at 450 nm, on Model 680 microplate reader (Bio-Rad, USA).

6.2.5.4.2. Indirect flow cytometry – Anti-HER2 mAbs

The activity of anti-HER2 monoclonal antibodies after purification through precipitation was determined by flow cytometry analysis. Cells were harvested with dissociation buffer (0.6 nM EDTA in PBS) and centrifuged at 300 x*g* for 5 min and resuspended in ice cold PBS with 3% (w/v) BSA (Sigma) to a final concentration of 1 x 10^6 cells/ml. Cell suspension with 1 x 10^5 cells were incubated with 0.5 µg of anti-HER2 mAbs samples for 30 min at 4ºC. Afterwards, the cells were washed twice by centrifugation at 300 x*g* for 5 min and resuspended in ice cold PBS with 3% (w/v) BSA. The detection was performed with addition of the secondary antibody Goat anti-Human IgG (H+L) Cross-Adsorbed Secondary Antibody conjugated with FITC (RRDI: AB_2535589, Invitrogen), diluted to a final concentration of 1:400. The secondary antibody was incubated for 30 min at 4ºC in the dark, the cells were then washed by centrifugation as previously described and 10 µl of propidium iodide (10 µg/ml, Sigma) added to the stained cells. Assessment of antibody binding were performed using Guava easyCyte™ (Merck Millipore). Flow cytometry data was analysed with FlowJo software (TreeStar).

6.3. Results and discussion

6.3.1. Screening conditions for antibody precipitation

Salts have a major effect in protein solubility and propensity to precipitate that many times follows the Hofmeister series. The Hofmeister series ranks the salt anions and cations according to their kosmotropic and chaotropic character, whether they have a salting-out or salting-in effect on proteins, respectively. An initial precipitation screen inspired in the Hofmeister series was designed for the precipitation of pure human polyclonal antibody (pAb) at 2 and 20 mg/ml (Figure 6.1A). All tested precipitation conditions lead to pAb precipitation, however the majority did exhibit a very low precipitation yield (<20%). In addition, when the precipitant concentration was constant, the 10-fold increase in protein concentration did not reflect a 10-fold increase in the precipitation yield. The combination of these results may indicate that the precipitant concentration is lower for the protein to precipitate in the set conditions. Nonetheless, and since protein-protein interactions also play a major role in protein precipitation, the same rational was applied to human serum, with a total protein concentration of 0.5 mg/ml, with the aim to precipitate and capture the pAb. Two additional precipitation conditions were tested – 20% (w/v) PEG3350 and 2.5 M NaCl (Figure 6.1B). Both conditions were unveiled by a high throughput precipitation screening in the HTX lab at EMBL Grenoble. Of the 21 precipitation conditions tested, 5 presented a precipitation yield higher than 40% – 300 mM $LiSO_4$; 300 mM $CaCl_2$; 300 mM $CaCl_2$ @pH7; 20% (w/v) PEG3350 and 2.5 M NaCl (Figure 6.1B). However, none of the different conditions enabled a selective precipitation of the pAb (Figure 6.1C).

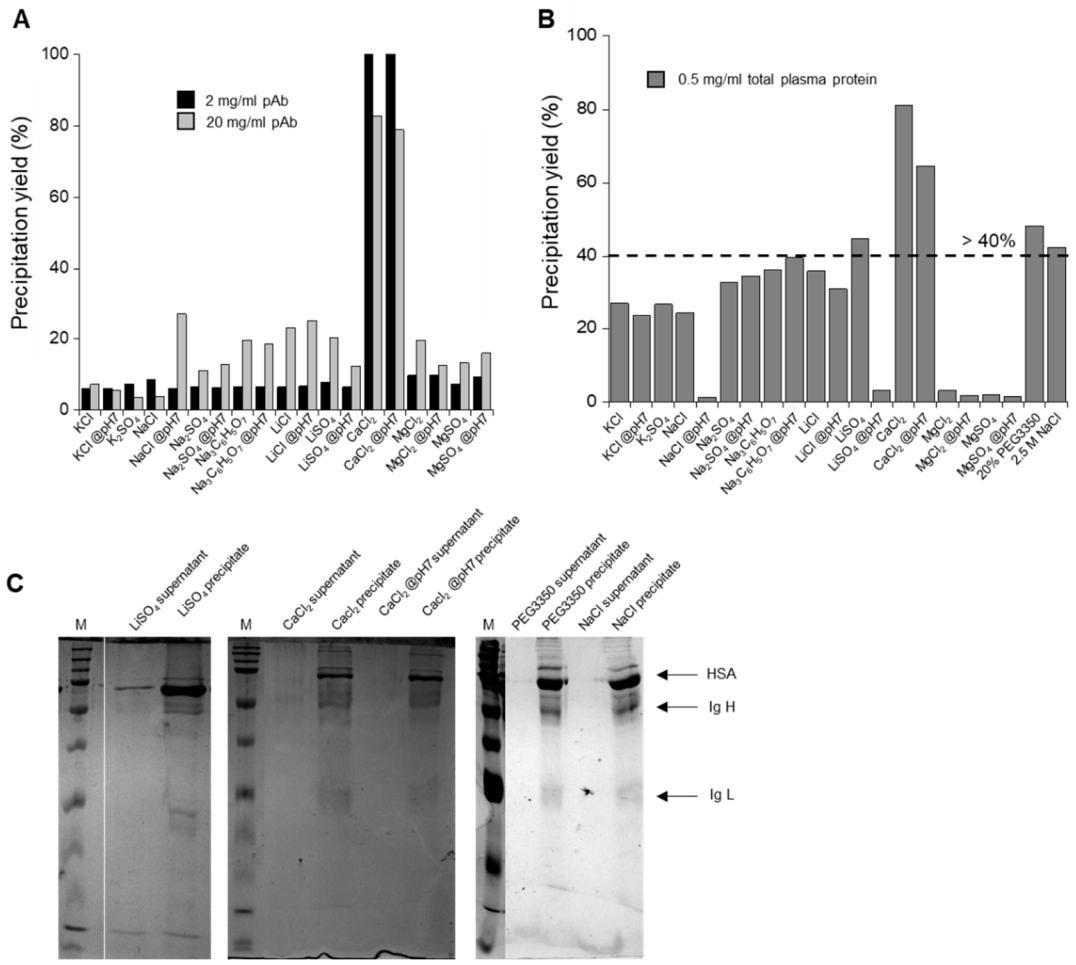

Figure 6.1. Precipitation screen for antibody precipitation using 300 mM precipitant, except if otherwise specified. Precipitation yield for (**A**) pure polyclonal antibody at 2 mg/ml (**black**) and 20 mg/ml (**grey**) and (**B**) human serum at 0.5 mg/ml total protein with a dashed line at 40% precipitation yield threshold. (**C**) SDS-PAGE for the precipitant condition with a precipitation yield higher than 40% with the supernatant and precipitation samples for each condition. **Lane ID**: **M**: Precious Plus Protein™ Dual Color Standards (from top to bottom: 200, 150, 100, 75, 50, 37, 25 and 20 kDa); arrows indicate HSA (66 kDa), Ig heavy (Ig H; 50 kDa) and light (Ig L; 25 kDa) chains.

6.3.2. Affinity magnetic precipitation – pAb capture from human serum

To provide antibody selectivity, magnetic particles functionalized with the 22/8 triazine (MP-22/8) synthetic ligand [227], were used as additives in the precipitant solution. The orbital shaking, temperature and incubation time of crude extract and precipitant with MP-22/8 were optimized (Figure 6.2) using human serum with a total protein concentration of 0.5 mg/ml. The orbital shaking (200 *vs* 0 RPM) had a great effect in the precipitation yield, however, depending on the precipitant, the orbital shaking had a positive, negative or neutral effect. For 300 mM $LiSO_4$ and $CaCl_2$, the lack of orbital shaking had a negative effect in the precipitation yield, whereas for 2.5 M NaCl the lack of orbital shaking had a positive effect in the precipitation yield. For 20% (w/v) PEG3350 the precipitation yield was not affected by the orbital shaking (Figure 6.2B). The orbital shaking at 200 RPM does improve the homogeneous dispersion of MPs in solution, nevertheless

both 2.5 M NaCl and 20% (w/v) PEG3350 precipitation conditions were unveiled in static crystallization assays. In the case of 20% (w/v) PEG3350, the orbital shaking, or lack of it, did not present any difference in the final precipitation yield, mainly due the MPs stability in this solution. On the other hand, in 2.5 M NaCl the same did not occur, the orbital shaking led to be a more stable condition to maintain the protein in solution, hence a lower precipitation yield (Figure 6.2B).

Protein-protein interactions mainly occur by weak interactions as hydrophobic interactions, hydrogen bonds, salt bridges or van der Walls forces [228]. Since precipitation is dependent on protein-protein interactions, and being these interactions temperature-dependent, the precipitation yield was assessed at 4ºC and 20ºC (Figure 6.2C), at high salt concentration or in the presence of hygroscopic species, such as PEG. This effect is more pronounced at lower temperatures, where hydrogen bonds and salt bridges are weakened [229], contributing to the destabilization of the proteins in solution. This explains the results obtained, since protein precipitation with 20% (w/v) PEG3350 and 2.5 M NaCl showed a greater increase in the magnetic precipitation yield from 20ºC to 4ºC. On the other hand, the change in temperature did not have a major influence in protein magnetic precipitation yield with 300 mM of $LiSO_4$ and $CaCl_2$. At last, the incubation time was optimized, and two time points were checked – 1 h and 24 h. In all conditions, without exception, the 24h incubation led to a lower magnetic precipitation yield (Figure 6.2D). This phenomenon can be due to the equilibrium that is established between protein in solution and protein precipitated Additionally, the lower precipitation yield was not proportional to a higher antibody purity and capture. In this way, the best incubation condition was 200 RPM at 4ºC for 1h. For the tested precipitants, the best performing one was 20% (w/v) PEG3350, as it was the condition with higher pAb content in the elution fraction. Since precipitant concentration does play a major role, three different concentrations of $LiSO_4$, $CaCl_2$ (100 mM; 200 mM and 300 mM), PEG3350 (10%; 20% and 30% (w/v)) and NaCl (1.5 M, 2.5 M and 3.5 M) were tested in the presence of MP-22/8 (Figure 6.3A), MP-Dextran (Figure 6.3B) and in the absence of MPs (Figure 6.3C). PEG3350 showed to be the best precipitant condition with higher antibody recovery and purity (Figure 6.3).

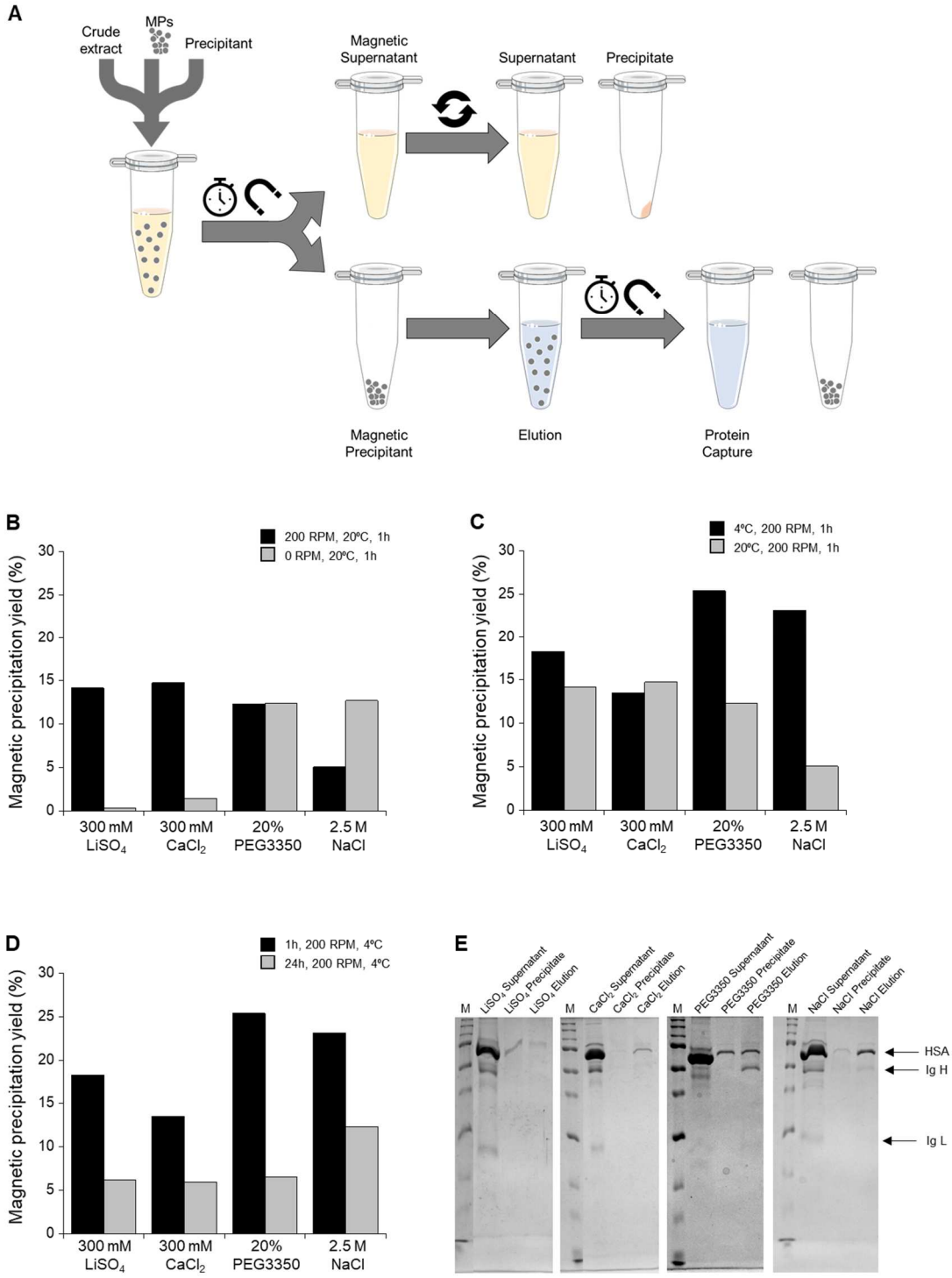

Figure 6.2. Magnetic precipitation optimization with MP-22/8. (**A**) Schematic representation of the Magnetic precipitation assay. (**B**) Optimization of the precipitation orbital shaking for 1 hour at 20ºC with 200 RPM (**black**) and 0 RPM (**grey**). (**C**) Optimization of the precipitation temperature for 1 hour at 200 RPM at 4ºC (**black**) and 20ºC (**grey**). (**D**) Optimization of the precipitation time at 4ºC with 200 RPM for 1 hour (**black**) and 24 hours (**grey**). (**E**) SDS-PAGE for the Magnetic precipitant at 4ºC for 1 hour at 200 RPM. **Lane ID: M:** Precious Plus Protein™ Dual Color Standards (from top to bottom: 200, 150, 100, 75, 50, 37, 25 and 20 kDa); arrows indicate HSA (66 kDa), Ig heavy (Ig H; 50 kDa) and light (Ig L; 25 kDa) chains.

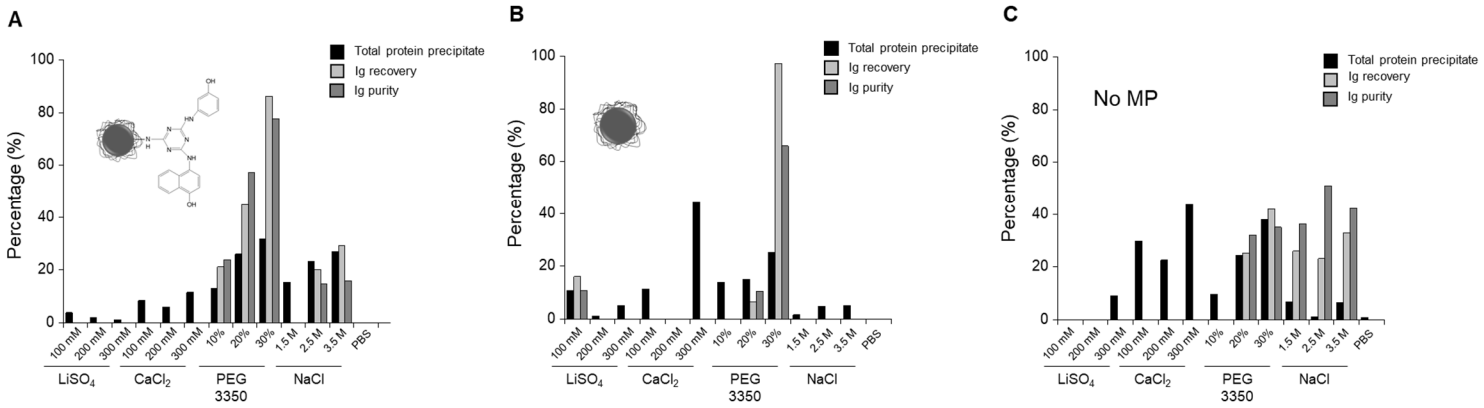

Figure 6.3. Magnetic precipitation of human serum for pAb recovery. In the presence of (**A**) MP-22/8, (**B**) MP-Dextran and (**C**) No MP, using the four main precipitants - $LiSO_4$, $CaCl_2$, at 100, 200 and 300 mM; PEG 3350 at 10, 20 and 30% (w/v) and NaCl at 1.5, 2.5 and 3.5 M. **Legend:** Total protein precipitate (**black**), Ig recovery (**light grey**) and Ig purity (**grey**).

Although the MPs were functionalized with a synthetic affinity ligand with a K_a of 7.7×10^5 M^{-1} in 50 mM phosphate buffer at pH 8 [136], the affinity between two molecules is regulated by the interactions established between them dependent on the solution conditions, such as ionic strength or pH. The 22/8 triazine affinity ligand interaction with antibodies, namely IgG, can be done at both the Fc and Fab domains, with higher affinity towards the Fc [230]. Nonetheless, affinity interactions are a combination of hydrophobic, H-bonding and electrostatic interactions, strongly dependent on the pH and ionic strength [230]. All precipitant solutions presented a 5-8 pH range, except $LiSO_4$ that had a 3-4 pH range. Even though theoretical and experimental data suggest that pH is the major factor for 22/8-IgG binding, the fact that the elution from MP-22/8 was performed with PBS at pH 7.4. This elution condition, suggests that the pH did not have the major contribution in the present situation, but the ionic strength of the precipitant solutions did, not only due to the elution buffer but also due to the best performing precipitant – 20% (w/v) PEG3350 – that presented the lower ionic strength. PEG is a polymer known to attract water molecules from the protein's surface increasing its interprotein interactions, leading to protein precipitation. Furthermore, in solution, PEG presents a amphiphilic character, exhibiting hydrophilic and hydrophobic characteristics, although neglectable PEG-protein interaction can induce protein conformational changes leading to the exposure of the protein hydrophobic residues that may interact with other proteins, PEG molecules or small molecules [231].

The increasing PEG3350 concentration (from 10% to 30% (w/v)) led to a higher pAb recovery and purity in the presence of MP-22/8 as additives, reaching 80% purity and 50% recovery, whereas when MP-Dextran was used as additive 43% pAb was recovered with 23% purity. When No MPs were added, similar results were obtained with 47% recovery and 32% purity (Figure 6.4A;B). In the absence of PEG, having only PBS in solution, no pAb was recovered in the elution fraction (Figure 6.4A;B). Without the presence of PEG, having only PBS in solution, no pAb was recovered in the elution fraction (Figure 6.4A;B). The low recovery yields obtained were due to the co-elution of human serum albumin (HSA), being the most abundant protein in human serum, and, even though most HSA did not precipitate or bind to the MPs (Figure 6.4C), a portion of this protein still precipitated and co-eluted with pAb. Nevertheless, at concentrations higher than 20% (w/v) PEG3350, pAb was only recovered in the elution fraction (Figure 6.4C).

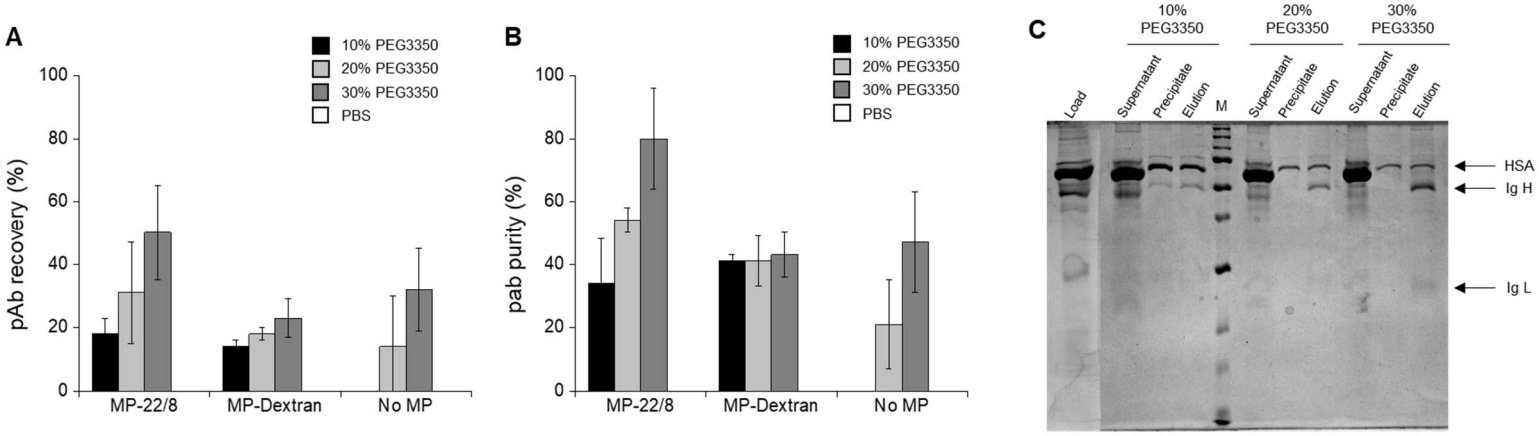

Figure 6.4. Magnetic Affinity Precipitation of human serum plasma crude extract for pAb purification. (**A**) pAb recovery and (**B**) pAb purity using MP-22/8, MP-Dextran and No MP with 10 (**black**), 20 (**light grey**) and 30% (w/v) (**grey**) PEG3350. (**C**) SDS-PAGE for the best affinity magnetic precipitation condition tested – MP-22/8 with 10, 20 and 30% (w/v). **Lane ID**: **M**: Precious Plus Protein™ Dual Color Standards (from top to bottom: 200, 150, 100, 75, 50, 37, 25 and 20 kDa); arrows indicate HSA (66 kDa), Ig heavy (Ig H; 50 kDa) and light (Ig L; 25 kDa) chains.

6.3.3. Affinity magnetic precipitation – mAb capture from CHO clarified supernatant

Affinity magnetic precipitation was tested for the capture of two monoclonal antibodies (mAbs), both IgG1– anti-TNFα and anti-HER2 – using PEG3350 as precipitant. The incubation condition was performed with 200 RPM at 4ºC for 1h with the respective precipitant solution. As MPs control, an assay with MP-Dextran and without MPs were conducted; while PBS at pH 7.4 was used as a precipitant control. MP-Dextran were used as control since they are an intermediate product of the MP-22/8 synthesis and the use of high salt solution (> 0.25 M) and PEG may lead to non-specific interactions between the medium proteins and the solid matrix [232].

For anti-TNFα mAb capture, three different PEG3350 concentrations were tested – 10%, 20% and 30% (w/v) – to assess IgG recovery and purity in the elution fraction (Figure 6.5). The maximum of recovery was observed with 20% (w/v) PEG3350. For 10% (w/v) PEG3350, approximately 10% of the mAb did not precipitate onto the magnetic particles and was leaked in the supernatant fraction. On the other hand, with 30% (w/v) PEG3350, 20% of the mAb precipitated without binding to MP-22/8 (Figure 6.5C). Although pure, the recovery of this fraction comprises an additional centrifugation step in the downstream pipeline of anti-TNFα mAb capture. In this way, the best recovery and purity yields were obtained with 20% (w/v) PEG3350 using MP-22/8, reaching a 97% recovery and 99% purity, as opposed to 31% recovery and 52% recovery from MP-Dextran and no MP, respectively, and 10% recovery using PBS (Figure 6.5).

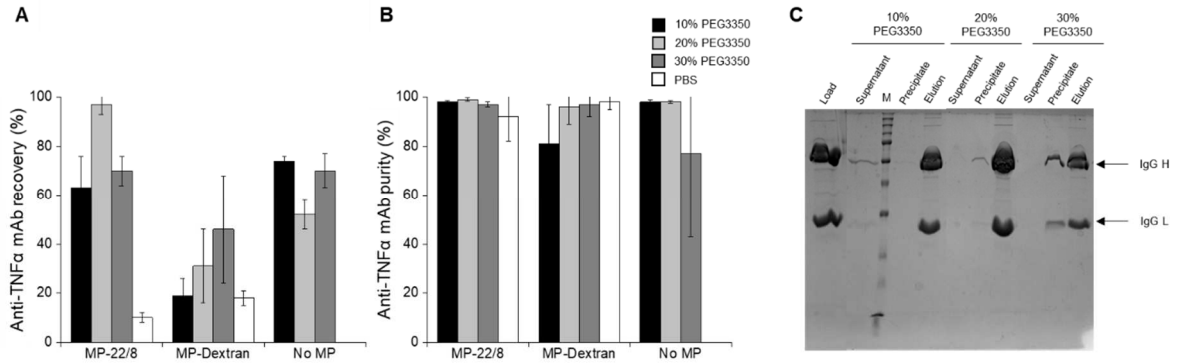

Figure 6.5. Magnetic Affinity Precipitation of anti-TNFα mAb crude extract. (**A**) mAb recovery and (**B**) mAb purity using MP-22/8, MP-Dextran and No MP with 10, 20 and 30% (w/v) PEG3350. (**C**) SDS-PAGE for the best affinity magnetic precipitation condition tested – MP-22/8 with 10, 20 and 30% (w/v). **Lane ID: M:** Precious Plus Protein™ Dual Color Standards (from top to bottom: 200, 150, 100, 75, 50, 37, 25 and 20 kDa); arrows indicate IgG heavy (Ig H; 50 kDa) and light (IgG L; 25 kDa) chains.

For anti-HER2 mAb, only the best precipitant solution was tested – 20% PEG3350 – with 200 RPM at 4ºC for 1h and the same MPs controls were established – MP-Dextran and no MP (Figure 6.6). The best results were obtained using MP-22/8 with 100% recovery and 63% purity, whereas for MP-Dextran 89% recovery and 55% purity was obtained. When no MPs were used, the recovery yield was 87% with 49% purity.

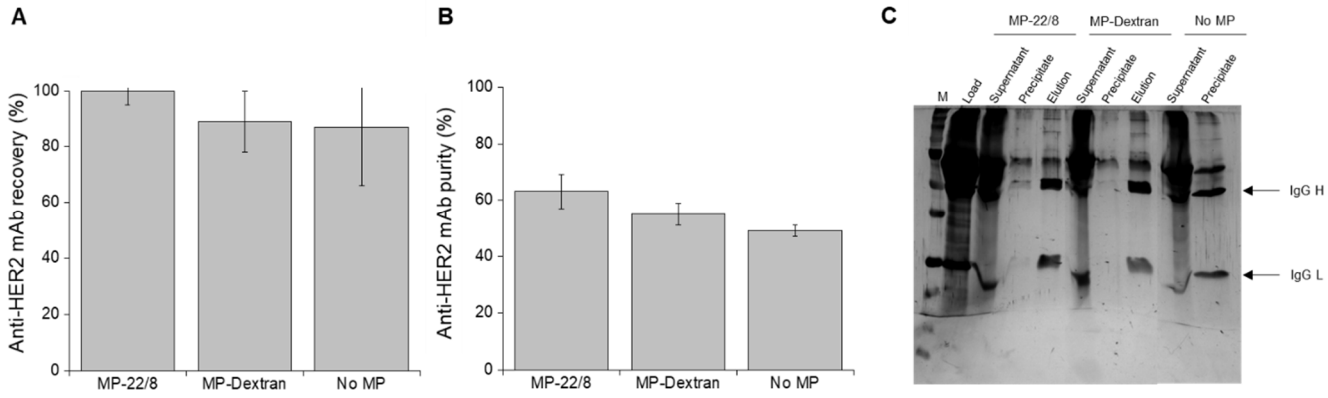

Figure 6.6. Magnetic Affinity Precipitation of anti-HER2 mAb crude extract with 20% (w/v) PEG3350. Anti-HER2 (**A**) recovery and (**B**) purity assessment using MP-22/8, MP-Dextran and No MP. (**C**) SDS-PAGE for the precipitant conditions tested. **Lane ID: M:** Precious Plus Protein™ Dual Color Standards (from top to bottom: 200, 150, 100, 75, 50, 37, 25 and 20 kDa); arrows indicate IgG heavy (Ig H; 50 kDa) and light (IgG L; 25 kDa) chains.

The two mAbs tested were produced in two different types of clarified CHO cell supernatant. While anti-TNFα mAb was produced in a serum free medium, anti-HER2 mAb was produced in a serum containing medium, making this a less pure medium with lower IgG to total protein ratio. Since protein concentration is one of the factors for protein precipitation – the higher the target protein concentration, the higher the precipitation yield – the ratio IgG to total protein should be as high as possible. On the other hand, if the ratio is low, multiple rounds of precipitation can be performed until higher purities are obtained.

The presence of aggregates and biological activity were evaluated after the antibodies capture by affinity magnetic precipitation. Three different techniques were used: (i) HPLC size-exclusion for both mAbs; (ii) indirect enzyme-linked immunosorbent assay (ELISA) for anti-TNFα mAbs and (iii) indirect flow cytometry for anti-HER2 mAbs, to verify the antibody integrity after capture.

Size exclusion chromatography was performed in order to evaluate if IgG aggregates were present or formed along the purification process. The magnetic precipitation of anti-TNFα mAbs in the presence of MP-22/8 did not show aggregates formation, presenting 98% HPLC-purity across all PEG3350 concentrations. The same behaviour was observed in the presence of MP-dextran, presenting 97% HPLC-purity. When no MPs were present, high HPLC-purities of 98% were only possible with 20% and 30% (w/v) PEG3350. For anti-HER2 mAb, magnetic precipitation with MP-22/8 showed the presence of possible mAb aggregates, representing 30%, being the mAb monomer present with 66% HPLC-purity. On the other hand, when MP-dextran was present, the aggregates formation was reduced to 3% and the mAb monomer HPLC-purity increased to 84%.

The biological activity of purified anti-TNFα mAb was evaluated by indirect ELISA (Figure 6.7A). The elution fractions from the magnetic precipitation using PEG 3350 as precipitant at different concentrations in the presence of either 22/8 or dextran-coated MPs were analyzed, as well as the eluted fractions of mAb precipitation without the presence of MPs. Magnetic precipitation - MPs in the presence of PEG3350 as precipitant - presented higher mAb activity when compared to magnetic fishing - MPs in the presence of PBS (Figure 6.7A) - indicating that PEG can stabilize the mAb along the precipitation steps and does not diminish nor interfere with the mAb biological activity. In the conditions tested, mAb activity varied depending on the MP present. Nonetheless, amongst the different PEG 3350, 10% (w/v) showed to be the best precipitant concentration with both MPs. In the presence of MP-22/8 with 10% (w/v) PEG3350 a 60% anti-TNFα mAb activity was observed. However, the highest mAb activity was achieved in the presence of MP-dextran with 10% (w/v) PEG3350, achieving 84% activity (Figure 6.7A).

For anti-HER2 mAb, since its antigen is the transmembrane protein HER2, its activity was evaluated by indirect flow cytometry (Figure 6.7B). Anti-HER2 mAb magnetic precipitation was evaluated in the presence of MP-22/8, MP-dextran and no MP presence having as precipitant 20% (w/v) PEG3350. For the flow cytometry analyses SKBR3 cells were used to evaluate the activity, whereas HeLa cells were used as a negative control. Overall, PEG3350 precipitation did not affect mAb activity, except when MP-dextran was present for the magnetic precipitation. A summary of mAb yield, purity and activity is reported in Table 6.2.

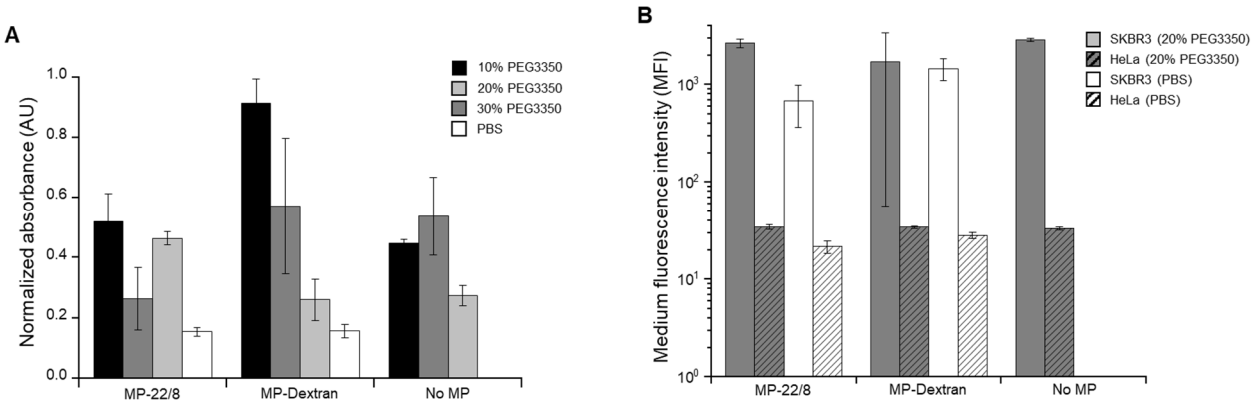

Figure 6.7. Activity of anti-TNFα and anti-HER2 mAbs purified by magnetic precipitation. (**A**) Indirect ELISA of the elution fraction of anti-TNFα mAb in the presence of MP-22/8, MP-dextran and No MP at different PEG3350 concentration (10%, 20% and 30% (w/v)) and PBS. (**B**) Indirect flow cytometry of the elution fraction of anti-HER2 mAb in the presence of 20% (w/v) PEG3350 and PBS for SKBR3 and HeLa cells.

Table 6.2. Summary of paramount parameters for affinity magnetic mAbs precipitation – yield, purity and activity at the elution fraction having as precipitant 20% (w/v) PEG3350 in the presence of MP-22/8 and MP-dextran.

	Yield		**Purity**		**Activity**	
	MP-22/8	MP-dextran	MP-22/8	MP-dextran	MP-22/8	MP-dextran
Anti-TNFα mAb *	97%	31%	98%	52%	+	++
Anti-HER2 mAb *	100%	89%	63%	55%	+++	++

*Precipitant: 20% (w/v) PEG3350

6.4. Conclusion

The viability of using affinity magnetic precipitation for antibody capture from clarified cell supernatant was for the first time demonstrated. Three different antibodies sources were tested: (i) pAbs from human serum, (ii) anti-TNFα mAb and (iii) anti-HER2 mAb from clarified CHO cell supernatant. The study comprised the discovery of the best precipitant and precipitation conditions using MPs functionalized with the 22/8 triazine synthetic ligand previously discovered to have affinity towards antibodies [227]. The addition of MPs was demonstrated to be crucial to achieve higher antibody purity and recovery. Nonetheless, the optimization of the precipitant and precipitation conditions also revealed to be essential to minimize antibody loss and maximize its purity. The best affinity magnetic precipitation condition was using PEG3350 as precipitant with varying concentration of 20% and 30% (w/v) for 1h at 4ºC with 200 RPM orbital shaking. For pAbs capture from human serum it was possible to reach 80% purity and 50% recovery with 30% (w/v) PEG3350. For both mAbs, the best result was accomplished with 20% (w/v) PEG3350 reaching a 97% recovery and 99% purity for anti-TNFα mAb and 100% recovery and 63% purity for anti-HER2 mAb. The elution was always performed using PBS at pH 7.4, this may lead not only to the antibody capture but also to conditioning and concentration in one single step. Contrary to the current Protein A affinity chromatography

harsh pH denaturing elution condition [219], the combination of the precipitant condition, with PEG, along with the elution condition with PBS makes this a biocompatible and mild capture process for mAbs purification [231,232].

In this way, and with the continuous growth of the biosimilar market, the lower costs associated, the scalability of precipitation process, and the use of an affinity synthetic ligand to provide selectivity towards the target molecule, makes affinity magnetic precipitation a new platform for the capture of high added value proteins directly from the complex cell supernatant.

General conclusion and Future work

The biopharmaceutical industry is currently under a great change, mainly due to the development and approval of high added value biosimilar molecules. Still, one of the bottlenecks in protein production is their downstream processing, namely its purification. The current gold standard in purification of high added value biopharmaceuticals rely in packed bed chromatographic strategies. Over the last 15 years, several researchers in industry and academy joined efforts in the search for affinity reagents based on fully biological or fully synthetic scaffolds for protein purification. Regardless, due to the limitations demonstrated by chromatographic techniques to deal with the high titers and volumes produced upstream, a new approach relies in Anything But Chromatography (ABC) methodologies.

In this work, the potential of having a combination of two ABC methods was evaluated for the development of a new non-chromatographic platform for biopharmaceutical purification. Inspired in protein crystallization, this work focused on developing a new precipitation process triggered by magnetic nano- and micro-particles used as additives, creating a new hybrid purification process named magnetic precipitation. The research strategy was divided in two sections. Firstly, protocols to develop new simpler affinity ligands towards relevant biopharmaceuticals (human serum albumin (HSA)) were done, followed by optimization of strategies for ligand attachment onto magnetic particles (MPs). Secondly, crystallization of model proteins having affinity driven magnetic particles was evaluated in terms of crystal growth and diffraction quality. Lastly, affinity driven magnetic precipitation was assessed in the purification of antibodies from complex media.

Firstly, we evaluated the potential of magnetic particle functionalization with synthetic ligands in a triazine-based scaffold that was rationally designed for the affinity purification of a biopharmaceutical relevant protein such as HSA. In order to produce stable ligands with a wide variability in binding capacities, the triazine-ring scaffold was chosen for the rational approach to define and produce 64 synthetic ligands to bind HSA domain II. Of the 64 ligands screened, two showed the most promising binding capacity to capture HSA from serum crude extract (100% recovery yield), however it was only possible to achieve high yield and purity with one triazine synthetic ligand, named A6A5. Once established the ability to used synthetic ligands in conventional packed bed chromatography support, we here demonstrated the functionalization of magnetic particles with biological ligands with affinity towards pharmaceutical relevant proteins, such as antibodies. The functionalization and capture with the affinity driven magnetic fishing led to high recovery and purity of polyclonal antibodies from complex crude extract as human serum.

The successful functionalization of two different solid supports and capture with high recovery yield and final protein purity led to the challenge to further improve the magnetic fishing method by coupling it with the precipitation method. The proof-of-concept was performed with three model proteins (of those, two were commercially available, HEWL and trypsin, and one produced in house, GFP), to evaluate the performance of magnetic particles in the crystallization of those proteins. The magnetic particles, here used as additives, did not hamper the crystallization, moreover crystallization conditions for trypsin were altered in the presence of affinity driven magnetic particles, as the usually used inhibitor (benzamidine) could be removed from the crystallization conditions without diminishing crystal quality or altering protein

structure. This work proved possible to add magnetic particles to a precipitation process maintaining the proteins' quality and enabling its incorporation in the purification pipeline of high added value proteins.

With the attempt to use magnetic precipitation in the proteins' purification train, different antibodies from different crude extracts were tested using specific precipitation conditions for the target proteins, as well as magnetic particles functionalized with a triazine synthetic affinity ligand to target and capture antibodies from the crude extract. The new method enabled the purification of antibodies, without any previous conditioning, with a final purity up to 99% and a recovery yield up to 97% in a single step.

This work highlights the synergy of different separation methods to accomplish a high purity and high recovery of biopharmaceutical relevant molecules, enabling to overcome the current bottlenecks in the conventional downstream processing regarding the high titers and working volumes produced upstream. The work developed here can be integrated in the current purification techniques, not with the objective of replacing the implemented chromatographic methods, but as an additional strategy to overcome the current challenges. Here, this method can cope with the demands from upstream processing enabling in step the capture, conditioning and concentration of the target molecule. Afterwards, the chromatographic train can be designed to provide a high quality and high purity product.

Although this was not studied in this work, the mechanism through which differently coated MPs influence and trigger nucleation and protein crystal growth deserves investigation. The current work was focused on a proof-of-concept to study the effect of MPs as additives in the crystallization of model proteins for structure determination. Future work will be done to test this technology in difficult-to-crystallize proteins or to replace required additives in protein crystallization. Furthermore, assays were centered in the vapor diffusion method. Although this is currently the most used protein crystallization method, it is of interest to evaluate the effect of MPs when used in other methods, such as batch or free interface diffusion.

As for the purification of antibodies, the integration of magnetic precipitation in the current downstream pipeline, having same adaptations to reduce costs and time, should be tested. In line with this, the scale-up of this method is critical for the hypothesis here raised, as well as working in cGMP conditions.

Overall, the work here presented reinforces that magnetic fishing and crystallization/precipitation techniques can be used in synergy for protein 3D structure determination and purification.

References

[1] M. Hall, G. Pave, D. Hill, Global Pharmaceuticals: 2018 industry statistics | Hardman & Co, 2019. https://www.hardmanandco.com/research/corporate-research/global-pharmaceuticals-2018-industry-statistics/ (accessed September 22, 2019).

[2] G. Walsh, Biopharmaceutical benchmarks 2018, Nat. Biotechnol. 36 (2018) 1136–1145. doi:10.1038/nbt.4305.

[3] Perciva, Press release: DSM and Crucell announce record achievement in PER.C6® technology, (2008).

[4] H. Broly, C. Mitchell-Logean, M.D. Costioli, C. Guillemot-Potelle, Cost of goods modeling and quality by design for developing cost-effective processes, BioPharm Int. 23 (2010) 26–35. http://www.biopharminternational.com/cost-goods-modeling-and-quality-design-developing-cost-effective-processes?id=&sk=&date=&%0A%09%09%09&pageID=2 (accessed January 20, 2016).

[5] M. Franzreb, E. Müller, J. Vajda, Cost estimation for protein A chromatography, Bioprocess Tech. 12 (2014) 44–52.

[6] M. Kuczewski, E. Schirmer, B. Lain, G. Zarbis-Papastoitsis, A single-use purification process for the production of a monoclonal antibody produced in a PER.C6 human cell line., Biotechnol. J. 6 (2011) 56–65. doi:10.1002/biot.201000292.

[7] A.A. Shukla, U. Gottschalk, Single-use disposable technologies for biopharmaceutical manufacturing, Trends Biotechnol. 31 (2013) 147–154. doi:10.1016/j.tibtech.2012.10.004.

[8] P. Borowicz, W. Slawinski, A. Plucienniczak, J. Mikolajczyk, T. Glabski, D. Kurzynoga, D. Mikiewicz-Sygula, A. Wojtowicz-Krawiec, M. Zielinski, M. Kesik-Brodacka, V. Cecuda-Adamczewska, I. Sokolowska, G. Plucienniczak, D. Stadnik, J. Antosik, J. Pstrzoch, J. Bernat, T. Pawlukowiec, J. Stepniewski, M. Bogiel, Instytut Biotechnologii I Antybiotykow. Insulin derivatives or its pharmaceutically acceptable salt, pharmaceutical composition, use of insulin derivative or its pharmaceutically acceptable salt and method of treatment, EP 2371853A2, 2006.

[9] W. Schneider, C. Friihlich, H. Fiedler, H. Lefevre, Plasmesco. Process for isolating albumin from blood, US Patent 4156681, 1979.

[10] R.M. Hewick, J.S. Seehra, Genetics Institute. Method for the purification of erythropoietin and erythropoietin compositions, US Patent 4677195, 1987.

[11] D. Hekmat, Large-scale crystallization of proteins for purification and formulation, Bioprocess Biosyst. Eng. (2015) 1209–1231. doi:10.1007/s00449-015-1374-y.

[12] R. dos Santos, C.S.M. Fernandes, S. Ottengy, A.C. Viecinski, G. Béhar, B. Mouratou, F. Pecorari, A.C.A. Roque, Affitins for protein purification by affinity magnetic fishing, J. Chromatogr. A. 1457 (2016) 50–58. doi:10.1016/j.chroma.2016.06.020.

[13] V.L. Dhadge, S.A.S.L. Rosa, A. Azevedo, R. Aires-Barros, A.C.A. Roque, Magnetic aqueous two phase fishing: A hybrid process technology for antibody purification, J. Chromatogr. A. 1339 (2014) 59–64. doi:10.1016/j.chroma.2014.02.069.

[14] U. Gottschalk, The renaissance of protein purification, Biopharm. Int. 19 (2006) 8–9. http://www.biopharminternational.com/renaissance-protein-purification (accessed November 16, 2015).

[15] M. Pathak, D. Dutta, A. Rathore, Analytical QbD: Development of a native gel electrophoresis method for measurement of monoclonal antibody aggregates., Electrophoresis. 35 (2014) 2163–2171. doi:10.1002/elps.201400055.

[16] M. Zhang, G.R. Miesegaes, M. Lee, D. Coleman, B. Yang, M. Trexler-Schmidt, L. Norling, P. Lester, K.A. Brorson, Q. Chen, Quality by design approach for viral clearance by protein A chromatography, Biotechnol. Bioeng. 111 (2014) 95–103. doi:10.1002/bit.24999.

[17] T. Barroso, T. Casimiro, A.M. Ferraria, F. Mattioli, A. Aguiar-Ricardo, A.C.A. Roque, Hybrid monoliths for magnetically-driven protein separations, Adv. Funct. Mater. 24 (2014) 4528–4541. doi:10.1002/adfm.201400022.

[18] V.L. Dhadge, S.A.S.L. Rosa, A. Azevedo, R. Aires-Barros, A.C.A. Roque, Magnetic aqueous two phase fishing: A hybrid process technology for antibody purification., J. Chromatogr. A. 1339 (2014) 59–64. doi:10.1016/j.chroma.2014.02.069.

[19] J. Dong, M.L. Bruening, Functionalizing microporous membranes for protein purification and protein digestion, Annu. Rev. Anal. Chem. 8 (2015) 81–100. doi:10.1146/annurev-anchem-071114-040255.

[20] M.J. Jacinto, R.R.G. Soares, A.M. Azevedo, V. Chu, A. Tover, J.P. Conde, M.R. Aires-Barros, Optimization and miniaturization of aqueous two phase systems for the purification of recombinant human immunodeficiency virus-like particles from a CHO cell supernatant, Sep. Purif. Technol. 154 (2015) 27–35. doi:10.1016/j.seppur.2015.09.006.

[21] V.L. Dhadge, A. Hussain, A.M. Azevedo, R. Aires-barros, A.C.A. Roque, Boronic acid-modified magnetic materials for antibody purification, J. R. Soc. Interface. 11 (2014) 20130875. doi:10.1098/rsif.2013.0875.

[22] I.L. Batalha, A. Hussain, A.C.A. Roque, Gum Arabic coated magnetic nanoparticles with affinity ligands specific for antibodies, J. Mol. Recognit. 23 (2010) 462–471. doi:10.1002/jmr.1013.

[23] P. Gronemeyer, R. Ditz, J. Strube, Trends in upstream and downstream process development for antibody manufacturing, Bioengineering. 1 (2014) 188–212. doi:10.3390/bioengineering1040188.

[24] N. Hammerschmidt, B. Hintersteiner, N. Lingg, A. Jungbauer, Continuous precipitation of IgG from CHO cell culture supernatant in a tubular reactor, Biotechnol. J. 10 (2015) 1196–1205. doi:10.1002/biot.201400608.

[25] R. Sommer, P. Satzer, A. Tscheliessnig, H. Schulz, B. Helk, A. Jungbauer, Combined polyethylene glycol and CaCl2 precipitation for the capture and purification of recombinant antibodies, Process Biochem. 49 (2014) 2001–2009. doi:10.1016/j.procbio.2014.07.012.

[26] S.-L. Sim, T. He, A. Tscheliessnig, M. Mueller, R.B.H. Tan, Protein precipitation by polyethylene glycol : A generalized model based on hydrodynamic radius, J. Biotechnol. 157 (2012) 315–319. doi:10.1016/j.jbiotec.2011.09.028.

[27] Y. Zang, B. Kammerer, M. Eisenkolb, K. Lohr, H. Kiefer, Towards protein crystallization as a process step in downstream processing of therapeutic antibodies: Screening and optimization at microbatch scale, PLoS One. 6 (2011) 3–10. doi:10.1371/journal.pone.0025282.

[28] B. Smejkal, N.J. Agrawal, B. Helk, H. Schulz, M. Giffard, M. Mechelke, F. Ortner, P. Heckmeier, B.L. Trout, D. Hekmat, Fast and scalable purification of a therapeutic full-length antibody based on process crystallization, Biotechnol. Bioeng. 110 (2013) 2452–2461. doi:10.1002/bit.24908.

[29] R.A. Judge, M.R. Johns, E.T. White, Protein purification by bulk crystallization: The recovery of ovalbumin, Biotechnol. Bioeng. 48 (1995) 316–323. doi:10.1002/bit.260480404.

[30] C. Jacobsen, J. Garside, M. Hoare, Nucleation and growth of microbial lipase crystals from clarified concentrated fermentation broths, Biotechnol. Bioeng. 57 (1998) 666–675.

[31] U.J. Lewis, D.E. Williams, N.G. Brink, Pancreatic elastase: Purification, properties and function, J Biol Chem. 222 (1956) 705–720.

[32] O.P. Srivastava, A.I. Aronson, Isolation and characterization of a unique protease from sporulating cells of Bacillus subtilis, Arch. Microbiol. 129 (1981) 227–232. doi:10.1007/BF00425256.

[33] D.B.M. Commins, R.A.B. Hard, T.A. Nickerson, Recovery of lactose from aqueous solutions: Precipitation with calcium hydroxide and sodiumm hydroxide, J. Food Sci. 45 (1980) 362–366. doi:10.1111/j.1365-2621.1980.tb02615.x.

[34] E.A. Miranda, A. Bernardo, G.A.M. Hirata, M. Giulietti, Crysallization of lactose and whey protein,

in: J.S. dos R. Coimbra, J.A. Teixeira (Eds.), Eng. Asp. Milk Dairy Prod., CRC Press, 2009: pp. 121–154.

[35] P. Gagnon, Technology trends in antibody purification., J. Chromatogr. A. 1221 (2012) 57–70. doi:10.1016/j.chroma.2011.10.034.

[36] S. Englard, S. Seifter, Precipitation techniques, Methods Enzymol. 182 (1990) 285–300. doi:10.1016/0076-6879(90)82024-V.

[37] S.C. Tan, B.C. Yiap, DNA, RNA, and protein extraction: The past and the present, J. Biomed. Biotechnol. 2009 (2009). doi:10.1155/2009/574398.

[38] E.J. Cohn, The properties and functions of the plasma proteins, with a consideration of the methods for their separation and purification, Chem. Rev. 28 (1941) 395–417. doi:10.1021/cr60090a007.

[39] W. Hinderer, S. Arnold, Process for the purification of recombinant human erythropoietin (EPO), EPO thus purified and pharmacceutical compositions comprising same, US Patent 2012/0264688 A1, 2012.

[40] R.D. Sheth, B. V. Bhut, M. Jin, Z. Li, W. Chen, S.M. Cramer, Development of an ELP-Z based mAb affinity precipitation process using scaled-down filtration techniques, J. Biotechnol. 192 (2014) 11–19. doi:10.1016/j.jbiotec.2014.09.020.

[41] R. Giegé, A historical perspective on protein crystallization from 1840 to the present day, FEBS J. 280 (2013) 6456–6497. doi:10.1111/febs.12580.

[42] F. Hünefeld, Fünftes capitel: Ueber die salze des bluts, in: F. Bockhaus (Ed.), Der Chemismus Der Thierischen Organ. Physiol. Untersuchungen Der Mater. Veränderungen, Oder Des Bild. Im Thierischen Org. Insbes. Des Blutbildungsprocesses, Der Natur Der Blutkörperchen Und Ihrer Kernchen, 1840: pp. 160–161.

[43] D.H. Thomas, A. Rob, D.W. Rice, A novel dialysis procedure for the crystallization of proteins, Protein Eng. Des. Sel. 2 (1989) 489–491. doi:10.1093/protein/2.6.489.

[44] F.R. Salemme, A free interface diffusion technique for the crystallization of proteins for X-ray crystallography, Arch. Biochem. Biophys. 151 (1972) 533–539. doi:10.1016/0003-9861(72)90530-9.

[45] I. Altan, P. Charbonneau, E.H. Snell, Computational crystallization, Arch. Biochem. Biophys. 602 (2016) 12–20. doi:10.1016/j.abb.2016.01.004.

[46] M. Sleutel, J. Lutsko, A.E.S. Van Driessche, M.A. Durán-Olivencia, D. Maes, Observing classical nucleation theory at work by monitoring phase transitions with molecular precision., Nat. Commun. 5 (2014) 5598. doi:10.1038/ncomms6598.

[47] J.F. Lutsko, M.A. Durán-Olivencia, Classical nucleation theory from a dynamical approach to nucleation, J. Chem. Phys. 138 (2013) 244908-244908–14. doi:doi:10.1063/1.4811490.

[48] N. Asherie, Protein crystallization and phase diagrams, Methods. 34 (2004) 266–272. doi:10.1016/j.ymeth.2004.03.028.

[49] P.G. Vekilov, Phase transitions of folded proteins, Soft Matter. 6 (2010) 5254–5272. doi:10.1039/c0sm00215a.

[50] J.A. Gavira, Current trends in protein crystallization, Arch. Biochem. Biophys. 602 (2015) 3–11. doi:10.1016/j.abb.2015.12.010.

[51] A. McPherson, J.A. Gavira, Introduction to protein crystallization, Acta Crystallogr. Sect. FStructural Biol. Commun. 70 (2014) 2–20. doi:10.1107/S2053230X13033141.

[52] K.D. Collins, Ions from the Hofmeister series and osmolytes: Effects on proteins in solution and in the crystallization process, Methods. 34 (2004) 300–311. doi:10.1016/j.ymeth.2004.03.021.

[53] Y. Zhang, P.S. Cremer, Interactions between macromolecules and ions: the Hofmeister series, Curr. Opin. Chem. Biol. 10 (2006) 658–663. doi:10.1016/j.cbpa.2006.09.020.

[54] Y. Zhang, P.S. Cremer, Chemistry of Hofmeister anions and osmolytes., Annu. Rev. Phys. Chem. 61 (2010) 63–83. doi:10.1146/annurev.physchem.59.032607.093635.

[55] A. McPherson, Crystallization of proteins from polyethylene glycol, J. Biol. Chem. 251 (1976) 6300–6303.

[56] D.H. Atha, K.C. Ingham, Mechanism of precipitation of proteins by polyethylene glycol. Analysis in terms of excluded volume, J. Biol. Chem. 256 (1981) 12108–12117.

[57] D.W. Bolen, Effects of naturally occurring osmolytes on protein stability and solubility: Issues important in protein crystallization, Methods. 34 (2004) 312–322. doi:10.1016/j.ymeth.2004.03.022.

[58] M. Kowacz, M. Marchel, L. Juknaitė, J.M.S.S. Esperança, M.J. Romão, A.L. Carvalho, L.P.N. Rebelo, Ionic-liquid-functionalized mineral particles for protein crystallization, Cryst. Growth Des. 15 (2015) 2994–3003. doi:10.1021/acs.cgd.5b00403.

[59] D. Ribeiro, A. Kulakova, P. Quaresma, E. Pereira, C. Bonifácio, M.J. Romão, R. Franco, A.L. Carvalho, Use of gold nanoparticles as additives in protein crystallization, Cryst. Growth Des. 14 (2014) 222–227. doi:10.1021/cg4014398.

[60] S.A. Oelmeier, C. Ladd-Effio, J. Hubbuch, Alternative separation steps for monoclonal antibody purification: Combination of centrifugal partitioning chromatography and precipitation, J. Chromatogr. A. 1319 (2013) 118–126. doi:10.1016/j.chroma.2013.10.043.

[61] A. Tscheliessnig, P. Satzer, N. Hammerschmidt, H. Schulz, B. Helk, A. Jungbauer, Ethanol precipitation for purification of recombinant antibodies, J. Biotechnol. 188 (2014) 17–28. doi:10.1016/j.jbiotec.2014.07.436.

[62] N. Hammerschmidt, S. Hobiger, A. Jungbauer, Continuous polyethylene glycol precipitation of recombinant antibodies: Sequential precipitation and resolubilization, Process Biochem. 51 (2015) 325–332. doi:10.1016/j.procbio.2015.11.032.

[63] T.A. Poor, A.S. Song, B.D. Welch, C.A. Kors, On the stability of parainfluenza virus 5 F proteins., J. Virol. 89 (2015) 3438–3441. doi:10.1128/JVI.03221-14.

[64] E.G. Baker, G.J. Bartlett, M.P. Crump, R.B. Sessions, N. Linden, C.F.J. Faul, D.N. Woolfson, Local and macroscopic electrostatic interactions in single α-helices, Nat. Chem. Biol. 11 (2015) 221–228. doi:10.1038/nchembio.1739.

[65] Z. Fu, E.R. Gilbert, D. Liu, Regulation of Insulin Synthesis and Secretion and Pancreatic Beta-Cell Dysfunction in Diabetes, Curr. Diabetes Rev. 9 (2013) 25. doi:doi.org/10.2174/157339913804143225.

[66] B. Kelley, Very large scale monoclonal antibody purification: The case for conventional unit operations, Biotechnol. Prog. 23 (2007) 995–1008. doi:10.1021/bp070117s.

[67] M.J. Adams, T.L. Blundell, E.J. Dodson, G.G. Dodson, M. Vijayan, E.N. Baker, M.M. Harding, D.C. Hodgkin, B. Rimmer, S. Sheat, Structure of rhombohedral 2 zinc insulin crystals, Nature. 224 (1969) 491–495. doi:10.1038/224491a0.

[68] D.A. Scott, Crystalline insulin, Biochem. J. 28 (1934) 1592–1602. doi:10.1073/pnas.12.2.132.

[69] K. Petersen, J. Schlichtkrull, Insulin crystals and preparations and processes for producing them, US Patent 692612, 1964.

[70] R. Jackson, Eli Lilly and Company. Processor the crystallization of the ammonium and alkali metal salts in insulin, US Patent 3719655, 1973.

[71] J. Curling, N. Goss, J. Bertolini, Production of plasma proteins for therapeutic use, in: J. Bertolini, N. Goss, J. Curling (Eds.), John Wiley & Sons, Inc., Hoboken, NJ, USA, 2012: pp. 1–28. doi:10.1002/9781118356807.

[72] G. Fanali, A. di Masi, V. Trezza, M. Marino, M. Fasano, P. Ascenzi, Human serum albumin: From bench to bedside., Mol. Aspects Med. 33 (2012) 209–90. doi:10.1016/j.mam.2011.12.002.

[73] J. Van Alstine, M. Berg, J. Kjorning, J. Shanagar, GE Healthcare Bio-Sciences. Plasma protein fractionation by sequential polyacid precipitation, US Patent 2014/0343253 A1, 2008.

[74] H.E. Broxmeyer, Erythropoietin: multiple targets, actions, and modifying influences for biological and clinical consideration., J. Exp. Med. 210 (2013) 205–8. doi:10.1084/jem.20122760.

[75] H.W.B. Cheng, K.Y. Chan, H.T. Lau, C.W. Man, S.C. Cheng, C. Lam, Use of erythropoietin-stimulating agents (ESA) in patients with end-stage renal failure decided to forego dialysis: Palliative perspective, Am. J. Hosp. Palliat. Care. (2015). doi:10.1177/1049909115624653.

[76] D. Tatkare, World erythropoietin drugs market - opportunities and forecasts, 2013 - 2020. Allied Market Research, 2015.

[77] T. Miyake, C.K. Hung, E. Goldwasser, Purification of human erythropoietin, J. Biol. Chem. 252 (1977) 5558–5564.

[78] F.K. Lin, S. Suggs, C.H. Lin, J.K. Browne, R. Smalling, J.C. Egrie, K.K. Chen, G.M. Fox, F. Martin, Z. Stabinsky, Cloning and expression of the human erythropoietin gene, Proc. Natl. Acad. Sci. U. S. A. 82 (1985) 7580–4. doi:10.1073/pnas.82.22.7580.

[79] J.W. Eschbach, J.C. Egrie, M.R. Downing, J.K. Browne, J.W. Adamson, Correction of the amenia of end-stage renal disease with recombinant human erythropoietin, N. Engl. J. Med. 316 (1987) 73–78. doi:10.1056/NEJM198701083160203.

[80] C.M. Carcagno, M. Criscuolo, C. Melo, J.A. Vidal, Methods of purifying recombinante human erythropoietin from cell culture supernatants, EP 1127063B1, 2001.

[81] J. Mongkolsapaya, J.M. Grimes, N. Chen, X.N. Xu, D.I. Stuart, E.Y. Jones, G.R. Screaton, Structure of the TRAIL-DR5 complex reveals mechanisms conferring specificity in apoptotic initiation, Nat. Struct. Biol. 6 (1999) 1048–1053. doi:10.1038/14935.

[82] S.R. Wiley, K. Schooley, P.J. Smolak, W.S. Din, C.P. Huang, J.K. Nicholl, G.R. Sutherland, T.D. Smith, C. Rauch, C.A. Smith, R.G. Goodwin, Identification and characterization of a new member of the TNF family that induces apoptosis, Immunity. 3 (1995) 673–682. doi:10.1016/1074-7613(95)90057-8.

[83] A. Ashkenazi, R.C. Pai, S. Fong, S. Leung, D.A. Lawrence, S.A. Marsters, C. Blackie, L. Chang, A.E. McMurtrey, A. Hebert, L. DeForge, I.L. Koumenis, D. Lewis, L. Harris, J. Bussiere, H. Koeppen, Z. Shahrokh, R.H. Schwall, Safety and antitumor activity of recombinant soluble Apo2 ligand., J. Clin. Invest. 104 (1999) 155–62. doi:10.1172/JCI6926.

[84] H. Flores, T.P. Lin, T.C. Matthews, R. Pai, Z. Shahrokh, Genentech. APO-2 ligand/TRAIL formulations, US Patent 7741285 B2, 2010.

[85] A.C.A. Roque, C.S.O. Silva, M.A. Taipa, Affinity-based methodologies and ligands for antibody purification: advances and perspectives., J. Chromatogr. A. 1160 (2007) 44–55. doi:10.1016/j.chroma.2007.05.109.

[86] J.B. Evans, B.A. Syed, From the analyst's couch: Next-generation antibodies., Nat. Rev. Drug Discov. 13 (2014) 413–4. doi:10.1038/nrd4255.

[87] J.G. Elvin, R.G. Couston, C.F. van der Walle, Therapeutic antibodies: Market considerations, disease targets and bioprocessing., Int. J. Pharm. 440 (2013) 83–98. doi:10.1016/j.ijpharm.2011.12.039.

[88] H.F. Liu, J. Ma, C. Winter, R. Bayer, Recovery and purification process development for monoclonal antibody production, MAbs. 2 (2010) 480–499. doi:10.4161/mabs.2.5.12645.

[89] H. Huettmann, M. Berkemeyer, W. Buchinger, A. Jungbauer, Preparative crystallization of a single chain antibody using an aqueous two-phase system, Biotechnol. Bioeng. 111 (2014) 2192–2199. doi:10.1002/bit.25287.

[90] C. Hildebrandt, L. Joos, R. Saedler, G. Winter, The "New polyethylene glycol dilemma": Polyethylene glycol impurities and their paradox role in mAb crystallization, J. Pharm. Sci. 104 (2015) 1938–1945. doi:10.1002/jps.24424.

[91] R. Sommer, A. Tscheliessnig, P. Satzer, H. Schulz, B. Helk, A. Jungbauer, Capture and intermediate purification of recombinant antibodies with combined precipitation methods, Biochem. Eng. J. 93 (2015) 200–211. doi:10.1016/j.bej.2014.10.008.

[92] C. Knevelman, J. Davies, L. Allen, N.J. Titchener-Hooker, High-throughput screening techniques for rapid PEG-based precipitation of IgG4 mAb from clarified cell culture supernatant, Biotechnol. Prog. 26 (2010) 697–705. doi:10.1002/btpr.357.

[93] S.-L. Sim, T. He, A. Tscheliessnig, M. Mueller, R.B.H. Tan, A. Jungbauer, Branched polyethylene glycol for protein precipitation, Biotechnol. Bioeng. 109 (2012) 736–746. doi:10.1002/bit.24343.

[94] R.D. Sheth, M. Jin, B. V. Bhut, Z. Li, W. Chen, S.M. Cramer, Affinity precipitation of a monoclonal antibody from an industrial harvest feedstock using an ELP-Z stimuli responsive biopolymer, Biotechnol. Bioeng. 111 (2014) 1595–1603. doi:10.1002/bit.25230.

[95] L. Janoschek, M. Freiherr von Roman, S. Berensmeier, Protein A affinity precipitation of human immunoglobulin G, J. Chromatogr. B Anal. Technol. Biomed. Life Sci. 965 (2014) 72–78. doi:10.1016/j.jchromb.2014.06.011.

[96] M.W. Handlogten, J.F. Stefanick, P.E. Deak, B. Bilgicer, Affinity-based precipitation via a bivalent peptidic hapten for the purification of monoclonal antibodies, Analyst. 139 (2014) 4247–4255. doi:10.1039/c4an00780h.

[97] S. Chollangi, R. Parker, N. Singh, Y. Li, M. Borys, Z. Li, Development of robust antibody purification by optimizing protein-A chromatography in combination with precipitation methodologies, Biotechnol. Bioeng. 112 (2015) 2292–2304. doi:10.1002/bit.25639.

[98] T. Burnouf, Modern Plasma Fractionation, Transfus. Med. Rev. 21 (2007) 101–117. doi:10.1016/j.tmrv.2006.11.001.

[99] R.E. Kontermann, Strategies to Extend Plasma Half-Lives of Recombinant Antibodies, BioDrugs. 23 (2009) 93–109. doi:10.2165/00063030-200923020-00003.

[100] B. Elsadek, F. Kratz, Impact of albumin on drug delivery — New applications on the horizon, J. Control. Release. 157 (2012) 4–28. doi:10.1016/j.jconrel.2011.09.069.

[101] Market Research Bureau Inc., The Worldwide Plasma Proteins Market, 2014.

[102] T. Burnouf, Integration of chromatography with traditional plasma protein fractionation methods, Bioseparation. 1 (1991) 383–396.

[103] Y. He, T. Ning, T. Xie, Q. Qiu, L. Zhang, Y. Sun, D. Jiang, K. Fu, F. Yin, W. Zhang, L. Shen, H. Wang, J. Li, Q. Lin, Y. Sun, H. Li, Y. Zhu, D. Yang, Large-scale production of functional human serum albumin from transgenic rice seeds, Proc. Natl. Acad. Sci. 108 (2011) 19078–19083. doi:10.1073/pnas.1109736108.

[104] M. Belew, Li, M. Yan, Zhang, Wei, K. Caldwell, Purification of Recombinant Human Serum Albumin (rHSA) Produced by Genetically Modified *Pichia Pastoris*, Sep. Sci. Technol. 43 (2008) 3134–3153. doi:10.1080/01496390802221857.

[105] J. Travis, J. Bowen, D. Tewksbury, D. Johnson, R. Pannell, Isolation of albumin from whole human plasma and fractionation of albumin-depleted plasma, Biochem. J. 157 (1976) 301–306.

[106] T. Burnouf, M. Radosevich, Affinity chromatography in the industrial purification of plasma proteins for therapeutic use, J. Biochem. Biophys. Methods. 49 (2001) 575–86. doi:10.1016/S0165-022X(01)00221-4.

[107] D. Hanggi, P. Carr, Analytical evaluation of the purity of commercial preparations of Cibacron Blue F3GA and related dyes, Anal. Biochem. 149 (1985) 91–104.

[108] C.R. Lowe, Combinatorial approaches to affinity chromatography, Curr. Opin. Chem. Biol. 5 (2001) 248–56. doi:10.1016/S1367-5931(00)00199-X.

[109] A.C.A. Roque, C.R. Lowe, Rationally designed ligands for use in affinity chromatography: an artificial protein L, in: M. Zachariou (Ed.), Methods Mol. Biol., Second, Humana Press, Totowa, NJ, 2008: pp. 93–109. doi:10.1007/978-1-59745-582-4_7.

[110] V.L. Dhadge, P.I. Morgado, F. Freitas, M.A. Reis, A. Azevedo, R. Aires-Barros, A.C.A. Roque, An extracellular polymer at the interface of magnetic bioseparations., J. R. Soc. Interface. 11 (2014) 20140743. doi:10.1098/rsif.2014.0743.

[111] K. Sproule, P. Morrill, J.C. Pearson, S.J. Burton, K.R. Hejnaes, H. Valore, S. Ludvigsen, C.R. Lowe, New strategy for the design of ligands for the purification of pharmaceutical proteins by affinity chromatography, J. Chromatogr. B Biomed. Sci. Appl. 740 (2000) 17–33. doi:10.1016/S0378-4347(99)00570-8.

[112] C.S.M. Fernandes, R. Castro, A.S. Coroadinha, A.C.A. Roque, Small synthetic ligands for the enrichment of viral particles pseudotyped with amphotropic murine leukemia virus envelope, J. Chromatogr. A. 1438 (2016) 160–170. doi:10.1016/j.chroma.2016.02.026.

[113] S.F. Teng, K. Sproule, A. Husain, C.R. Lowe, Affinity chromatography on immobilized “biomimetic” ligands: Synthesis, immobilization and chromatographic assessment of an immunoglobulin G-binding ligand, J. Chromatogr. B Biomed. Sci. Appl. 740 (2000) 1–15. doi:10.1016/S0378-4347(99)00549-6.

[114] S.F. Teng, K. Sproule, A. Hussain, C.R. Lowe, A strategy for the generation of biomimetic ligands for affinity chromatography. Combinatorial synthesis and biological evaluation of an IgG binding ligand, J. Mol. Recognit. 12 (1999) 67–75. doi:10.1002/(SICI)1099-1352(199901/02)12:1<67::AID-JMR443>3.0.CO;2-4.

[115] J. Ghuman, P.A. Zunszain, I. Petitpas, A.A. Bhattacharya, M. Otagiri, S. Curry, Structural Basis of the Drug-binding Specificity of Human Serum Albumin, J. Mol. Biol. 353 (2005) 38–52. doi:10.1016/j.jmb.2005.07.075.

[116] G.M. Morris, R. Huey, W. Lindstrom, M.F. Sanner, R.K. Belew, D.S. Goodsell, A.J. Olson, AutoDock4 and AutoDockTools4: Automated docking with selective receptor flexibility, J. Comput. Chem. 30 (2009) 2785–2791.

[117] A.W. Schüttelkopf, D.M.F. van Aalten, PRODRG: a tool for high-throughput crystallography of protein-ligand complexes., Acta Crystallogr. D. Biol. Crystallogr. 60 (2004) 1355–1363. doi:10.1107/S0907444904011679.

[118] Y. Pang, P. Reid, D. Brooks, Solubility and distribution of halothane in human blood, Br. J. Anaesth. 52 (1980) 851–862. doi:10.1093/bja/52.9.851.

[119] J. Johansson, R. Eckenhoff, P. Dutton, Binding of halothane to serum albumin demonstrated using tryptophan fluorescence, Anesthesiology. 83 (1995) 316–324.

[120] P. Ascenzi, A. Bocedi, S. Notari, G. Fanali, R. Fesce, M. Fasano, Allosteric Modulation of Drug Binding to Human Serum Albumin, Mini Rev. Med. Chem. 6 (2006) 483–489. doi:10.2174/138955706776361448.

[121] I.-M. Frick, P. Åkesson, J. Cooney, U. Sjöbring, K.-H. Schmidt, H. Gomi, S. Hattori, C. Tagawa, F. Kishimoto, L. Björck, Protein H - a surface protein of Streptococcus pyogenes with separate binding sites for IgG and albumin, Mol. Microbiol. 12 (1994) 143–151. doi:10.1111/j.1365-2958.1994.tb01003.x.

[122] A. Jonsson, J. Dogan, N. Herne, L. Abrahmsen, P.-A. Nygren, Engineering of a femtomolar affinity binding protein to human serum albumin, Protein Eng. Des. Sel. 21 (2008) 515–527. doi:10.1093/protein/gzn028.

[123] H. Jonsson, L. Frykberg, L. Rantamäki, B. Guss, MAG, a novel plasma protein receptor from Streptococcus dysgalactiae, Gene. 143 (1994) 85–89. doi:10.1016/0378-1119(94)90609-2.

[124] H. Jonsson, H. Lindmark, B. Guss, A protein G-related cell surface protein in Streptococcus zooepidemicus, Infect. Immun. 63 (1995) 2968–2975.

[125] S. Lejon, I.-M. Frick, L. Bjorck, M. Wikstrom, S. Svensson, Crystal Structure and Biological Implications of a Bacterial Albumin Binding Module in Complex with Human Serum Albumin, J. Biol. Chem. 279 (2004) 42924–42928. doi:10.1074/jbc.M406957200.

[126] V. Oganesyan, M.M. Damschroder, K.E. Cook, Q. Li, C. Gao, H. Wu, W.F. Dall’Acqua, Structural

insights into neonatal Fc receptor-based recycling mechanisms., J. Biol. Chem. 289 (2014) 7812–7824. doi:10.1074/jbc.M113.537563.

[127] J.T. Andersen, J. Dee Qian, I. Sandlie, The conserved histidine 166 residue of the human neonatal Fc receptor heavy chain is critical for the pH-dependent binding to albumin, Eur. J. Immunol. 36 (2006) 3044–3051. doi:10.1002/eji.200636556.

[128] K.M.K. Sand, M. Bern, J. Nilsen, B. Dalhus, K.S. Gunnarsen, J. Cameron, A. Grevys, K. Bunting, I. Sandlie, J.T. Andersen, Interaction with Both Domain I and III of Albumin Is Required for Optimal pH-dependent Binding to the Neonatal Fc Receptor (FcRn), J. Biol. Chem. 289 (2014) 34583–34594. doi:10.1074/jbc.M114.587675.

[129] R.E. Kontermann, Half-Life Modulating Strategies–An Introduction, in: R. Kontermann (Ed.), Ther. Proteins Strateg. to Modul. Their Plasma Half-Lives, Wiley-VCH Verlag GmbH & Co. KGaA, Weinheim, Germany, 2012: pp. 1–21. doi:10.1002/9783527644827.ch1.

[130] T. Arakawa, Y. Kita, Stabilizing effects of caprylate and acetyltryptophanate on heat-induced aggregation of bovine serum albumin, Biochim. Biophys. Acta - Protein Struct. Mol. Enzymol. 1479 (2000) 32–36. doi:10.1016/S0167-4838(00)00061-3.

[131] A. Kawai, V.T.G. Chuang, Y. Kouno, K. Yamasaki, S. Miyamoto, M. Anraku, M. Otagiri, Crystallographic analysis of the ternary complex of octanoate and N-acetyl-l-methionine with human serum albumin reveals the mode of their stabilizing interactions, Biochim. Biophys. Acta - Proteins Proteomics. 1865 (2017) 979–984. doi:10.1016/J.BBAPAP.2017.04.004.

[132] A. Yepremyan, A. Mehmood, S.M. Brewer, M.M. Barnett, B.G. Janesko, G. Akkaraju, E. Simanek, K.N. Green, A new triazine bearing a pyrazolone group capable of copper, nickel, and zinc chelation, RSC Adv. 8 (2018) 3024–3035. doi:10.1039/c7ra09459k.

[133] A.C.A. Roque, A. Bicho, I.L. Batalha, A.S. Cardoso, A. Hussain, Biocompatible and bioactive gum Arabic coated iron oxide magnetic nanoparticles, J. Biotechnol. 144 (2009) 313–320. doi:10.1016/j.jbiotec.2009.08.020.

[134] A. Roque, M.A. Taipa, C.R. Lowe, Synthesis and screening of a rationally designed combinatorial library of affinity ligands mimicking protein L from Peptostreptococcus magnus., J. Mol. Recognit. 18 (2005) 213–24. doi:10.1002/jmr.733.

[135] I.L. Batalha, H. Zhou, K. Lilley, C.R. Lowe, A.C.A. Roque, Mimicking nature: Phosphopeptide enrichment using combinatorial libraries of affinity ligands, J. Chromatogr. A. In Press (2016). doi:10.1016/j.chroma.2016.06.032.

[136] S.D.F. Santana, V.L. Dhadge, A.C.A. Roque, Dextran-coated magnetic supports modified with a biomimetic ligand for IgG purification., ACS Appl. Mater. Interfaces. 4 (2012) 5907–5914. doi:10.1021/am301551n.

[137] M. Levisson, R.B. Spruijt, I.N. Winkel, S.W.M. Kengen, J. Van Der Oost, Phage Display of Engineered Binding Proteins, in: N.E. Labrou (Ed.), Protein Downstr. Process., Humana Press, Totowa, NJ, 2014: pp. 211–229. doi:10.1007/978-1-62703-977-2.

[138] I. Safarik, M. Safarikova, Magnetic techniques for the isolation and purification of proteins and peptides, Biomagn. Res. Technol. 2 (2004). doi:10.1186/1477-044X-2-7.

[139] V.J.B. Ruigrok, M. Levisson, M.H.M. Eppink, H. Smidt, J. van der Oost, Alternative affinity tools: more attractive than antibodies?, Biochem. J. 436 (2011) 1–13. doi:10.1042/BJ20101860.

[140] L. Miller, J. Michel, G. Vogt, J. Döllinger, D. Stern, J. Piesker, A. Nitsche, Identification and characterization of a phage display-derived peptide for orthopoxvirus detection., Anal. Bioanal. Chem. 406 (2014) 7611–7621. doi:10.1007/s00216-014-8150-8.

[141] A. Twair, S. Al-Okla, M. Zarkawi, A.Q. Abbady, Characterization of camel nanobodies specific for superfolder GFP fusion proteins., Mol. Biol. Rep. 41 (2014) 6887–6898. doi:10.1007/s11033-014-3575-x.

[142] A. Correa, S. Pacheco, A.E. Mechaly, G. Obal, G. Béhar, B. Mouratou, P. Oppezzo, P.M. Alzari, F. Pecorari, Potent and specific inhibition of glycosidases by small artificial binding proteins

(affitins)., PLoS One. 9 (2014) e97438. doi:10.1371/journal.pone.0097438.

[143] B. Mouratou, F. Schaeffer, I. Guilvout, D. Tello-Manigne, A.P. Pugsley, P.M. Alzari, F. Pecorari, Remodeling a DNA-binding protein as a specific in vivo inhibitor of bacterial secretin PulD, Proc. Natl. Acad. Sci. U. S. A. 104 (2007) 17983–17988. doi:10.1073/pnas.0702963104.

[144] G. Béhar, M. Bellinzoni, M. Maillasson, L. Paillard-Laurance, P.M. Alzari, X. He, B. Mouratou, F. Pecorari, Tolerance of the archaeal Sac7d scaffold protein to alternative library designs: characterization of anti-immunoglobulin G Affitins, Protein Eng. Des. Sel. 26 (2013) 267–275. doi:10.1093/protein/gzs106.

[145] S.P. Edmondson, J.W. Shriver, DNA binding proteins Sac7d and Sso7d from Sulfolobus, Methods Enzymol. 334 (2001) 129–45. doi:10.1016/S0076-6879(01)34463-4.

[146] H. Robinson, Y.G. Gao, B.S. McCrary, S.P. Edmondson, J.W. Shriver, A.H. Wang, The hyperthermophile chromosomal protein Sac7d sharply kinks DNA., Nature. 392 (1998) 202–5. doi:10.1038/32455.

[147] F. Pecorari, P. Alzari, OB-fold used as scaffold for engineering new binders, Patent Publication Nos. PCT/IB2007/004388, 2008.

[148] M. Krehenbrink, M. Chami, I. Guilvout, P.M. Alzari, F. Pécorari, A.P. Pugsley, Artificial binding proteins (Affitins) as probes for conformational changes in secretin PulD., J. Mol. Biol. 383 (2008) 1058–68. doi:10.1016/j.jmb.2008.09.016.

[149] G. Béhar, S. Pacheco, M. Maillasson, B. Mouratou, F. Pecorari, Switching an anti-IgG binding site between archaeal extremophilic proteins results in Affitins with enhanced pH stability, J. Biotechnol. 192 (2014) 123–129. doi:10.1016/j.jbiotec.2014.10.006.

[150] G. Béhar, A. Renodon-Cornière, B. Mouratou, F. Pecorari, Affitins as robust tailored reagents for affinity chromatography purification of antibodies and non-immunoglobulin proteins, J. Chromatogr. A. 1441 (2016) 44–51. doi:10.1016/j.chroma.2016.02.068.

[151] A. Ditsch, J. Yin, P.E. Laibinis, D.I.C. Wang, T.A. Hatton, Ion-exchange purification of proteins using magnetic nanoclusters, Biotechnol. Prog. 22 (2006) 1153–1162. doi:10.1021/bp050290t.

[152] I. Safarik, M. Safarikova, Magnetic nano- and microparticles in biotechnology, Chem. Pap. 63 (2009) 497–505. doi:10.2478/s11696-009-0054-2.

[153] D. Horák, M. Babic, H. Macková, M.J. Benes, Preparation and properties of magnetic nano- and microsized particles for biological and environmental separations, J. Sep. Sci. 30 (2007) 1751–1772. doi:10.1002/jssc.200700088.

[154] A.S. Pina, Í.L. Batalha, C.S. Fernandes, M.A. Aoki, A.C.A. Roque, Exploring the potential of magnetic antimicrobial agents for water disinfection, Water Res. 6 (2014) 2–10. doi:10.1016/j.watres.2014.08.024.

[155] J. Kong, S. Yu, Fourier Transform Infrared Spectroscopic analysis of protein secondary structures, Acta Biochim. Biophys. Sin. (Shanghai). 39 (2007) 549–559. doi:10.1111/j.1745-7270.2007.00320.x.

[156] S.I.C.J.C.J. Palma, M. Marciello, A. Carvalho, S. Veintemillas-Verdaguer, M.D.P. Morales, A.C.A.A. Roque, Effects of phase transfer ligands on monodisperse iron oxide magnetic nanoparticles, J. Colloid Interface Sci. 437 (2015) 147–155. doi:10.1016/j.jcis.2014.09.019.

[157] F. Rubio, J. Rubio, J.L. Oteo, A FT-IR Study of the Hydrolysis of Tetraethylorthosilicate (TEOS)., Spectrosc. Lett. 31 (1998) 199–219. doi:10.1080/00387019808006772.

[158] R. Shukla, S. Shukla, V. Bivolarski, I. Iliev, I. Ivanova, A. Goyal, Structural characterization of insoluble dextran produced by Leuconostoc mesenteroides NRRL B-1149 in the presence of maltose, Food Technol. Biotechnol. 49 (2011) 291–296. doi:10.13140/2.1.2567.7442.

[159] A. Ditsch, P.E. Laibinis, D.I.C. Wang, T.A. Hatton, Controlled clustering and enhanced stability of polymer-coated magnetic nanoparticles, Langmuir. 21 (2005) 6006–6018. doi:10.1021/la047057+.

[160] W. Wu, Q. He, C. Jiang, Magnetic iron oxide nanoparticles: synthesis and surface functionalization strategies, Nanoscale Res. Lett. 3 (2008) 397–415. doi:10.1007/s11671-008-9174-9.

[161] H. Gu, K. Xu, C. Xu, B. Xu, Biofunctional magnetic nanoparticles for protein separation and pathogen detection, Chem. Commun. (Camb). (2006) 941–949. doi:10.1039/B514130C.

[162] R. Strang, Purification of egg-white lysozyme by ion-exchange chromatography, Biochem. Educ. 12 (2010) 57–59. doi:10.1016/0307-4412(84)90003-7.

[163] J. Chen, Y. Lin, L. Jia, Preparation of anionic polyelectrolyte modified magnetic nanoparticles for rapid and efficient separation of lysozyme from egg white, J. Chromatogr. A. 1388 (2015) 43–51. doi:10.1016/j.chroma.2015.02.032.

[164] I. Safarik, Z. Sabatkova, O. Tokar, M. Safarikova, Magnetic cation exchange isolation of lysozyme from native hen egg white, Food Technol. Biotechnol. 45 (2007) 355–359.

[165] L. Borlido, A.M. Azevedo, A.G. Sousa, P.H. Oliveira, A.C.A. Roque, M.R. Aires-Barros, Fishing human monoclonal antibodies from a CHO cell supernatant with boronic acid magnetic particles, J. Chromatogr. B Anal. Technol. Biomed. Life Sci. 903 (2012) 163–170. doi:10.1016/j.jchromb.2012.07.014.

[166] P.A.J. Rosa, A.M. Azevedo, S. Sommerfeld, M. Mutter, W. Bäcker, M.R. Aires-Barros, Continuous purification of antibodies from cell culture supernatant with aqueous two-phase systems: From concept to process, Biotechnol. J. 8 (2013) 352–362. doi:10.1002/biot.201200031.

[167] R. dos Santos, S.A.S.L. Rosa, M.R. Aires-Barros, A. Tover, A.M. Azevedo, Phenylboronic acid as a multi-modal ligand for the capture of monoclonal antibodies: development and optimization of a washing step., J. Chromatogr. A. 1355 (2014) 115–24. doi:10.1016/j.chroma.2014.06.001.

[168] X.-D. Tong, B. Xue, Y. Sun, A novel magnetic affinity support for protein adsorption and purification., Biotechnol. Prog. 17 (2001) 134–139. doi:10.1021/bp000134g.

[169] G. Bayramoglu, T. Tekinay, V.C. Ozalp, M.Y. Arica, Fibrous polymer grafted magnetic chitosan beads with strong poly(cation-exchange) groups for single step purification of lysozyme, J. Chromatogr. B. 990 (2015) 84–95. doi:10.1016/j.jchromb.2015.03.030.

[170] M.A. Magdeldin Sameh, Affinity Chromatography: Principles and Applications, in: D.S. Magdeldin (Ed.), Affin. Chromatogr., InTech, 2012: pp. 3–26.

[171] J.J. Gray, High-resolution protein-protein docking, Curr. Opin. Struct. Biol. 16 (2006) 183–193. doi:10.1016/j.sbi.2006.03.003.

[172] J. Hu, S. Huang, X. Huang, Z. Kang, N. Gan, Superficially mesoporous Fe3O4@SiO2 core shell microspheres: Controlled syntheses and attempts in protein separations, Microporous Mesoporous Mater. 197 (2014) 180–184. doi:10.1016/j.micromeso.2014.06.014.

[173] J.D. Westbrook, S.K. Burley, How Structural Biologists and the Protein Data Bank Contributed to Recent FDA New Drug Approvals, Structure. 27 (2019) 211–217. doi:10.1016/j.str.2018.11.007.

[174] A.-L. Noresson, O. Aurelius, C.T. Öberg, O. Engström, A.P. Sundin, M. Håkansson, O. Stenström, M. Akke, D.T. Logan, H. Leffler, U.J. Nilsson, Designing interactions by control of protein–ligand complex conformation: tuning arginine–arene interaction geometry for enhanced electrostatic protein–ligand interactions, Chem. Sci. 9 (2018) 1014–1021.

[175] J.F. Darby, M. Atobe, J.D. Firth, P. Bond, G.J. Davies, P. O'Brien, R.E. Hubbard, Increase of enzyme activity through specific covalent modification with fragments, Chem. Sci. 8 (2017) 7772–7779. doi:10.1039/c7sc01966a.

[176] C. Kotlowski, M. Larisika, P.M. Guerin, C. Kleber, T. Kröber, R. Mastrogiacomo, C. Nowak, P. Pelosi, S. Schütz, A. Schwaighofer, W. Knoll, Fine discrimination of volatile compounds by graphene-immobilized odorant-binding proteins, Sensors Actuators B Chem. 256 (2018) 564–572. doi:10.1016/j.snb.2017.10.093.

[177] G. Houlihan, P. Gatti-Lafranconi, D. Lowe, F. Hollfelder, Directed evolution of anti-HER2 DARPins by SNAP display reveals stability/function trade-offs in the selection process., Protein Eng. Des. Sel. 28 (2015) 269–79. doi:10.1093/protein/gzv029.

[178] R. Li, V. Dows, D.J. Stewart, S.J. Burton, C.R. Lowe, Design, synthesis, and application of a Protein A mimetic, Nat. Biotechnol. 16 (1998) 190–195. doi:10.1038/nbt0898-773.

[179] C. Sauter, J.D. Ng, B. Lorber, G. Keith, Philippe Brion, M. Wais Hosseini, J.-M. Lehn, R. Giegé, Additives for the crystallization of proteins and nucleic acids, J. Cryst. Growth. 196 (1999) 365–376. doi:10.1016/S0022-0248(98)00852-5.

[180] E. Girard, S. Olivier Maury, S. Engilberge, F. RiobéRiob, S. Di Pietro, L. Lassalle, N. Coquelle, C.-A. Arnaud, D. Pitrat, J.-C. Mulatier, D. Madern, E. Breyton, O. Maury, Crystallophore: a versatile lanthanide complex for protein crystallography combining nucleating effects, phasing properties, and luminescence, Chem. Sci. 8 (2017) 5909–5917. doi:10.1039/c7sc00758b.

[181] B. Zhang, A.R. Mei, M.A. Isbell, D. Wang, Y. Wang, S.F. Tan, X.L. Teo, L. Xu, Z. Yang, J.Y.Y. Heng, DNA Origami as Seeds for Promoting Protein Crystallization, ACS Appl. Mater. Interfaces. 10 (2018) 44240–44246. doi:10.1021/acsami.8b15629.

[182] X.-Z. Yang, C.-Y. Zhang, Q.-J. Wang, Y.-Z. Guo, C. Dong, E.-K. Yan, W.-J. Liu, X.-W. Zheng, D.-C. Yin, Utilization of Cyclodextrins and Its Derivative Particles as Nucleants for Protein Crystallization, Cryst. Growth Des. 17 (2017) 6189–6200. doi:10.1021/acs.cgd.7b00455.

[183] P. Asanithi, E. Saridakis, L. Govada, I. Jurewicz, E.W. Brunner, R. Ponnusamy, J.A.S. Cleaver, A.B. Dalton, N.E. Chayen, R.P. Sear, Carbon-nanotube-based materials for protein crystallization, ACS Appl. Mater. Interfaces. 1 (2009) 1203–1210. doi:10.1021/am9000858.

[184] Y.W. Chen, C.H. Lee, Y.L. Wang, T.L. Li, H.C. Chang, Nanodiamonds as Nucleating Agents for Protein Crystallization, Langmuir. 33 (2017) 6521–6527. doi:10.1021/acs.langmuir.7b00578.

[185] S. Khurshid, E. Saridakis, L. Govada, N.E. Chayen, Porous nucleating agents for protein crystallization, Nat. Protoc. 9 (2014) 1621–1633. doi:10.1038/nprot.2014.109.

[186] S. Ko, H.Y. Kim, I. Choi, J. Choe, Gold nanoparticles as nucleation-inducing reagents for protein crystallization, Cryst. Growth Des. 17 (2017) 497–503. doi:10.1021/acs.cgd.6b01346.

[187] N.E. Chayen, E. Saridakis, R. El-Bahar, Y. Nemirovsky, Porous silicon: An effective nucleation-inducing material for protein crystallization, J. Mol. Biol. 312 (2001) 591–595. doi:10.1006/jmbi.2001.4995.

[188] L. Borlido, L. Moura, A.M. Azevedo, A.C.A. Roque, M.R. Aires-Barros, J.P.S. Farinha, Stimuli-Responsive magnetic nanoparticles for monoclonal antibody purification, Biotechnol. J. 8 (2013) 709–717. doi:10.1002/biot.201200329.

[189] L. Borlido, A.M. Azevedo, A.C.A. Roque, M.R. Aires-Barros, Potential of boronic acid functionalized magnetic particles in the adsorption of human antibodies under mammalian cell culture conditions, J. Chromatogr. A. 1218 (2011) 7821–7827. doi:10.1016/j.chroma.2011.08.084.

[190] R. Valenzuela, M.C. Fuentes, C. Parra, J. Baeza, N. Duran, S.K. Sharma, M. Knobel, J. Freer, Influence of stirring velocity on the synthesis of magnetite nanoparticles (Fe3O4) by the co-precipitation method, J. Alloys Compd. 488 (2009) 227–231. doi:10.1016/J.JALLCOM.2009.08.087.

[191] A. Leyva, A. Quintana, M. Sánchez, E.N. Rodríguez, J. Cremata, J.C. Sánchez, Rapid and sensitive anthrone-sulfuric acid assay in microplate format to quantify carbohydrate in biopharmaceutical products: Method development and validation, Biologicals. 36 (2008) 134–141. doi:10.1016/j.biologicals.2007.09.001.

[192] M.H.M.E. Alves, G.A. Nascimento, M.P. Cabrera, S.I. da C. Silvério, C. Nobre, J.A. Teixeira, L.B. de Carvalho, Trypsin purification using magnetic particles of azocasein-iron composite, Food Chem. 226 (2017) 75–78.

[193] A.S. Pina, A.M.G.C. Dias, F.I. Ustok, G. El Khoury, C.S.M. Fernandes, R.J.F. Branco, C.R. Lowe,

A.C.A. Roque, Mild and cost-effective green fluorescent protein purification employing small synthetic ligands, J. Chromatogr. A. 1418 (2015) 83–93. doi:10.1016/j.chroma.2015.09.036.

[194] A.S. Pina, M. Guilherme, A.S. Pereira, C.S.M. Fernandes, R.J.F. Branco, G. El Khoury, C.R. Lowe, A.C.A. Roque, A Tailor-Made "Tag-Receptor" Affinity Pair for the Purification of Fusion Proteins, ChemBioChem. 15 (2014) 1423–1435. doi:10.1002/cbic.201400018.

[195] M.D. Winn, C.C. Ballard, K.D. Cowtan, E.J. Dodson, P. Emsley, P.R. Evans, R.M. Keegan, E.B. Krissinel, A.G.W. Leslie, A. McCoy, S.J. McNicholas, G.N. Murshudov, N.S. Pannu, E.A. Potterton, H.R. Powell, R.J. Read, A. Vagin, K.S. Wilson, Overview of the CCP4 suite and current developments, Acta Crystallogr. Sect. D Biol. Crystallogr. 67 (2011) 235–242. doi:10.1107/S0907444910045749.

[196] A.J. McCoy, R.W. Grosse-Kunstleve, P.D. Adams, M.D. Winn, L.C. Storoni, R.J. Read, Phaser crystallographic software, J. Appl. Crystallogr. 40 (2007) 658–674.

[197] P.D. Adams, P. V. Afonine, G. Bunkóczi, V.B. Chen, I.W. Davis, N. Echols, J.J. Headd, L.-W. Hung, G.J. Kapral, R.W. Grosse-Kunstleve, A.J. McCoy, N.W. Moriarty, R. Oeffner, R.J. Read, D.C. Richardson, J.S. Richardson, T.C. Terwilliger, P.H. Zwart, IUCr, *PHENIX* : a comprehensive Python-based system for macromolecular structure solution, Acta Crystallogr. Sect. D Biol. Crystallogr. 66 (2010) 213–221. doi:10.1107/S0907444909052925.

[198] P. Emsley, B. Lohkamp, W.G. Scott, K. Cowtan, Biological Crystallography Features and development of Coot, Acta Crystallogr. Sect. D Biol. Crystallogr. 66 (2010) 486–501. doi:10.1107/S0907444910007493.

[199] P. V. Afonine, R.W. Grosse-Kunstleve, N. Echols, J.J. Headd, N.W. Moriarty, M. Mustyakimov, T.C. Terwilliger, A. Urzhumtsev, P.H. Zwart, P.D. Adams, Towards automated crystallographic structure refinement with phenix.refine, Acta Crystallogr. Sect. D Biol. Crystallogr. 68 (2012) 352–367.

[200] J. Skujins, A. Pukite, A.D. Mclaren, Adsorption and reactions of chitinase and lisozyme on chitin, Mol. Cell. Biochem. 2 (1973) 221–228. https://link.springer.com/content/pdf/10.1007%2FBF01795475.pdf (accessed May 26, 2019).

[201] N. Suzuki, M. Hiraki, Y. Yamada, N. Matsugaki, N. Igarashi, R. Kato, I. Dikic, D. Drew, S. Iwata, S. Wakatsuki, M. Kawasaki, Crystallization of small proteins assisted by green fluorescent protein, Acta Crystallogr. Sect. D Biol. Crystallogr. 66 (2010) 1059–1066. doi:10.1107/S0907444910032944.

[202] J. Ménétrey, T. Isabet, V. Ropars, M. Mukherjea, O. Pylypenko, X. Liu, J. Perez, P. Vachette, H.L. Sweeney, A.M. Houdusse, Processive steps in the reverse direction require uncoupling of the lead head lever arm of myosin VI., Mol. Cell. 48 (2012) 75–86. doi:10.1016/j.molcel.2012.07.034.

[203] P.E. Czabotar, D. Westphal, G. Dewson, S. Ma, C. Hockings, W.D. Fairlie, E.F. Lee, S. Yao, A.Y. Robin, B.J. Smith, D.C.S. Huang, R.M. Kluck, J.M. Adams, P.M. Colman, Bax crystal structures reveal how BH3 domains activate Bax and nucleate its oligomerization to induce apoptosis., Cell. 152 (2013) 519–31. doi:10.1016/j.cell.2012.12.031.

[204] J. Schiebel, R. Gaspari, T. Wulsdorf, K. Ngo, C. Sohn, T.E. Schrader, A. Cavalli, A. Ostermann, A. Heine, G. Klebe, Intriguing role of water in protein-ligand binding studied by neutron crystallography on trypsin complexes., Nat. Commun. 9 (2018) 3559. doi:10.1038/s41467-018-05769-2.

[205] L. Kovari, C. Momany, M. Rossmann, The use of antibody fragments for crystallization and structure determinations, Structure. 3 (1995) 1291–1293. https://www.cell.com/action/showPdf?pii=S0969-2126%2801%2900266-0 (accessed July 13, 2019).

[206] D.M. Ecker, S.D. Jones, H.L. Levine, The therapeutic monoclonal antibody market., MAbs. 7 (2015) 9–14. doi:10.4161/19420862.2015.989042.

[207] M.X. Yang, B. Shenoy, M. Disttler, R. Patel, M. McGrath, S. Pechenov, A.L. Margolin, Crystalline monoclonal antibodies for subcutaneous delivery, PNAS. 100 (2003) 6934–6939.

www.pnas.orgcgidoi10.1073pnas.1131899100 (accessed July 13, 2019).

[208] N.S. Lipman, L.R. Jackson, L.J. Trudel, F. Weis-Garcia, Monoclonal Versus Polyclonal Antibodies: Distinguishing Characteristics, Applications, and Information Resources, ILAR J. 46 (2005) 258–268. https://academic.oup.com/ilarjournal/article-abstract/46/3/258/738903 (accessed July 13, 2019).

[209] A.A. Shukla, L.S. Wolfe, S.S. Mostafa, C. Norman, Evolving trends in mAb production processes, Bioeng. Transl. Med. 2 (2017) 58–69.

[210] D. Hekmat, Large-scale crystallization of proteins for purification and formulation, Bioprocess Biosyst. Eng. 38 (2015) 1209–1231. doi:10.1007/s00449-015-1374-y.

[211] D. Hekmat, M. Huber, C. Lohse, N. von den Eichen, D. Weuster-Botz, Continuous Crystallization of Proteins in a Stirred Classified Product Removal Tank with a Tubular Reactor in Bypass, Cryst. Growth Des. 17 (2017) 4162–4169. doi:10.1021/acs.cgd.7b00436.

[212] E. Trilisky, R. Gillespie, T.D. Osslund, S. Vunnum, Crystallization and Liquid-Liquid Phase Separation of Monoclonal Antibodies and Fc-Fusion Proteins: Screening Results, Biotechnol. Prog. 27 (2011) 1054–1067. doi:http://dx.doi.org/10.1002/btpr.621.

[213] U. Weichsel, D. Segets, S. Janeke, W. Peukert, Enhanced Nucleation of Lysozyme Using Inorganic Silica Seed Particles of Different Sizes, Cryst. Growth Des. 15 (2015) 3582–3593. doi:10.1021/cg501681g.

[214] E. Kadar, Í.L. Batalha, A. Fisher, A.C.A. Roque, The interaction of polymer-coated magnetic nanoparticles with seawater, Sci. Total Environ. 487 (2014) 771–777. doi:10.1016/j.scitotenv.2013.11.082.

[215] M. Cerff, A. Scholz, M. Franzreb, I.L. Batalha, A.C.A. Roque, C. Posten, In situ magnetic separation of antibody fragments from Escherichia coli in complex media, BMC Biotechnol. 13 (2013) 44. doi:10.1186/1472-6750-13-44.

[216] R. dos Santos, A.L. Carvalho, A.C.A. Roque, Renaissance of protein crystallization and precipitation in biopharmaceuticals purification, Biotechnol. Adv. 35 (2017). doi:10.1016/j.biotechadv.2016.11.005.

[217] B. Somasundaram, K. Pleitt, E. Shave, K. Baker, L.H.L. Lua, Progression of continuous downstream processing of monoclonal antibodies: Current trends and challenges, Biotechnol. Bioeng. 115 (2018) 2893–2907. doi:10.1002/bit.26812.

[218] A.S. Rathore, D. Kumar, N. Kateja, Recent developments in chromatographic purification of biopharmaceuticals, Biotechnol. Lett. 40 (2018) 895–905. doi:10.1007/s10529-018-2552-1.

[219] A.M. Ramos-de-la-Peña, J. González-Valdez, O. Aguilar, Protein A chromatography: Challenges and progress in the purification of monoclonal antibodies, J. Sep. Sci. 42 (2019) 1816–1827. doi:10.1002/jssc.201800963.

[220] A.L. Grilo, A. Mantalaris, The Increasingly Human and Profitable Monoclonal Antibody Market, Trends Biotechnol. 37 (2019) 9–16. doi:10.1016/J.TIBTECH.2018.05.014.

[221] C. Schuster, J. Matzinger, A. Jungbauer, Micro-Phase Separation within Epoxy Resin Yields Ultrathin Mesoporous Membranes with Increased Scalability by Conversion from Spin- to Dip-Coating Process, Macromol. Mater. Eng. 304 (2019) 1900321. doi:10.1002/mame.201900321.

[222] M.N. São Pedro, A.M. Azevedo, M.R. Aires-Barros, R.R.G. Soares, Minimizing the Influence of Fluorescent Tags on IgG Partition in PEG–Salt Aqueous Two-Phase Systems for Rapid Screening Applications, Biotechnol. J. 14 (2019) 1800640. doi:10.1002/biot.201800640.

[223] A. Trapp, A. Faude, N. Hörold, S. Schubert, S. Faust, T. Grob, S. Schmidt, Multiple functions of caprylic acid-induced impurity precipitation for process intensification in monoclonal antibody purification, J. Biotechnol. 279 (2018) 13–21. doi:10.1016/J.JBIOTEC.2018.05.001.

[224] D. Wang, Y. Ye, H. Liu, H. Ma, W. Zhang, Effect of alkaline precipitation on Cr species of Cr(III)-bearing complexes typically used in the tannery industry, Chemosphere. 193 (2018) 42–49.

doi:10.1016/J.CHEMOSPHERE.2017.11.006.

[225] Y. Zhang, Y. Hu, L. Wang, W. Sun, Systematic review of lithium extraction from salt-lake brines via precipitation approaches, Miner. Eng. 139 (2019) 105868. doi:10.1016/J.MINENG.2019.105868.

[226] A.M.G.C. Dias, A. Hussain, A.S. Marcos, A.C.A. Roque, A biotechnological perspective on the application of iron oxide magnetic colloids modified with polysaccharides, Biotechnol. Adv. 29 (2011) 142–155. doi:10.1016/j.biotechadv.2010.10.003.

[227] S.F. Teng, K. Sproule, A. Hussain, C.R. Lowe, A strategy for the generation of biomimetic ligands for affinity chromatography. Combinatorial synthesis and biological evaluation of an IgG binding ligand, J. Mol. Recognit. 12 (1999) 67–75. doi:10.1002/(SICI)1099-1352(199901/02)12:1<67::AID-JMR443>3.0.CO;2-4.

[228] S. Jones, J.M. Thornton, Principles of protein-protein interactions., Proc. Natl. Acad. Sci. U. S. A. 93 (1996) 13–20. http://www.ncbi.nlm.nih.gov/pubmed/8552589 (accessed December 27, 2018).

[229] T.I. Mizan, P.E. Savage, R.M. Ziff, Temperature dependence of hydrogen bonding in supercritical water, J. Phys. Chem. 100 (1996) 103–408.

[230] R.J.F. Branco, A.M.G.C. Dias, A.C.A. Roque, Understanding the molecular recognition between antibody fragments and protein A biomimetic ligand, J. Chromatogr. A. 1244 (2012) 106–115. doi:10.1016/j.chroma.2012.04.071.

[231] J. Wu, C. Zhao, W. Lin, R. Hu, Q. Wang, H. Chen, L. Li, S. Chen, J. Zheng, Binding characteristics between polyethylene glycol (PEG) and proteins in aqueous solution, J. Mater. Chem. B. 2 (2014) 2983–2992. doi:10.1039/c4tb00253a.

[232] R.W. Thompson, R.F. Latypov, Y. Wang, A. Lomakin, J.A. Meyer, S. Vunnum, G.B. Benedek, Evaluation of effects of pH and ionic strength on colloidal stability of IgG solutions by PEG-induced liquid-liquid phase separation, J. Chem. Phys. 145 (2016) 185101. doi:10.1063/1.4966708.

Annexes

Annex 1 – Monoclonal antibodies production: Anti-TNFα monoclonal antibody and anti-HER2 monoclonal antibody

The anti-tumor necrosis factor alpha (anti-TNFα) mAb and anti-human epidermal growth factor receptor 2 (anti-HER2) mAb were produced in FreeStyle™ 293-F cells (Thermo Fisher Scientific, Waltham, Massachusetts, USA) transfected using polyethylenimine (PEI) (Polysciences, Warrington, Pennsylvania). Cell culture of FreeStyle™ 293-F cells was conducted at 200 RPM (Inova incubator) with 8% CO_2. MAbs were produced in a small (3 ml) scale in Nunc 24-well plate, with round untreated bottom, and larger (100 ml) scale in 500 ml culture Erlenmeyer flask. For the small-scale production, 24 hours previously to the transfection, cells were inoculated at 0.5 x 10^6 cells/mL, and in the following day transferred to a culture plate at a 1.0 x 10^6 cells/mL in 3 ml of fresh FreeStyle™ 293 medium (Thermo Fisher Scientific), for anti-TNFα mAbs production and in fresh DMEM medium (Dulbecco's Modified Eagle's Medium) (Gibco®, Carlsbad, CA) supplemented with 5% FBS (fetal bovine serum) for anti-HER2 mAbs production. PEI (4.5 µg or 9 µg) and polycistronic mAb DNA plasmid (1.5 µg or 3 µg) for the heavy and light chains were separately diluted in fresh FreeStyle™ 293 medium and mixed at a 1:3 ratio of DNA to PEI, for a final volume of 300 µl. After 30 min incubation at room temperature, the PEI:DNA mixture was added to the cell suspension. Protein expression was evaluated 72 hours after transfection by Western Blot. For mAb large scale production, 24 hours before the transfection, 100 ml of 0.5 x 10^6 cells/ml were seeded. In the following day, cells at 1.0 x 10^6 cells/mL were transfected with PEI:DNA mixture. DNA plasmid and PEI were separately diluted in fresh FreeStyle™ 293 medium, for anti-TNFα mAb production and DMEM medium supplemented with 5% FBS, for anti-HER2 mAbs production, and mixed in a 1:3 ratio and incubated for 15 min at room temperature for further cell transfection. The cells were harvested after seven days in culture by centrifugation at 300 *xg* at room temperature for 10 min and the supernatant filtrated through a 0.45 µm filter.